

KINETIC ANALYSES OF THE EFFECTS OF TEMPERATURE AND LIGHT
INTENSITY ON GROWTH, HYDROGEN PRODUCTION, AND ORGANIC
ACID UTILIZATION BY RHODOBACTER CAPSULATUS

A THESIS SUBMITTED TO
THE GRADUATE SCHOOL OF NATURAL AND APPLIED SCIENCES
OF
MIDDLE EAST TECHNICAL UNIVERSITY

BY

PELİN SEVİNÇ

IN PARTIAL FULFILLMENT OF THE REQUIREMENTS
FOR
THE DEGREE OF MASTER OF SCIENCE
IN
BIOTECHNOLOGY

JUNE 2010

Approval of the thesis:

KINETIC ANALYSES OF THE EFFECTS OF TEMPERATURE AND LIGHT INTENSITY ON GROWTH, HYDROGEN PRODUCTION AND ORGANIC ACID UTILIZATION BY RHODOBACTER CAPSULATUS

submitted by **PELİN SEVİNÇ** in partial fulfillment of the requirements for the degree of **Master of Science in Biotechnology Department, Middle East Technical University** by,

Prof. Dr. Canan Özgen
Dean, Graduate School of **Natural and Applied Sciences** _____

Prof. Dr. İnci Eroğlu
Head of Department, **Biotechnology** _____

Prof. Dr. Ufuk Gündüz
Supervisor, **Biological Sciences Dept., METU** _____

Prof. Dr. İnci Eroğlu
Co-Supervisor, **Chemical Engineering Dept., METU** _____

Examining Committee Members:

Asst. Prof. Dr. Can Özen
Biotechnology Dept., METU _____

Prof. Dr. Ufuk Gündüz
Biological Sciences Dept., METU _____

Prof. Dr. İnci Eroğlu
Chemical Engineering Dept., METU _____

Dr. Tuba Hande Ergüder
Environmental Engineering Dept., METU _____

Dr. Başar Uyar
Chemical Engineering Dept., Kocaeli University _____

Date: 28.06.2010

I hereby declare that all information in this document has been obtained and presented in accordance with academic rules and ethical conduct. I also declare that, as required by these rules and conduct, I have fully cited and referenced all material and results that are not original to this work.

Name, Last name : Pelin Sevinç

Signature :

ABSTRACT

KINETIC ANALYSES OF THE EFFECTS OF TEMPERATURE AND LIGHT INTENSITY ON GROWTH, HYDROGEN PRODUCTION AND ORGANIC ACID UTILIZATION BY RHODOBACTER CAPSULATUS

Sevinç, Pelin

M.Sc., Department of Biotechnology

Supervisor: Prof. Dr. Ufuk Gündüz

Co-Supervisor: Prof. Dr. İnci Eroğlu

June 2010, 189 pages

Effects of temperature and light intensity on photofermentative hydrogen production by *Rhodobacter capsulatus* DSM1710 by use of acetic and lactic acids as substrates were studied. Experiments were conducted at 20, 30 and 38°C incubator temperatures under light intensities in the 1500 – 7000 lux range. pH of the medium and quantity of hydrogen forming together with quantity of biomass, and concentrations of acetic, lactic, formic, butyric and propionic acids in the medium were determined periodically. Growth took place and hydrogen was produced under all experimental conditions. Growth was found to increase with increase in temperature but to decrease with increase in light intensity. Total hydrogen produced increased with light intensity up to 6000 lux at 20°C, 5000 lux at 30°C and 3000 lux

at 38°C and decreased beyond these values. Medium temperature of about 30°C was found to be optimum for cumulative hydrogen. pH was found to increase slightly and almost all of lactic acid and most of acetic acid was consumed while formic, butyric and propionic acids were first formed and then consumed in the experiments. Growth data fitted well to the logistic model and hydrogen production data fitted well to the Modified Gompertz Model. Lactic acid was found to be almost completely consumed by first order kinetics in early times. Consumption of acetic acid was found to follow zero order kinetics in the early times when lactic acid existed in the system but the order shifted to one later when most of lactic acid was consumed.

Keywords: *Rb. capsulatus*, Biological Hydrogen Production, Light Intensity, Temperature, Kinetic Modelling

ÖZ

RHODOBACTER CAPSULATUS'TA SICAKLIK VE IŞIK YOĞUNLUĞUNUN HÜCRE ÜREMESİ, HİDROJEN ÜRETİMİ VE ORGANİK ASİT KULLANIMINA ETKİLERİNİN KİNETİK YÖNTEMLE İNCELENMESİ

Sevinç, Pelin

Yüksek Lisans, Biyoteknoloji Bölümü

Tez Yöneticisi: Prof. Dr. Ufuk Gündüz

Ortak Tez Yöneticisi: Prof. Dr. İnci Eroğlu

Haziran 2010, 189 sayfa

Rhodobacter capsulatus DSM1710'da, asetik asit ve laktik asit kullanımı ile fotofermentatif hidrojen üretimi üzerinde sıcaklık ve ışık yoğunluğunun etkileri çalışılmıştır. Deneyler 20, 30 ve 38°C incubator sıcaklıklarında 1500 – 7000 lux aralığındaki ışık yoğunluklarında gerçekleştirilmiştir. Ortamın pH'sı ve oluşan hidrojenin miktarı ile ortamdaki biyokütle miktarı ve asetik, laktik, formik, bütirik ve propiyonik asitlerin konsantrasyonları zamana bağlı olarak belirlenmiştir. Bütün deney şartlarında hücre büyümesi gerçekleşmiş ve hidrojen üretilmiştir. Hücre büyümesinin artan sıcaklıkla arttığı ancak artan ışık yoğunluğu ile azaldığı bulunmuştur. Toplam hidrojen miktarının 20 derecede 6000 lux, 30 derecede 5000 lux ve 38 derecede 3000 lux'e kadar arttığı daha yüksek değerlerde azaldığı

bulunmuştur. Toplam hidrojen açısından optimum ortam sıcaklığı yaklaşık 30°C olarak bulunmuştur. Deneyleerde ortamın pH'sının biraz arttığı, laktik asidin hemen hemen tamamının ve asetik asidin de önemli kısmının kullanıldığı, buna karşılık formik, bütirik ve propiyonik asitlerin önce oluştuğu daha sonra kullanıldığı bulunmuştur.

Büyüme verilerinin lojistik model ve hidrojen üretimi verilerinin de Modifiye Gompertz Modeline iyi uyduğu bulunmuştur. Laktik asidin hemen hemen tümü erken sürelerde birinci derece hız denklemine uygun şekilde harcanmıştır. Asetik asit tüketimi sistemde laktik asidin bulunduğu erken sürelerde sıfırıncı derece hız denklemine ve laktik asidin hemen hemen tümünün kullanılması sonrasında ise birinci derece hız denklemine uygun olarak gerçekleştiği bulunmuştur.

Anahtar Kelimeler: *Rb. capsulatus*, Biyolojik Hidrojen Üretimi, Işık Şiddeti, Sıcaklık, Kinetik Modelleme

To my Family

ACKNOWLEDGEMENTS

I would like to thank to my supervisor Prof. Dr. Ufuk Gündüz and to my co-supervisor Prof. Dr. İnci Erođlu for their continual guidance, advice and support throughout this study. I would also thank to Prof. Dr. Meral Yücel for her valuable ideas and suggestions.

I would like to express my sincere gratitude to Dr. Başar Uyar, Dr. Ebru Özgür and dr. Gökhan Kars for their great helps and friendships. All Hydrogen Research Laboratory members, Nilüfer Afşar, Endam Özkan, Gökçe Avcıođlu, Dominic Deo Androga, Muazzez Gürđan, Begüm Peksel, Efe Boran, Kamal Elkahlout, were of great help as they provided support and suggested very useful ideas in addition to their friendship.

I would also like to give my special thanks to my labmates, Gülşah Pekgöz, Yaprak Dönmez, Zelha Nil, Sevilay Akköse, Esra Güç for their support and suggestions. The members of Lab 206 are gratefully acknowledged for their friendship.

I would like to thank deeply to my close friends Melis Atala, Pınar Zorlutuna and Pınar Karpuz for their sincere friendship, patience and concern.

Finally, I want to thank my mother, Sevil Sevinç and to my father, Naci Sevinç for all their love, care, support and never ending patience.

This study was supported by 6th frame European Union Project “Hyvolution”, TÜBİTAK 1001 Project 108T455 and BAP project with number of 2006.07.02.00.01.

TABLE OF CONTENTS

ABSTRACT.....	iv
ÖZ.....	vi
ACKNOWLEDGEMENTS.....	ix
TABLE OF CONTENTS.....	x
LIST OF TABLES.....	xiv
LIST OF FIGURES.....	xix
LIST OF SYMBOLS AND ABBREVIATIONS.....	xxv
CHAPTERS	
1. INTRODUCTION	1
1.1 Hydrogen Production Methods.....	1
1.2 Biological Hydrogen Production.....	4
1.2.1 Biophotolysis.....	4
1.2.2 Fermentative Production (Dark fermentation).....	7
1.2.3 Photofermentation.....	10
1.2.4 Integrated Systems.....	12
1.3 HYVOLUTION Project.....	13
1.4 General Characteristics of Purple Non-sulphur Bacteria.....	14
1.5 Hydrogen Production Metabolism.....	16
1.6 Enzymes in Hydrogen Production.....	19
1.6.1 Hydrogenase Enzyme.....	19
1.6.2 Nitrogenase Enzyme.....	20
1.7 By-Products.....	21
1.8 Factors Affecting Hydrogen Production.....	22
1.8.1 The Effect of Temperature on Hydrogen Production.....	23
1.8.2 The Effect of Light Intensity on Hydrogen Production.....	24
1.9 Aim of This Study.....	27

2. MATERIALS AND METHODS	28
2.1 The Microorganism.....	28
2.2 Culture Media.....	28
2.2.1 Media Preperation.....	28
2.2.2 Liquid Media.....	28
2.2.2.1 Growth Media.....	28
2.2.2.2 Hydrogen Production Media.....	29
2.2.3 Solid Media.....	29
2.3 Experimental Setup for Hydrogen Production.....	29
2.4 Experimental Procedure.....	32
2.5 Analyses.....	33
2.5.1 Cell Concentration.....	33
2.5.2 pH Analysis.....	33
2.5.3 Gas Composition Analysis.....	34
2.5.4 Organic Acid Analysis.....	34
3. RESULTS AND DISCUSSIONS.....	36
3.1 The Medium Temperature Affected by Light Intensity.....	36
3.2 The Effect of Light Intensity and Temperature on Cell Growth.....	38
3.3 Variation of pH at Different Temperatures and Light Intensities.....	50
3.4 The Effect of Light Intensity and Temperature on Hydrogen Production.....	52
3.4.1 Modeling of Hydrogen Production Results.....	58
3.4.2 Substrate Conversion Efficiency, Yield, Molar Productivity, Light Conversion Efficiency and Product Yield Factor Determinations....	63
3.5 Organic Acid Consumption and Production.....	71
3.5.1 Lactic Acid Consumption.....	71
3.5.2 Acetic Acid Consumption.....	80
3.5.3 Other Organic Acids.....	86
5. CONCLUSIONS.....	93
REFERENCES.....	95

APPENDICES

A. COMPOSITION OF THE GROWTH AND HYDROGEN PRODUCTION MEDIA.....	106
B. OPTICAL DENSITY – DRY WEIGHT CALIBRATION CURVE.....	108
C. SAMPLE GAS CHROMOTOGRAM.....	109
D. ORGANIC ACID ANALYSIS.....	110
D1. Sample HPLC Chromotogram.....	110
D2. Sample Acetic Acid Calibration Curve.....	111
E. LOGISTIC MODEL.....	112
E1-E6. Curves fitted to the logistic model together with the experimental data for different light intensities at 20°C.....	112
E7-E13. Curves fitted to the logistic model together with the experimental data for different light intensities at 30°C.....	115
E14-E18. Curves fitted to the logistic model together with the experimental data for different light intensities at 38°C.....	119
F. MODIFIED GOMPERTZ MODEL.....	122
F1-F6. Curves fitted to the Modified Gompertz Model together with the experimental data for different light intensities at 20°C.....	122
F7-F13. Curves fitted to the Modified Gompertz Model together with the experimental data for different light intensities at 30°C.....	125
F7-F13. Curves fitted to the Modified Gompertz Model together with the experimental data for different light intensities at 38°C.....	129
G. LACTIC ACID CONSUMPTION KINETICS.....	132
G1-G7. Lactic Acid Consumption Kinetics together with the experimental data for different light intensities at 20°C.....	132
G8-G13. Lactic Acid Consumption Kinetics together with the experimental data for different light intensities at 30°C.....	136
G14-G18. Lactic Acid Consumption Kinetics together with the experimental data for different light intensities at 38°C.....	139

H.	ACETIC ACID CONSUMPTION KINETICS.....	142
	H1-H6. Acetic Acid Consumption Kinetics together with the experimental data for different light intensities at 20°C.....	142
	H7-H13. Acetic Acid Consumption Kinetics together with the experimental data for different light intensities at 30°C.....	145
	H14-H18. Lactic Acid Consumption Kinetics together with the experimental data for different light intensities at 38°C.....	149
I.	EXPERIMENTAL DATA.....	152

LIST OF TABLES

TABLES

Table 1.1	The taxonomy of <i>Rb. capsulatus</i>	15
Table 2.1	Temperatures and light intensities used in the experiments.....	30
Table 3.1	The maximum photobioreactor temperatures measured under different light intensities at 20, 30 and 38°C incubator temperatures and change in temperature expressed as percentage of the incubator temperature	37
Table 3.2	Comparison of experimental and logistic model constants of <i>Rb.capsulatus</i> at 20°C and different light intensities.....	46
Table 3.3	Comparison of experimental and logistic model constants of <i>Rb.capsulatus</i> at 30°C and different light intensities.....	46
Table 3.4	Comparison of experimental and logistic model constants of <i>Rb. capsulatus</i> at 38°C and different light intensities.....	47
Table 3.5	Comparison of the Modified Gompertz Model parameters with the experimental values obtained at 20°C and different light intensities	60
Table 3.6	Comparison of the Modified Gompertz Model parameters with the experimental values obtained at 30°C and different light intensities	61
Table 3.7	Comparison of the Modified Gompertz Model parameters with the experimental values obtained at 38°C and different light intensities	61
Table 3.8	Differential and the integrated forms of the 0 th , 1 st and 2 nd order rate equations.....	74
Table 3.9	Extent of the fits and rate constants for lactic acid consumption at 20°C.....	75

Table 3.10	Extent of the fits and rate constants for lactic acid consumption at 30°C.....	75
Table 3.11	Extent of the fits and rate constants for lactic acid consumption at 38°C.....	76
Table 3.12	Activation energies for lactic acid consumption under different light intensities	78
Table 3.13	Half-life for lactate consumption.....	79
Table 3.14	Kinetic Analysis for Acetate Consumption at 20°C.....	82
Table 3.15	Kinetic Analysis for Acetate Consumption at 30°C.....	83
Table 3.16	Kinetic Analysis for Acetate Consumption at 38°C.....	83
Table 3.17	Activation energies for acetic acid consumption under different light intensities.....	86
Table A.1	The constituents of the growth and hydrogen production medium per liter of solution.....	106
Table A.2	The composition of 1 liter vitamin solution	106
Table A.3	The composition of 1 liter trace element solution.....	107
Table I.1	OD, cell dry weight, pH and cumulative hydrogen produced values for 20°C and 1500 lux (Mean of 2 runs).....	152
Table I.2	Organic Acid concentrations for 20°C and 1500 lux (Mean of 2 runs).....	153
Table I.3	OD, cell dry weight, pH and cumulative hydrogen produced values for 20°C and 2000 lux (Mean of 2 runs).....	154
Table I.4	Organic Acid concentrations for 20°C and 2000 lux (Mean of 2 runs).....	155
Table I.5	OD, cell dry weight, pH and cumulative hydrogen produced values for 20°C and 3000 lux (Mean of 2 runs).....	156
Table I.6	Organic Acid concentrations for 20°C and 3000 lux (Mean of 2 runs).....	157
Table I.7	OD, cell dry weight, pH and cumulative hydrogen produced values for 20°C and 4000 lux (Mean of 2 runs).....	158

Table I.8	Organic Acid concentrations for 20°C and 4000 lux (Mean of 2 runs).....	159
Table I.9	OD, cell dry weight, pH and cumulative hydrogen produced values for 20°C and 5000 lux (Mean of 2 runs).....	160
Table I.10	Organic Acid concentrations for 20°C and 5000 lux (Mean of 2 runs).....	161
Table I.11	OD, cell dry weight, pH and cumulative hydrogen produced values for 20°C and 6000 lux (Mean of 2 runs).....	162
Table I.12	Organic Acid concentrations for 20°C and 6000 lux (Mean of 2 runs).....	163
Table I.13	OD, cell dry weight, pH and cumulative hydrogen produced values for 20°C and 7000 lux (Mean of 2 runs).....	164
Table I.14	Organic Acid concentrations for 20°C and 7000 lux (Mean of 2 runs).....	165
Table I.15	OD, cell dry weight, pH and cumulative hydrogen produced values for 30°C and 1500 lux (Mean of 2 runs).....	166
Table I.16	Organic Acid concentrations for 30°C and 1500 lux (Mean of 2 runs).....	167
Table I.17	OD, cell dry weight, pH and cumulative hydrogen produced values for 30°C and 2000 lux (Mean of 2 runs).....	168
Table I.18	Organic Acid concentrations for 30°C and 2000 lux (Mean of 2 runs).....	169
Table I.19	OD, cell dry weight, pH and cumulative hydrogen produced values for 30°C and 3000 lux (Mean of 2 runs).....	170
Table I.20	Organic Acid concentrations for 30°C and 3000 lux (Mean of 2 runs).....	171
Table I.21	OD, cell dry weight, pH and cumulative hydrogen produced values for 30°C and 4000 lux (Mean of 2 runs).....	172
Table I.22	Organic Acid concentrations for 30°C and 4000 lux (Mean of 2 runs).....	173

Table I.23	OD, cell dry weight, pH and cumulative hydrogen produced values for 30°C and 5000 lux (Mean of 2 runs).....	174
Table I.24	Organic Acid concentrations for 30°C and 5000 lux (Mean of 2 runs).....	175
Table I.25	OD, cell dry weight, pH and cumulative hydrogen produced values for 30°C and 6000 lux (Mean of 2 runs).....	176
Table I.26	Organic Acid concentrations for 30°C and 6000 lux (Mean of 2 runs).....	177
Table I.27	OD, cell dry weight, pH and cumulative hydrogen produced values for 30°C and 7000 lux (Mean of 2 runs).....	178
Table I.28	Organic Acid concentrations for 30°C and 7000 lux (Mean of 2 runs).....	179
Table I.29	OD, cell dry weight, pH and cumulative hydrogen produced values for 38°C and 1500 lux (Mean of 2 runs).....	180
Table I.30	Organic Acid concentrations for 38°C and 1500 lux (Mean of 2 runs).....	181
Table I.31	OD, cell dry weight, pH and cumulative hydrogen produced values for 38°C and 2000 lux (Mean of 2 runs).....	182
Table I.32	Organic Acid concentrations for 38°C and 2000 lux (Mean of 2 runs).....	183
Table I.33	OD, cell dry weight, pH and cumulative hydrogen produced values for 38°C and 3000 lux (Mean of 2 runs).....	184
Table I.34	Organic Acid concentrations for 38°C and 3000 lux (Mean of 2 runs).....	185
Table I.35	OD, cell dry weight, pH and cumulative hydrogen produced values for 38°C and 4000 lux (Mean of 2 runs).....	186
Table I.36	Organic Acid concentrations for 38°C and 4000 lux (Mean of 2 runs).....	187
Table I.37	OD, cell dry weight, pH and cumulative hydrogen produced values for 38°C and 5000 lux (Mean of 2 runs).....	188

Table I.38	Organic Acid concentrations for 38°C and 5000 lux (Mean of 2 runs).....	189
------------	---	-----

LIST OF FIGURES

FIGURES

Figure 1.1	Feedstock used in the current global production of hydrogen.....	3
Figure 1.2	Direct Biophotolysis.....	5
Figure 1.3	Indirect Biophotolysis.....	6
Figure 1.4	The conversion of carbohydrates to H ₂ , CO ₂ , organic acids and solvents by Clostridia genera during dark fermentation	8
Figure 1.5	The scheme of photofermentative hydrogen production.....	11
Figure 1.6	The overall scheme of HYVOLUTION project.....	13
Figure 1.7	The microscopic picture of <i>Rb. capsulatus</i>	16
Figure 1.8	A simplified overall scheme of the carbon metabolism in PNS bacteria.....	17
Figure 1.9	The overall scheme of hydrogen production by PNS bacteria.....	18
Figure 2.1	The schematic diagram of experimental set up	31
Figure 2.2	The photograph of the experimental set up for hydrogen production experiments.....	32
Figure 3.1	The schematic cell growth curve.....	39
Figure 3.2	Cell growth for different light intensities at 20°C.....	39
Figure 3.3	Cell growth for different light intensities at 30°C.....	40
Figure 3.4	Cell growth for different light intensities at 38°C.....	40
Figure 3.5	Initial and maximum dry cell weights and their differences at (a) 20°C, (b) 30°C and (c) 38°C.....	41
Figure 3.6	The logistic growth model at 20°C and 2000 lux.....	45
Figure 3.7	Variation of pH with time for different light intensities at 20°C	51
Figure 3.8	Variation of pH with time for different light intensities at 30°C.....	51
Figure 3.9	Variation of pH with time for different light intensities at 38°C.....	52

Figure 3.10	Cumulative Hydrogen Production for different light intensities at 20°C.....	53
Figure 3.11	Cumulative Hydrogen Production for different light intensities at 30°C.....	53
Figure 3.12	Cumulative Hydrogen Production for different light intensities at 38°C.....	54
Figure 3.13	Total amount of hydrogen produced at different incubator temperatures and light intensities.....	54
Figure 3.14	A schematic curve for the Modified Gompertz Model.....	58
Figure 3.15	Comparison of hydrogen production data with Modified Gompertz Model at 20°C and 2000 lux.....	60
Figure 3.16	Substrate Conversion Efficiency Results for Different Light Intensities and Temperatures.....	64
Figure 3.17	Molar Productivity Values for Different Light Intensities and Temperatures.....	65
Figure 3.18	Hydrogen Yield Values for Different Light Intensities and Temperatures.....	67
Figure 3.19	Light Conversion Efficiencies for Different Light Intensities and Temperatures.....	69
Figure 3.20	Product Yield Factor Values for Different Light Intensities and Temperatures.....	70
Figure 3.21	Lactic Acid Consumption at different light intensities and 20°C.....	72
Figure 3.22	Lactic Acid Consumption at different light intensities and 30°C.....	72
Figure 3.23	Lactic Acid Consumption at different light intensities and 38°C.....	73
Figure 3.24	First Order Kinetics for Lactic acid consumption at 30°C 4000 lux...	76
Figure 3.25	Variation of $\ln k_1$ with reciprocal of temperature for lactate consumption at 4000 lux.....	78
Figure 3.26	Acetic Acid Consumption at different light intensities and 20°C.....	80
Figure 3.27	Acetic Acid Consumption at different light intensities and 30°C.....	80
Figure 3.28	Acetic Acid Consumption at different light intensities and 38°C.....	81

Figure 3.29	Comparison of model and experimental results of acetic acid consumption at 20°C and 1500 lux.....	84
Figure 3.30	Variation of Formic Acid Concentration with time for different light intensities at 20°C.....	87
Figure 3.31	Variation of Formic Acid Concentration with time for different light intensities at 30°C.....	87
Figure 3.32	Variation of Formic Acid Concentration with time for different light intensities at 38°C.....	88
Figure 3.33	Variation of Butyric Acid Concentration with time for different light intensities at 20°C.....	88
Figure 3.34	Variation of Butyric Acid Concentration with time for different light intensities at 30°C.....	89
Figure 3.35	Variation of Butyric Acid Concentration with time for different light intensities at 38°C.....	89
Figure 3.36	Variation of Propionic Acid Concentration with time for different light intensities at 20°C.....	90
Figure 3.37	Variation of Propionic Acid Concentration with time for different light intensities at 30°C.....	90
Figure 3.38	Variation of Propionic Acid Concentration with time for different light intensities at 38°C.....	91
Figure B.	Calibration curve and the regression trend line for <i>Rhodobacter capsulatus</i> (DSM 1710) dry weight versus OD660.....	108
Figure C	Sample Gas Analysis Chromotogram.....	109
Figure D.1	Sample HPLC analysis chromatogram. Peak 1(mobile phase- H ₂ SO ₄), Peak 2 (lactic acid), Peak 3(Formic acid) and Peak 4(acetic acid).....	110
Figure D.2	Sample Acetic Acid Calibration Curve.....	111
Figure E.1	The logistic growth model at 20°C and 1500 lux.....	112
Figure E.2	The logistic growth model at 20°C and 3000 lux.....	113
Figure E.3	The logistic growth model at 20°C and 4000 lux.....	113
Figure E.4	The logistic growth model at 20°C and 5000 lux.....	114

Figure E.5	The logistic growth model at 20°C and 6000 lux.....	114
Figure E.6	The logistic growth model at 20°C and 7000 lux.....	115
Figure E.7	The logistic growth model at 30°C and 1500 lux.....	115
Figure E.8	The logistic growth model at 30°C and 2000 lux.....	116
Figure E.9	The logistic growth model at 30°C and 3000 lux.....	116
Figure E.10	The logistic growth model at 30°C and 4000 lux.....	117
Figure E.11	The logistic growth model at 30°C and 5000 lux.....	117
Figure E.12	The logistic growth model at 30°C and 6000 lux.....	118
Figure E.13	The logistic growth model at 30°C and 7000 lux.....	118
Figure E.14	The logistic growth model at 38°C and 1500 lux.....	119
Figure E.15	The logistic growth model at 38°C and 2000 lux.....	119
Figure E.16	The logistic growth model at 38°C and 3000 lux.....	120
Figure E.17	The logistic growth model at 38°C and 4000 lux.....	120
Figure E.18	The logistic growth model at 38°C and 5000 lux.....	121
Figure F.1	The Modified Gompertz Model at 20°C and 1500 lux.....	122
Figure F.2	The Modified Gompertz Model at 20°C and 3000 lux.....	123
Figure F.3	The Modified Gompertz Model at 20°C and 4000 lux.....	123
Figure F.4	The Modified Gompertz Model at 20°C and 5000 lux.....	124
Figure F.5	The Modified Gompertz Model at 20°C and 6000 lux.....	124
Figure F.6	The Modified Gompertz Model at 20°C and 7000 lux.....	125
Figure F.7	The Modified Gompertz Model at 30°C and 1500 lux.....	125
Figure F.8	The Modified Gompertz Model at 30°C and 2000 lux.....	126
Figure F.9	The Modified Gompertz Model at 30°C and 3000 lux.....	126
Figure F.10	The Modified Gompertz Model at 30°C and 4000 lux.....	127
Figure F.11	The Modified Gompertz Model at 30°C and 5000 lux.....	127
Figure F.12	The Modified Gompertz Model at 30°C and 6000 lux.....	128
Figure F.13	The Modified Gompertz Model at 30°C and 7000 lux.....	128
Figure F.14	The Modified Gompertz Model at 38°C and 1500 lux.....	129
Figure F.15	The Modified Gompertz Model at 38°C and 2000 lux.....	129
Figure F.16	The Modified Gompertz Model at 38°C and 3000 lux.....	130
Figure F.17	The Modified Gompertz Model at 38°C and 4000 lux.....	130

Figure F.18	The Modified Gompertz Model at 38°C and 5000 lux.....	131
Figure G.1	First Order Kinetics for Lactic Acid Consumption at 20°C 1500 lux.....	132
Figure G.2	First Order Kinetics for Lactic Acid Consumption at 20°C 2000 lux.....	133
Figure G.3	First Order Kinetics for Lactic Acid Consumption at 20°C 3000 lux.....	133
Figure G.4	First Order Kinetics for Lactic Acid Consumption at 20°C 4000 lux.....	134
Figure G.5	First Order Kinetics for Lactic Acid Consumption at 20°C 5000 lux.....	134
Figure G.6	First Order Kinetics for Lactic Acid Consumption at 20°C 6000 lux.....	135
Figure G.7	First Order Kinetics for Lactic Acid Consumption at 20°C 7000 lux.....	135
Figure G.8	First Order Kinetics for Lactic Acid Consumption at 30°C 1500 lux.....	136
Figure G.9	First Order Kinetics for Lactic Acid Consumption at 30°C 2000 lux.....	136
Figure G.10	First Order Kinetics for Lactic Acid Consumption at 30°C 3000 lux.....	137
Figure G.11	First Order Kinetics for Lactic Acid Consumption at 30°C 5000 lux.....	137
Figure G.12	First Order Kinetics for Lactic Acid Consumption at 30°C 6000 lux.....	138
Figure G.13	First Order Kinetics for Lactic Acid Consumption at 30°C 7000 lux.....	138
Figure G.14	First Order Kinetics for Lactic Acid Consumption at 38°C 1500 lux.....	139
Figure G.15	First Order Kinetics for Lactic Acid Consumption at 38°C 2000 lux.....	139

Figure G.16	First Order Kinetics for Lactic Acid Consumption at 38°C 3000 lux.....	140
Figure G.17	First Order Kinetics for Lactic Acid Consumption at 38°C 4000 lux.....	140
Figure G.18	First Order Kinetics for Lactic Acid Consumption at 38°C 5000 lux.....	141
Figure H.1	Kinetic Curves for Acetic Acid Consumption at 20°C 2000 lux.....	142
Figure H.2	Kinetic Curves for Acetic Acid Consumption at 20°C 3000 lux.....	143
Figure H.3	Kinetic Curves for Acetic Acid Consumption at 20°C 4000 lux.....	143
Figure H.4	Kinetic Curves for Acetic Acid Consumption at 20°C 5000 lux.....	144
Figure H.5	Kinetic Curves for Acetic Acid Consumption at 20°C 6000 lux.....	144
Figure H.6	Kinetic Curves for Acetic Acid Consumption at 20°C 7000 lux.....	145
Figure H.7	Kinetic Curves for Acetic Acid Consumption at 30°C 1500 lux.....	145
Figure H.8	Kinetic Curves for Acetic Acid Consumption at 30°C 2000 lux.....	146
Figure H.9	Kinetic Curves for Acetic Acid Consumption at 30°C 3000 lux.....	146
Figure H.10	Kinetic Curves for Acetic Acid Consumption at 30°C 4000 lux.....	147
Figure H.11	Kinetic Curves for Acetic Acid Consumption at 30°C 5000 lux.....	147
Figure H.12	Kinetic Curves for Acetic Acid Consumption at 30°C 6000 lux.....	148
Figure H.13	Kinetic Curves for Acetic Acid Consumption at 30°C 7000 lux.....	148
Figure H.14	Kinetic Curves for Acetic Acid Consumption at 38°C 1500 lux.....	149
Figure H.15	Kinetic Curves for Acetic Acid Consumption at 38°C 2000 lux.....	149
Figure H.16	Kinetic Curves for Acetic Acid Consumption at 38°C 3000 lux.....	150
Figure H.17	Kinetic Curves for Acetic Acid Consumption at 38°C 4000 lux.....	150
Figure H.18	Kinetic Curves for Acetic Acid Consumption at 38°C 5000 lux.....	151

LIST OF SYMBOLS AND ABBREVIATIONS

A	Irradiated area (m^2)
ADP	Adenosine di-Phosphate
ATP	Adenosine tri-Phosphate
C_A	Concentration of acetate (mM)
C_A^*	Concentration of acetic acid where order of acetate consumption reaction shifts, mM
C_L	Concentration of lactate, mM
C_L^*	Concentration of lactic acid where order of acetate consumption reaction shifts, mM
C_o	Initial organic acid concentration, mM
E	Activation Energy, J/mol
Fd	Ferredoxin
GC	Gas Chromotograph
gdw	Gram dry weight of bacteria
H	Experimental cumulative hydrogen produced, mmol/L
$H_{\text{max,e}}$	Maximum cumulative hydrogen production obtained from experimental results, mmol/L
$H_{\text{max,m}}$	Cumulative hydrogen production obtained by Modified Gompertz Model, mmol/L
HPLC	High Performance Liquid Chromatography
hup ⁻	Uptake hydrogenase deficient

I	light intensity, W/m^2
k'	Constant in Arrhenius equation
k_0	Rate constant for a zero order reaction, mM/h
k_1	Rate constant for a first order reaction, $1/\text{h}$
k_2	Rate constant for a second order reaction, $1/\text{mM-h}$
k_c	Specific growth rate constant obtained by logistic model, $1/\text{h}$
mmol	Millimole
n	Order of the reaction
NAD	Nicotinamide adenine dinucleotide
OD	Optical Density
PHB	Poly- β -hydroxy butyric acid
PNS	Purple Non-Sulphur
r	Extent of the fit
R	Universal gas constant
R^2	Coefficient of determination value
<i>Rb. capsulatus</i>	<i>Rhodobacter capsulatus</i>
<i>Rb. sphaeroides</i>	<i>Rhodobacter sphaeroides</i>
$R_{\text{max,e}}$	Maximum hydrogen production rate obtained from experimental results, mmol/L.h
$R_{\text{max,m}}$	maximum hydrogen production rate obtained from Modified Gompertz Model, mmol/L.h
<i>Rp. faecalis</i>	<i>Rhodopseudomonas faecalis</i>

<i>Rp. palustris</i>	<i>Rhodopseudomonas palustris</i>
<i>Rs. rubrum</i>	<i>Rhodospirillum rubrum</i>
t	Time, hour
t*	Time where order of acetate consumption reaction shifts
t _{1/2}	Half life, h
TCA	Tricarboxylic acid
t ₀	Initial time, h
V	Volume, ml or L
X	Dry cell weight, gdw/L
X _{max,e}	Experimental maximum bacterial concentration, (gdw/L)
X _{max,m}	Maximum bacterial concentration obtained by logistic model, (gdw/L)
X _{0,e}	Experimental initial bacterial concentration, (gdw/L)
X _{0,m}	Initial bacterial concentration obtained by logistic model, (gdw/L)

CHAPTER 1

INTRODUCTION

Today, nearly 80% of energy demand is obtained from fossil fuels (oil, coal and gas). Although the fossil fuels currently meet the energy need of the world, they will fail to do so in the future due to the uncontrollable growth in human population. Besides, greenhouse gases forming as a result of combustion of these fuels is one of the most important reasons of global warming. Therefore, studies are conducted on, renewable and environmentally friendly, alternative energy sources. One of these alternative energy sources is hydrogen. Hydrogen is the lightest and most abundant chemical element. Combustion reaction of hydrogen gives only water as product and this makes hydrogen a “clean” fuel. In this chapter studies in literature related with hydrogen production are summarized, emphasizing biological hydrogen production.

1.1 Hydrogen Production Methods:

Hydrogen is currently used in plenty of industrial sectors. The usage of hydrogen in the industry could be itemized as petrochemical production, oil and fat hydrogenation, fertilizer production, metallurgical applications, electronics and aerospace industries.

Hydrogen can be produced from a variety of feedstock; from fossil resources such as natural gas and coal, and from renewable resources such as biomass and water with input from renewable energy sources. (e.g. sunlight, wind, wave or hydro-power) (Riis et al., 2005) Chemical, biological, electrolytic, photolytic and thermo-chemical

methods can be used for producing hydrogen. These methods are briefly summarized below; (Holladay et al., 2008)

1. Fuel processing

- Hydrocarbon reforming: Reforming is the cracking of H₂ from hydrocarbons such as



Natural gas and coal are the most used hydrocarbons. Hydrogen production from hydrocarbon fuels can be classified as partial oxidation, autothermal reforming (ATR) and steam reforming. In partial oxidation, hydrocarbons are partially combusted by air in a reformer to produce a hydrogen rich gas mixture. In ATR, hydrocarbons are reacted with a mixture of oxygen and carbon dioxide or steam at the end of which a gas mixture containing hydrogen is produced. Steam reforming is the conversion of hydrocarbons (mostly methane) to hydrogen and carbon monoxide by reaction with water vapor. This technology is extensively used for H₂ production; 96% of total H₂ production is by reforming of fossil fuels.

2. Hydrogen from water

- Electrolysis: Electrolysis is the process of splitting water into hydrogen and oxygen by use of electricity. This technology is commercially available and 4% of H₂ is produced by this method.
- Thermochemical water splitting: Decomposition of water to hydrogen and oxygen in presence of heat. The decomposition process is not practicable in one step because required temperatures are above 2500°C. The process is carried out in steps requiring lower temperatures.
- Photoelectrolysis: Photoelectrolysis is the process of decomposition of water into hydrogen and oxygen by using sunlight. In this process a device

called photoelectrolyzer which consists of photovoltaic cells (converts sunlight to electricity) and an electrolyzer generates hydrogen.

3. Hydrogen from biomass

- Biomass gasification: With the addition of steam and oxygen biomass is converted to a syngas in which H_2 to CO ratio is 2:1. Gasification method is the variation of pyrolysis process.
- Biological hydrogen production: Biological hydrogen production processes are catalyzed by microorganisms by contrast with other production methods.

The resources and the proportions of feedstock which are commonly used to produce hydrogen with these methods are shown in Figure 1.1. This figure reveals that 96% of feedstock for hydrogen production is from fossil fuels. There is indirect usage of fossil fuels for the remaining 4% because electricity used in these processes is mostly produced via fossil fuels.

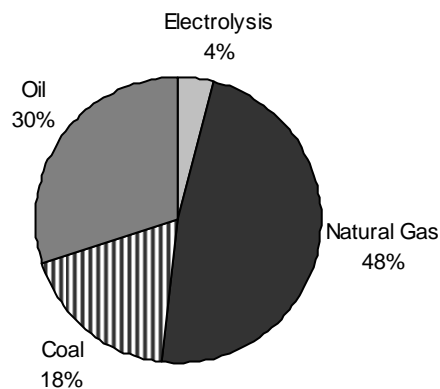


Figure 1.1- Feedstock used in the current global production of hydrogen (Kothari et al., 2008).

The main disadvantage of using fossil fuels for hydrogen production is the released greenhouse gases. The increase in the concentrations of greenhouse gases in the atmosphere causes temperature to rise in the world resulting in global warming. Use of renewable sources instead of or a supplement to fossil fuels should be important to overcome these drawbacks. Biological hydrogen production using renewable sources and operating under ambient conditions is one of the most important ways to decrease the use of fossil fuels in hydrogen production.

1.2 Biological Hydrogen Production

There are several microorganisms which produce hydrogen as a by-product of growth by using renewable sources such as water, biomass and sun light. All processes of biological hydrogen production are fundamentally dependent upon the presence of hydrogen-producing enzymes which catalyze the reaction: (Hallenbeck and Benemann, 2002)



Biological hydrogen production has been classified by Das and Veziroğlu, 2001 as follows:

- Biophotolysis of water using algae and cyanobacteria.
- Fermentative hydrogen production from organic compounds,
- Photodecomposition of organic compounds by photo-synthetic bacteria.
- Hybrid systems using photosynthetic and fermentative bacteria.

1.2.1 Biophotolysis

Biophotolysis is the biological dissociation of water into hydrogen and oxygen by the action of light energy by microorganisms. The biophotolysis of water takes place by green algae and cyanobacteria (blue-green algae) via direct and indirect biophotolysis, respectively.

In direct biophotolysis light energy is captured by photosynthetic apparatus and recovered energy provides splitting of water into O₂ and H⁺. Electrons, which are transferred to hydrogenase or nitrogenase enzyme by ferredoxin, reduce H⁺ to H₂. The net reaction and the scheme of direct biophotolysis are shown below:

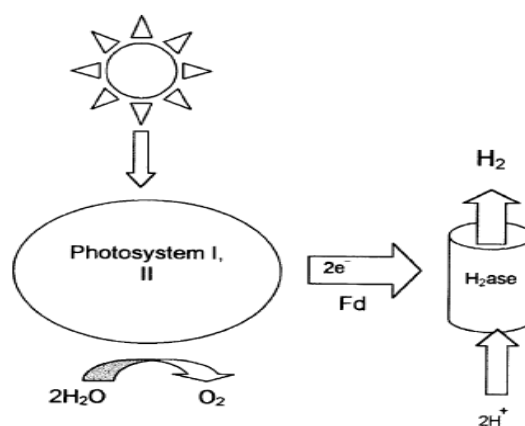
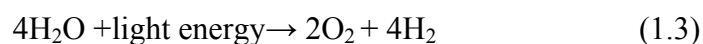


Figure 1.2- Direct Biophotolysis (Hallenbeck and Benemann, 2002)

The main advantage of this process is the capability of producing hydrogen directly from water. But the generated oxygen during decomposition of water inhibits both nitrogenase and hydrogenase enzymes. Also, a problem with separation of H₂ and O₂ makes this approach costly and economically challenging (Melis, 2002).

Cyanobacteria have photosynthetic pigments such as carotenoids and chlorophyll a and produce hydrogen by indirect biophotolysis. Like direct biophotolysis hydrogen production reaction is catalyzed both by hydrogenase and nitrogenase enzymes. In this process CO₂ is first fixed from air and energy-rich organic compounds are produced by using CO₂ as a C source. Then these organic compounds are used for

hydrogen production. The equations and scheme of indirect biophotolysis are shown below:

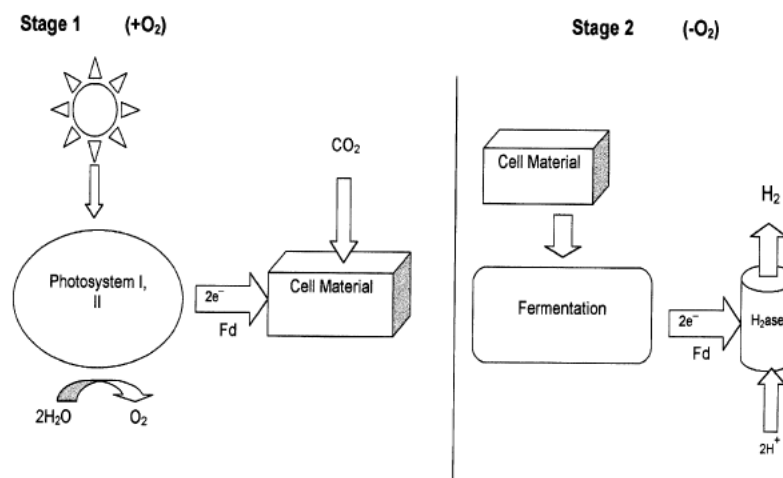
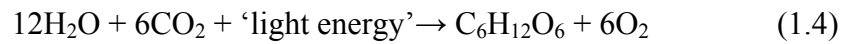


Figure 1.3- Indirect Biophotolysis (Hallenbeck and Benemann, 2002)

As seen from Figure 1.3, the oxygen and hydrogen evolution steps are separated. As a result of this separation, the inhibition of hydrogen producing enzymes because of O₂ sensitivity at direct biophotolysis is prohibited. This characteristic makes the process very attractive. The major disadvantage of this process is the lower photochemical efficiency. Also the uptake hydrogenase enzyme, which consumes part of produced hydrogen, must be removed in order to prevent the degradation of the hydrogen (Nath and Das, 2004). The indirect biophotolysis process is still of questionable economics and remain to be demonstrated even on an experimental level (Hallenbeck and Benemann, 2002).

1.2.2 Fermentative Production (Dark fermentation)

In dark fermentation process, anaerobic bacteria decompose organic substrates to small organic compounds by oxidation during heterotrophic growth. The metabolic energy required for growth of bacteria is provided by this reaction. The electrons obtained from this oxidation reaction are used for reducing protons which eventuates with production of molecular hydrogen as a by-product. The enzyme which catalyzes the hydrogen production is hydrogenase. Figure 1.4 illustrates the detailed scheme of the conversion of carbohydrates to H_2 , CO_2 , organic acids and solvents by Clostridia genera during dark fermentation.

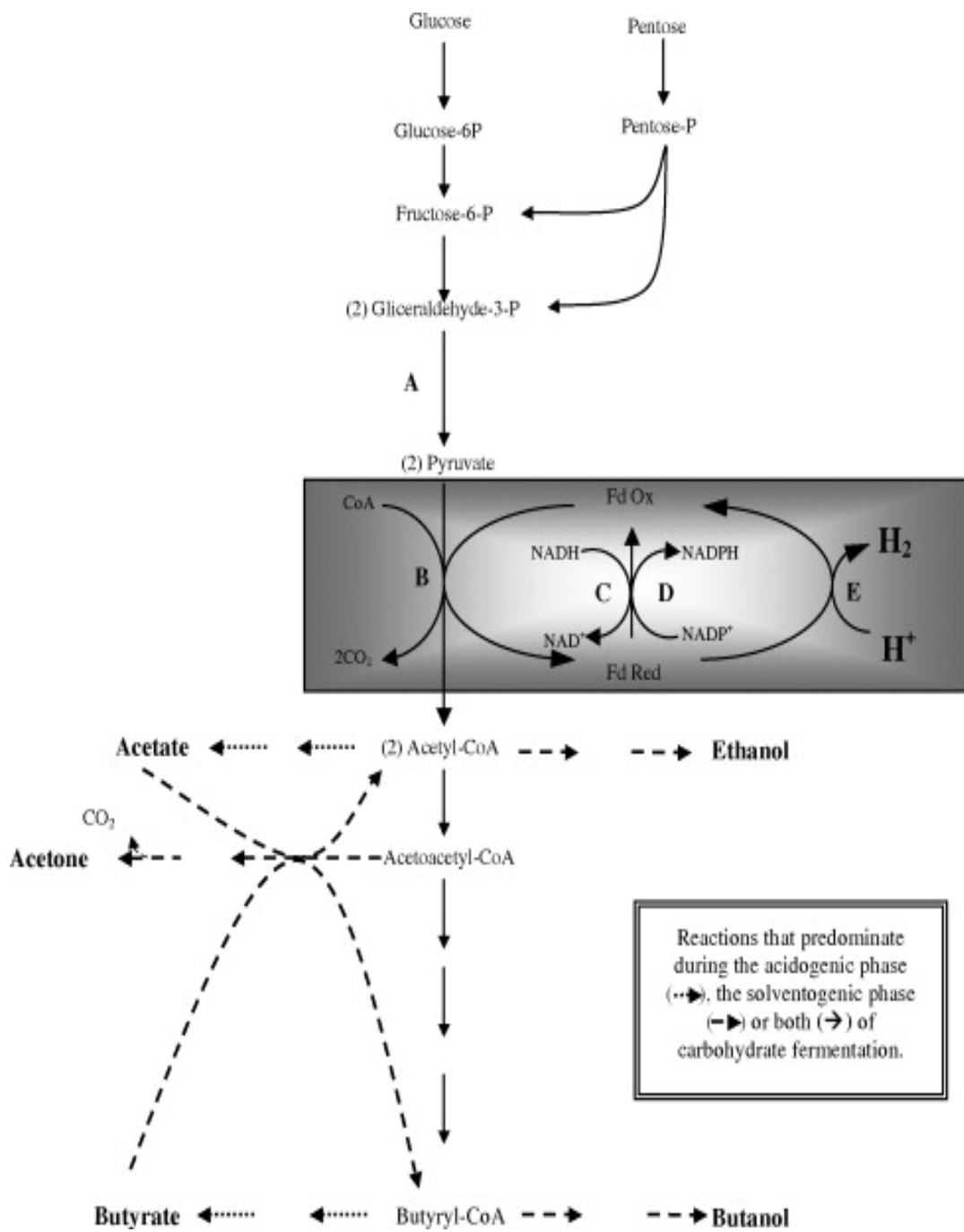


Figure 1.4. The conversion of carbohydrates to H_2 , CO_2 , organic acids and solvents by *Clostridia* genera during dark fermentation. (Valdez-Vazquez and Poggi-Varaldo, 2009)

Dark microbial H₂ production is driven by the anaerobic metabolism of the key intermediate, pyruvate (Kovács et al., 2006). Pyruvate which is converted from glucose by glycolytic pathway is oxidized to acetyl-CoA in the absence of light. During pyruvate oxidation ferredoxin is reduced. The reduced ferredoxin transfers the electrons to hydrogenase enzyme which catalyzes the production reaction of molecular hydrogen. *Clostridium* sp. (*Clostridium butyricum*, *Clostridium acetobutyricum*, *Clostridium beijerinckii*, *C. thermolacticum*, *C. saccharoperbutylacetonicum*, *Clostridium tyrobutyricum*, *C.thermocellum* and *Clostridium paraputrificum*) (Chong et al., 2009) and *Caldicellulosiruptor saccharolyticus* (Vrije et al., 2007) are typical strict anaerobic bacteria producing hydrogen by dark fermentation.

Facultative anaerobic bacteria can consume oxygen by aerobic respiration and switch to anaerobic fermentation. Because of these characteristic facultative anaerobes also produce hydrogen by dark fermentation. Although less sensitivity to oxygen is an advantage for facultative anaerobes, the yield of hydrogen production is lower. For 1 mol of glucose, 2 moles and 4 moles of hydrogen is produced by facultative anaerobes and strict anaerobes, respectively. *Enterobacter* sp. is the most common gram negative and facultative anaerobe with the ability to produce hydrogen (Chong et al., 2009).

During dark fermentation simple sugars such as glucose, lactose and sucrose could be used as substrates since they could be degraded easily. However, using pure biodegradable sources is economically expensive. In order to make the process cheaper carbohydrate rich, starch or cellulose containing solid wastes and food industry wastewaters could be used as substrates (Kapdan and Kargi, 2006).

There are several advantages for hydrogen production by fermentative bacteria. Several carbon sources could be used as substrate, all day production could be possible since fermentation does not need light and valuable products such as acetic acid and lactic are produced as by-products. The major drawback of dark

fermentation is the relatively lower yields of H₂ production. When the hydrogen production yield increases the reaction becomes thermodynamically unfavorable (Nath and Das, 2004).

1.2.3 Photofermentation

Purple sulphur and purple non-sulphur bacteria perform anoxygenic photosynthesis and produce hydrogen as a by product in the presence of light. Hydrogen production by photosynthetic bacteria is mediated by nitrogenase activity, although hydrogenases may be active for both hydrogen production and hydrogen uptake under some conditions (Miyamoto, 1997).

Purple sulphur bacteria use reduced sulphur compounds such as sulphide, thiosulphide and elementary sulphur as electron donors. *Halorhodospira halophila* is a purple sulphur photosynthetic bacterium which produces hydrogen during photoautotrophic growth. The hydrogen production reaction in this species is catalysed by nitrogenase enzyme (Tsuihiji et al, 2006).

Kovacs et al. (2006) studied hydrogen production by a phototrophic purple sulphur bacterium, *Thiocapsa roseopersicina* and showed that *T. roseopersicina* has the capability to produce hydrogen in vivo both by its nitrogenase enzyme and using the Hox hydrogenase enzyme.

Purple non-sulphur (PNS) bacteria produce hydrogen and CO₂ by utilizing volatile organic acids such as acetate, lactate and glutamate by using light energy under anaerobic conditions. The reaction and the scheme of photofermentative hydrogen production are shown below (Reaction 1.6 and Figure 1.5). The detailed characteristics and hydrogen production mechanism of PNS bacteria will be discussed later.

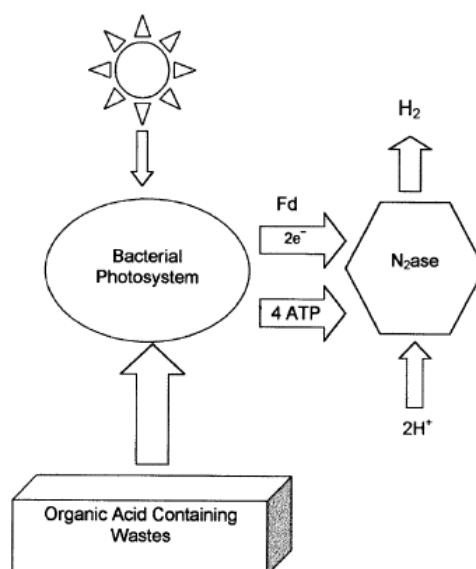


Figure 1.5 The scheme of photofermentative hydrogen production (Hallenbeck and Benemann, 2002)

Phototrophic bacteria are indicated in the current literature as the most promising microbial system for the biological production of hydrogen (Das and Veziroğlu, 2001; Basak and Das, 2007). The main advantages are listed as follows:

- High substrate to product conversion yield,
- Lack of oxygen-evolving activity, which is desirable for biohydrogen production,
- Ability to use a wide wavelength of light,
- Capability to use organic substrates (derived from wastes) for hydrogen generation that also helps in the bioremediation process.

1.2.4 Integrated Systems:

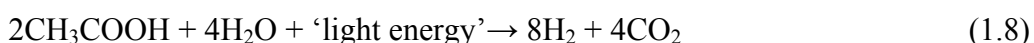
The microbial production of hydrogen can be enhanced by an integrated system which is the combination of dark fermentation and photofermentation. The first step of this sequential process is the conversion of organic substrates to low molecular weight organic acids by dark fermentation. Then these organic acids are used as a substrate for photofermentation.

For economical applications a yield of 8 mol H₂/mol glucose is considered sufficient whereas no single organism is capable of performing the conversion with this efficiency (Redwood and Macaskie, 2006). Combination of dark fermentation and photofermentation results in a theoretical maximum yield of 12 mol H₂/mol glucose as shown in the equations below (Kotay and Das, 2007).

Dark fermentation;



Photofermentation;



Integrated System;



Tao et al. (2007) found 3.67 mmolH₂/mmol sucrose hydrogen production by dark fermentation. When the fatty acids produced in dark fermentation were subsequently converted to H₂ by photofermentation by *Rhodobacter sphaeroides* SH2C total hydrogen production was increased to 6.63 mmol H₂/mmol sucrose. In another study Chen et al. (2008) found hydrogen yield of 3.80 mol H₂/mol sucrose in dark

fermentation by *Clostridium pasteurianum* CH₄ to increase to 10.2 mol H₂/mol sucrose with integrated system of dark fermentation and photofermentation by use of *Rhodospseudomonas palustris* WP3-5. Su et al. (2009) studied the optimization of hydrogen production from glucose by two-stage system using *Clostridium butyricum* as dark fermentative bacteria and *Rhodospseudomonas palustris* as photofermentative bacteria. Results showed that hydrogen yield increased from 1.59 mol H₂/mol glucose in dark fermentation to 5.48 mol H₂/mol glucose in the two stage process. These studies show that integrated biohydrogen production processes increase hydrogen production significantly.

1.3 HYVOLUTION Project:

Non-thermal production of pure hydrogen from biomass is an EU 6th framework integrated project, HYVOLUTION. Figure 1.6 demonstrates the overall scheme of HYVOLUTION project.

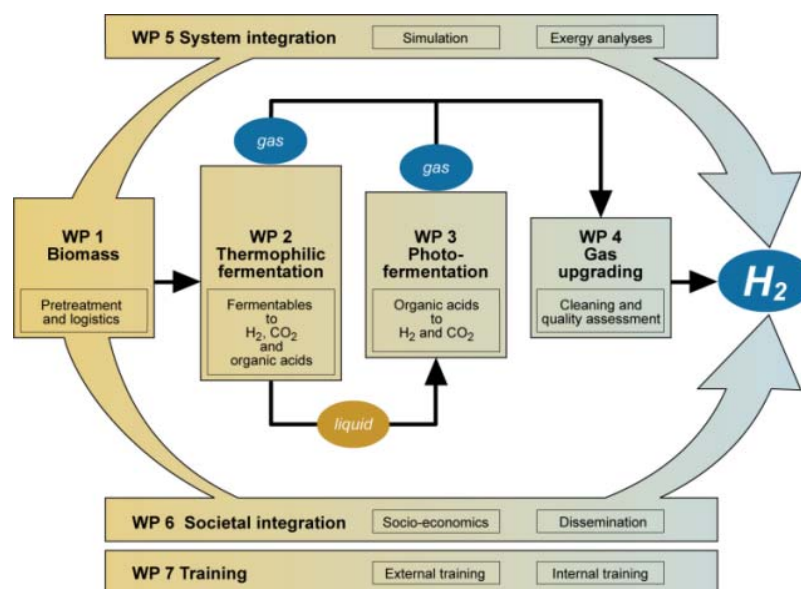


Figure 1.6- The overall scheme of HYVOLUTION project (<http://www.biohydrogen.nl>, <http://www.biohydrogen.nl/hyvolution/24172/5/0/20>, Last access date: June 10, 2010)

The main objective of this project is to develop a two stage bioprocess for the cost-effective production of pure hydrogen from multiple biomass feedstocks (Claassen and Vrije, 2006). The first stage of the bioprocess is the thermophilic fermentation of different feed stocks such as molasses, potato steam peel and thick juice to H₂, CO₂ and organic acids. In the second stage the dark fermenter effluents are converted to H₂ and CO₂ by photofermentation.

METU Biohydrogen group is a member of the project and the coordinator of a work package (WP3) which is the photofermentation part. The main aim of this work package is to investigate the optimization of photofermentative hydrogen production from organic acids with high yields and to construct a prototype photobioreactor.

1.4 General Characteristics of Purple Non-Sulphur Bacteria

The purple non-sulphur (PNS) bacteria are aquatic gram negative organisms. They are found in a wide variety of environments like freshwater, marine habitats and in the soil. The cells are ovoid to rod shaped and motile or nonmotile. They divide by binary fission and have vesicular photosynthetic membranes (Imhoff et al., 1984).

They can grow by several metabolic growth modes such as photoheterotropic growth, photoautotropic growth and chemotropic growth. These growth modes can be switched from one mode to another depending on the physiological conditions such as carbon sources and light intensity. The availability of carbon source determines the growth mode. If the media contains CO₂ as carbon source bacteria grows autotrophically. If the C source is organic acids they grow heterotrophically. Also the availability of a light source affects growth mode. They need light for phototropic growth (Basak and Das, 2007).

PNS bacteria have only a single photosystem which is in the intracellular membrane. This photosystem does not have enough power to split water. Because of the lack of photosystem II they can carry anoxygenic photosynthesis. Photoheterotropic growth

mode is the preferable mode for biological hydrogen production. For phototropic growth they need one or more water soluble vitamins. They can live in both dark and light conditions. The growth can occur in the pH range of 6-9 and the optimum temperature for growth is between 25 and 35°C (Sasikala et al., 1991)

The term “non-sulphur” is used because PNS bacteria were considered not to use hydrogen sulphide as an electron donor while growing photoautotrophically. However, PNS bacteria can use sulphide as an electron donor but not at high concentrations like sulphur bacteria. The PNS bacteria exhibits a yellowish brown to greenish and deep brown colour when grown anaerobically in the presence of light but turn red in the presence of oxygen; carotenoids are converted to corresponding ketocarotenoids that cause the red colour change (Pellerin and Gest, 1983).

Rhodobacter capsulatus is a gram negative PNS bacterium and belongs to α subdivision of Protobacteria. The taxonomy of *Rb. capsulatus* is shown in Table 1.1

Table 1.1 The taxonomy of *Rb. capsulatus*

Super Kingdom	Prokaryota
Kingdom	Monera
Sub Kingdom	Eubacteria
Phylum	Gracilicutes
Class	Photosynthetic eubacteria
Order	Rhodospirillates
Family	Rhodospirillaceae
Genus	Rhodobacter
Species	capsulatus

Rb. capsulatus has a rod shaped cell with a diameter of 0.5-1.2 μm and divides by binary fission producing capsules and slime (Imhoff et al., 1995). The microscopic picture of *Rb. capsulatus* bacterium is shown in Figure 1.7

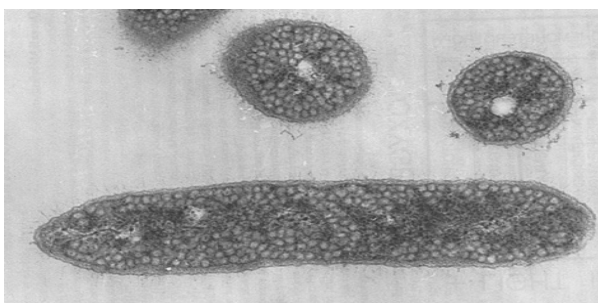


Figure 1.7 The microscopic picture of *Rb. capsulatus*

(<http://ecoserver.imbb.forth.gr>, http://ecoserver.imbb.forth.gr/microbiology/IMAGES/Rhodobacter_capsulatus.jpg, Last access date: June 10, 2010)

1.5 Hydrogen Production Metabolism

Rb. capsulatus and other PNS bacteria produce hydrogen by breaking down organic acids such as acetate, lactate and malate under anaerobic conditions and illumination. They use light as primary energy source and organic acids as carbon source. Hydrogen production reaction is catalysed by nitrogenase enzyme and this reaction occurs in the absence of molecular nitrogen.

Mainly, the mechanism of photofermentative hydrogen generation is a membrane bound electron transfer process (Basak and Das, 2007). In hydrogen production metabolism, the organic acids are oxidized in TCA (Tricarboxylic acid or Citric acid) cycle. The products of this oxidation are CO_2 , protons and electrons. A simplified overall scheme of the carbon metabolism in PNS bacteria is shown Figure 1.8.

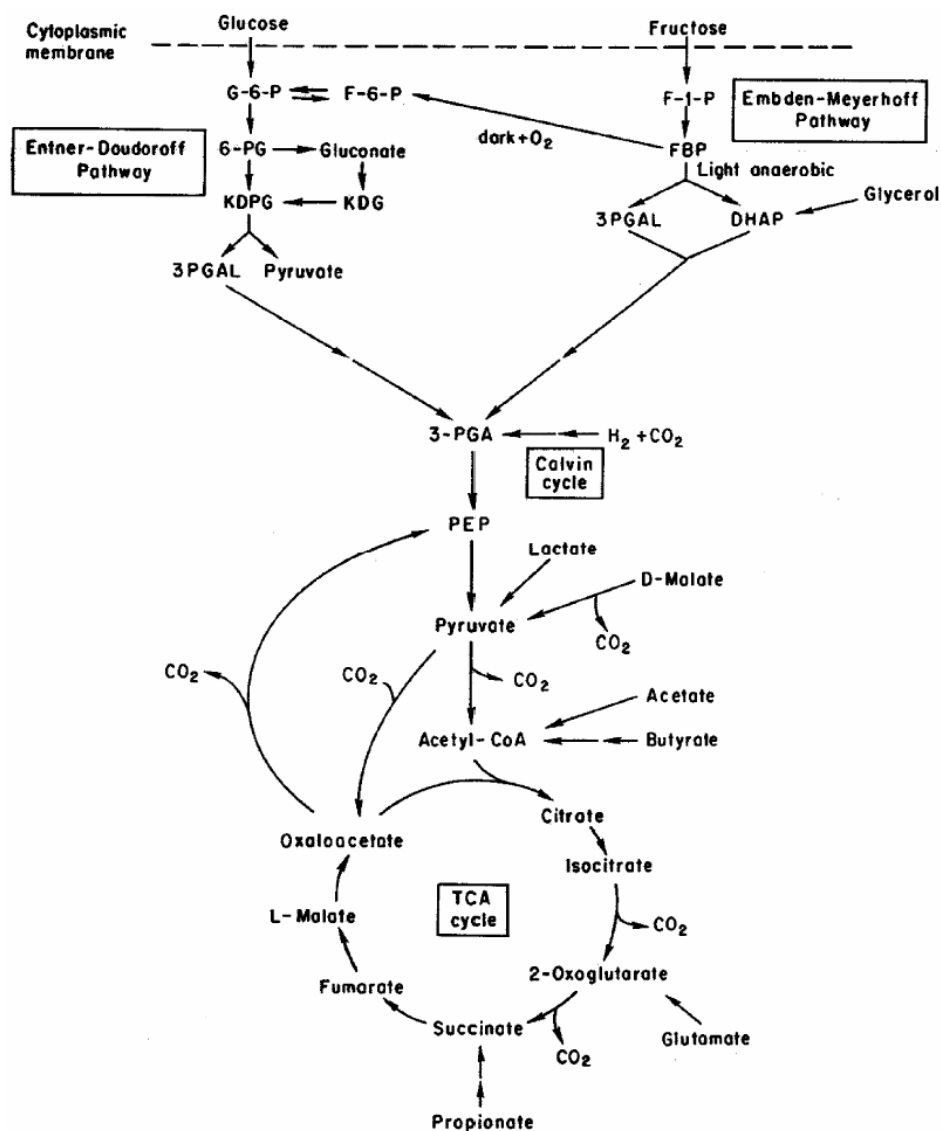


Figure 1.8 A simplified overall scheme of the carbon metabolism in PNS bacteria (Koku et al., 2002)

The electrons and protons which are released from TCA cycle are directly channelled to nitrogenase enzyme. The transfer of electrons from TCA cycle to nitrogenase enzyme is provided by a sequential oxidation and reduction reactions of electron carriers which are NAD (nicotinamide adenine dinucleotide) and Fd (ferredoxin) (Koku et al., 2002). The hypothesized electron path is:

Substrate → TCA-cycle → NAD=NADH → (Fd) ox= (Fd) red → Nitrogenase (1.10)

The ATP which is converted by photosynthetic membrane apparatus from light energy is also directed to nitrogenase enzyme. The protons are supplied in part by the TCA cycle. The remaining protons are supplied by the action of ATP-synthase. This enzyme works as a part of the photosynthetic apparatus. Finally, nitrogenase enzyme produces molecular hydrogen by reducing protons (Sasikala et al., 1990). Hydrogenase enzyme acts as an uptake enzyme which consumes the produced hydrogen. Therefore, the net collected hydrogen amount is the amount produced by nitrogenase minus the amount consumed by uptake hydrogenase (Vignais et al., 1985). In this metabolism some by-products such as Poly-β-hydroxy butyric acid (PHB) and caretenoids are also produced. The overall scheme of hydrogen production by PNS bacteria is shown in Figure 1.9.

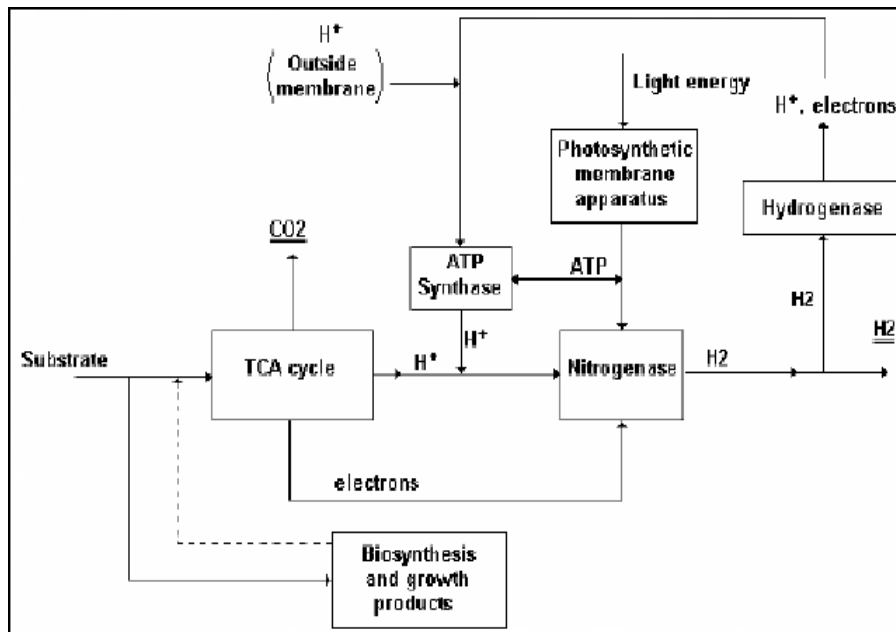


Figure 1.9 The overall scheme of hydrogen production by PNS bacteria (Koku et al., 2002)

1.6 Enzymes in Hydrogen Production:

Hydrogen Production metabolism by *Rb. capsulatus* involves two enzymes, hydrogenase and nitrogenase.

1.6.1 Hydrogenase Enzyme:

Hydrogenase enzymes catalyze oxidation of molecular hydrogen by the reversible reaction given below.

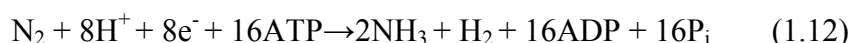


In presence of molecular hydrogen and an electron acceptor it will catalyse the consumption of hydrogen. In presence of an electron donor of low potential it may use protons as electron acceptors and release H₂. In *Rb. capsulatus* hydrogenase enzyme is membrane bound and mainly function as an H₂ uptake (consumption) enzyme (Uyar, 2008).

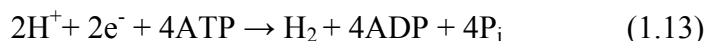
Presence of uptake hydrogenase enzyme decreases the overall yield of hydrogen since it consumes part of produced hydrogen. In order to overcome this problem, hydrogenase enzyme may be inactivated or deleted. Kars et al. (2008) developed a hup⁻ mutant strain of *Rb. sphaeroides* O.U.001 for improving the hydrogen production capacity of the cells. They inactivated the uptake hydrogenase enzyme by site directed mutagenesis. The results showed that the produced hydrogen with hup⁻ mutant strain was 20% higher than the wild type strain. In another study uptake hydrogenase enzyme of *Rb. capsulatus* MT1131 was deleted through interposon mutagenesis which developed a hup⁻ mutant strain (YO3). The results with YO3 mutant showed that total produced hydrogen, hydrogen production rate and substrate conversion efficiency were higher than those with wild type *Rb. capsulatus* MT1131 strain (Öztürk et al., 2006).

1.6.2 Nitrogenase Enzyme

Hydrogen production by PNS bacteria takes place mainly by nitrogenase enzyme. Nitrogenase enzyme complex is responsible for nitrogen fixation. When molecular nitrogen is available nitrogenase enzyme is responsible for the reduction of dinitrogen to ammonia. The nitrogen fixation reaction is shown below at equation 1.12.



Under anaerobic conditions and in absence of molecular nitrogen, nitrogenase enzyme catalyzes the following molecular hydrogen formation reaction.



The nitrogenase complex consists of two components which are dinitrogenase reductase (Fe protein) and dinitrogenase (MoFe protein). The subunits of nitrogenase are encoded by *nif* HDK operon. Nitrogenase reductase component has two subunits which are encoded by *nif* H gene and dinitrogenase subunits are encoded by *nif* D and *nif* K genes. *nif* A is the transcriptional activator of *nif* HDK operon (Henson et al, 2004).

Oxygen is known to decrease nitrogenase enzyme activity (Akköse, 2008; Hockman and Burris, 1981; Fu and Burris, 1989) and to repress synthesis of nitrogenase component proteins (Fay, 1992; Akköse, 2008). Akköse et al. (2009), in a study conducted with *Rb. sphaeroides* O.U.001, found that hydrogen produced under anaerobic conditions is 3 times as higher than under aerobic conditions. Hockman and Burris (1981) studied the effect of dissolved oxygen concentration on nitrogenase activity in three different photosynthetic bacteria and found that O₂ inhibited the enzyme activity by 50%; oxygen concentrations resulting in this decrease were different for different strains. They also demonstrated that the

inhibition of nitrogenase activity is usually reversible in *Rb. capsulatus* and when the anaerobic conditions are reestablished nitrogenase activity is restored.

High ammonium concentrations also repress nitrogenase activity (Pierrard et al, 1993; Fu and Burris, 1989) and expression of nitrogen fixation genes at different regulatory levels. (Pashen et al., 2001) Akköse et al. (2009) studied the different ammonium chloride concentrations for photofermentation with *Rb. sphaeroides* O.U. 001 and found that cumulative hydrogen production and hydrogen production rate decreased with increasing ammonium concentration. They also found that there was no hydrogen production at NH_4Cl concentrations higher than 2 mM. Waligórska et al. (2009) studied kinetic modeling by *Rb. sphaeroides* in the presence of NH_4^+ ions. The results of this study showed that higher hydrogen production and rate were observed with low ammonium ion concentrations.

1.7 By-Products of Biohydrogen Production

Simultaneous production of by-products occurs in the metabolism of PNS bacteria as seen in the overall scheme of hydrogen production (Figure 1.9). Biomass may be considered a by product. PHB and carotenoid are two other valuable by-products produced by the photosynthetic bacteria (Uyar, 2008).

PHB (Poly- β -hydroxy butyric acid) is a biodegradable thermoplastic that can be synthesized during unfavorable growth conditions, especially under stress, as a storage material. PHB is accumulated under conditions of excess carbon sources when growth is limited by deficiency of nitrogen, sulphur or phosphorus sources (Hustede et al., 1993). Hydrogen production and PHB accumulation are competing processes. In a study which was conducted by wild type and *phb⁻* mutant strains of *Rb. sphaeroides* KD131 maximum hydrogen production with the mutant strain was 1.3 fold higher compared with the wild type strain (Kim et al., 2006).

Carbon source, nitrogen availability and pH of the medium are some factors that affect the PHB accumulation inside the cells of photosynthetic bacteria (Rocha et al., 2001). Khatipov et al. (1998) studied the accumulation of PHB on various carbon (lactate, acetate, pyruvate and glucose) and nitrogen (ammonium and glutamate) sources with *Rb. sphaeroides* RV. They found that acetate containing media were most advantageous for PHB accumulation and indicated that ammonium must be present for high amount of PHB accumulation. They also found that higher PHB content was achieved by increasing the initial pH. Hustede et al. (1993) investigated the competition between PHB accumulation and hydrogen production with two wild type photosynthetic bacteria and their PHB deficient strains in different carbon sources. They found a competitive effect only with acetate as organic carbon compound. Waligórska et al. (2009) found carbon to nitrogen ratio to affect the PHB accumulation. They found that increasing C/N ratio from 6 to 120 increased PHB accumulation by a factor of 30.

1.8 Factors Affecting Hydrogen Production

There are different factors which affect hydrogen production by PNS bacteria. Carbon and nitrogen sources, C/N ratio, pH, light intensity and temperature are some factors that effect hydrogen production. These environmental factors may also affect the regulation of nitrogenase enzyme (Akköse, 2008).

The optimum pH values for growth and hydrogen production was studied by Sasikala et al. (1991) with *Rb. sphaeroides* O.U.001. The results showed that growth was observed at a pH range of 6-9 while optimum biomass was observed at 6.8-7.0 pH value. They found that the optimum value for hydrogen production is at pH 7.0. The effects of temperature and light intensity on hydrogen production were examined in this study. Some of the other studies related to effects of temperature and light intensity on hydrogen production are summarized below.

1.8.1 The Effect of Temperature on Hydrogen Production

Since photofermentation process is an enzymatic process hydrogen production by PNS bacteria is strongly affected by temperature. There are few studies in which the effect of temperature on photofermentation by PNS bacteria has been investigated.

Sasikala et al. (1991) studied the effect of temperature on growth and hydrogen production by *Rb. sphaeroides* O.U. 001 strain. They used malate as carbon source and light intensity was 4000 lux. They found that there was no growth taking place below 20°C and above 45°C and the optimum biomass yield was obtained between the temperatures of 30-35°C. For hydrogen production experiments the optimum temperature range was reported as 30°C-40°C.

Uyar (2008) studied growth and hydrogen production at 5 different temperatures, 31, 34, 37, 42 and 48°C, by *Rb. sphaeroides* O.U.001. The results showed that there was growth and hydrogen production at 31, 34 and 37°C whereas there was no growth and production of hydrogen at 42 and 48°C.

He et al. (2006) studied the effect of temperature on growth and hydrogen production by two mutant strains of *Rb. capsulatus* on 30 mM lactate and 5 mM glutamate at 26, 30 and 34°C. The increase in temperature resulted in faster growth rate for both strains. They observed the maximum dry cell weights at 34°C. They found the maxima of hydrogen production rate, substrate conversion efficiency and the yield at 30°C.

In a study (Stevens et al., 1984) six strains of *Rb. capsulatus* were tested on acetate and glutamate for their ability to produce hydrogen at 20, 25, 30 and 35°C. They found that three of the tested strains (B100, ST410 and ST 407) showed better acetate conversion efficiencies at 20°C compared to other temperatures. The optimal temperature was 30°C for two of the tested strains (ATCC 23782 and ATCC 17013) and was 35°C for the last strain (DSM 152). They also found that the total hydrogen

production time at the higher temperature was shorter in comparison to the lower temperatures.

Ünlü et al. (2009) studied the expression analyses of *nif* A and *nif* H genes of *Rb. sphaeroides* O.U.001 at different temperatures. They grew the bacteria at 20, 30 and 38°C in separate incubators under continuous illumination of 3000 lux. They found that the highest expression levels of both *nif* H and *nif* A genes were obtained at 30°C. They found that the expression level of *nif* H decreased significantly at 20 and 38°C; the decrease in *nif* A expression was not significant at the same confidence level.

Özgür et al. (2010) studied hydrogen production of *Rb. capsulatus* DSM 1710 in both indoor and outdoor conditions on acetate and glutamate at 200 W/m². The results showed that there was a significant decrease in substrate conversion efficiency, yield and the hydrogen production rate at fluctuating temperatures (between 15-40°C) compared to those at constant temperature of 30°C. In outdoor experiments under sunlight they examined hydrogen production by *Rb. capsulatus* YO3 mutant strain keeping the reactor temperatures below 30, 33, 35 and 40°C. The highest productivity and yield were observed when the temperature of the reactor was kept below 33°C.

1.8.2 The Effect of Light Intensity on Hydrogen Production:

Light intensity is one of the most important factors that affect hydrogen production by PNS bacteria. As mentioned before hydrogen production by PNS bacteria is mediated by nitrogenase enzyme and the required energy for hydrogen production is provided by the conversion of light energy to ATP by photosynthetic membrane apparatus. Nitrogenase synthesis, which affects hydrogen production, is strongly stimulated by light (Koku et al., 2002). Because of these reasons the light intensity to which the cells are exposed is a very important factor for hydrogen production.

Sasikala et al. (1991) studied the effect of light intensity on growth and hydrogen production by *Rb. sphaeroides* O.U. 001. They found that increasing light intensity has no effect on final biomass but it affects the growth rate of *Rb. sphaeroides* O.U. 001. They also stated that growth was better under continuous light compared to light dark cycle. They represented that increasing light intensity has an effect on produced hydrogen amount. They found that photoproduction of hydrogen increased with increasing light intensity up to 5000 lux. Saturation was observed after this light intensity and there was no photoinhibition.

Uyar et al. (2007) also studied the effect of light intensity on hydrogen production by *Rb. sphaeroides* O.U. 001 in malate/glutamate containing medium. They found that hydrogen production rate increased with increase in light intensity up to 4000 lux (270 W/m²) and increasing the light intensity after 4000 lux did not change the rate and there was no inhibition.

Although there was no photoinhibition in the studies of Sasikala et al. (1991) and Uyar et al. (2007) photoinhibition was observed in a study with *Rb. sphaeroides* O.U.001 in acetate/glutamate containing medium by Akköse (2008) who found total hydrogen production at 6500 lux to be half of that at 3500 lux light intensity.

Kim et al. (2006) studied the effects of light intensity on both growth and hydrogen production with *Rb. sphaeroides* KD131. Hydrogen production and pH were found first to increase and then decrease with increasing light intensity. They compared the growth and hydrogen production of *Rb. sphaeroides* KD131 with different mutants. Their results showed highest hydrogen production with the strain for which the growth was lowest and lowest hydrogen production with the strain growth was highest.

Obeid et al. (2009) studied the effect of light intensity on growth and hydrogen production on *Rb. capsulatus* IR3 strain at 30°C. They studied the effect of light intensity in the range of 6000 to 50000 lux (Na-vapor lamp- 600W) on lactate and

glutamate. They found that when the light intensity increased from 6000 to 50000 lux the final protein concentration increased by 30%. This increase was correlated with biomass concentration. They also found that hydrogen conversion yield increased with increasing light intensity up to 25000 lux. The yield was stabilized above this light intensity. They modelled the growth data with Monod's model and hydrogen production data with Baly's model. They found that hydrogen production rate at 50000 lux light intensity was 6 fold higher than that at 6000 lux.

Nath and Das (2009) studied the effect of different light intensities of 3.75; 7.5; 10.5 and 15 W/m² (2500 lux=3.75 W/m²) on growth and hydrogen production of *Rb. sphaeroides* O.U. 001. They found that cells reached a higher biomass concentration when they grew under higher illumination. They also found that hydrogen production amount and rate increased with increasing light intensity. Light conversion efficiency was found to decrease with increase in light intensity. The total amount of hydrogen produced was increased from 0.0348 mmol/L to 0.0553 mmol/L when light intensity was increased from 3.75 W/m² to 15 W/m². However same increase in light intensity decreased light conversion efficiency from 0.51 % to 0.19 %.

The effect of illumination on growth and hydrogen production by *Rb. sphaeroides* ZX-5 was investigated at both standing and shaking cultures by Li et al. (2009). The light intensity range used was 2000 to 9000 lux. They found at 30°C that final optical density (OD₆₆₀) value decreased from 1.91 to 1.56 with increasing light intensity. They found that substrate conversion efficiency and volumetric hydrogen production values increased with increase in light intensity in the 2000 to 5000 lux range. After 5000 lux the values decreased slightly. However, hydrogen production rate was found to increase consistently with increasing light intensity.

1.9. Aim of This Study:

The ultimate goal for biological hydrogen production is production of hydrogen on industrial scale. It is important to determine the optimum conditions for such a production. Photofermentative hydrogen production is affected by temperature and light intensity and several studies have been undertaken on the effects of light intensity and temperature on hydrogen production as mentioned above. These studies have primarily concentrated on the effect of light intensity at a constant (or a narrow range of) temperature or on the effect of temperature at a constant (or narrow range of) light intensity. Further, light sources, media, carbon sources, strains, reactors used in these studies were also different. This study was undertaken with the objective of gathering data on the effects of both temperature and light intensity within wide ranges on hydrogen production by *Rb .capsulatus*. Such data should be useful to understand the relationship between temperature and light intensity conditions and quantities like bacterial growth, hydrogen production, pH, substrate concentrations (learning models) and to develop phenomenological model equations and to predict how these quantities will be affected by changing temperature and light intensity conditions (predictive model). There may be systems where it may not be practical to control the medium temperature in industrial scale hydrogen production. It should therefore be important to determine the effect of ambient temperature (outdoor temperature under outdoor conditions and incubator temperature under indoor conditions) on hydrogen production. Incubator temperature was controlled in the present study and medium temperature was measured.

CHAPTER 2

MATERIALS AND METHODS

2.1 The Microorganisms

Rhodobacter capsulatus strain (DSM 1710) was obtained from Deutsche Sammlung von Mikroorganismen (DSM, Braunschweig Germany).

2.2 Culture Media

2.2.1 Media Preparation

Some modifications were done on minimal Biebl and Pfennig (1981) medium. Acetate and lactate were added as carbon source and glutamate was added as nitrogen source to Biebl and Pfennig medium. Vitamins, trace elements and iron-citrate were added to media. The compositions of the growth medium, vitamins, trace elements and iron-citrate are given in Appendix A.

2.2.2 Liquid Media

2.2.2.1 Growth Media

Acetate (20 mM), lactate (7.5 mM) and glutamate (10 mM) were added to minimal Biebl and Pfennig medium. The elements of medium were dissolved in distilled water and pH was adjusted to 6.3-6.4. The sterilization of medium, trace elements and iron-citrate was done by autoclaving. Vitamin solution (Biotin, Thiamin and Niacin) sterilization was done by filtration using 0.2 μm sterile filters since high temperatures may cause the degradation.

2.2.2.2 Hydrogen Production Media

The composition and preparation of hydrogen production media was similar with growth media except for amounts of carbon and nitrogen sources. In hydrogen production media, acetate (40mM), lactate (7.5 mM) and glutamate (2 mM) was added to minimal Biebl and Pfennig medium.

2.2.3 Solid Media

The solid media was used for activation of stock bacteria. The composition of solid media was the same with liquid media. In order to make the media solid, agar (1.5%) was used. In preparation of solid media agar was dissolved in growth medium before autoclaving. After sterilization the media was poured into sterile plates. The inoculation of stock bacteria was done after solidification of the agar media.

2.3 Experimental Setup for Hydrogen Production

Experiments were carried out in 55 ml glass bottles (photobioreactors). The bottles were filled with a mixture of 45 ml media and 5 ml culture. The bottles were sealed with rubber tap. The sterilization of bottles and rubber tap were done by autoclaving. In order to keep the temperature constant all photobioreactors were kept in a cooling incubator (Nüve, ES250). Inner temperatures of photobioreactors were determined by a digital thermometer (Maxi-T). Illumination was provided by means of 75-100 W tungsten lamps. Light intensity measurements were done by luxmeter (Lutron LX-105 Light Meter). The conversion factor was determined as $1 \text{ W/m}^2 = 17.5 \text{ lux}$ (Uyar, 2008) for indoor experiments. The selected temperatures and light intensities are shown in Table 2.1

Table 2.1 Temperatures and light intensities used in the experiments

Light Intensity (lux)	Light Intensity (W/m ²)	Incubator Temperature (°C)
1500	85	20
		30
		38
2000	114	20
		30
		38
3000	171	20
		30
		38
4000	228	20
		30
		38
5000	285	20
		30
		38
6000	342	20
		30
7000	400	20
		30

The amount of the evolved gas was determined volumetrically. Gas collection tubes were filled with distilled water and the tubes were sealed with rubber taps. The outer surface of the rubber top was covered with parafilm to prevent the flow of air into the tubes. The photobioreactors and the gas collection tubes were connected by plastic pipes which had needles at both ends. Evolved gas was accumulated in the gas collection tubes by replacing with water. The schematic diagram and the photograph of the experimental setup are shown in Figure 2.1 and 2.2, respectively.

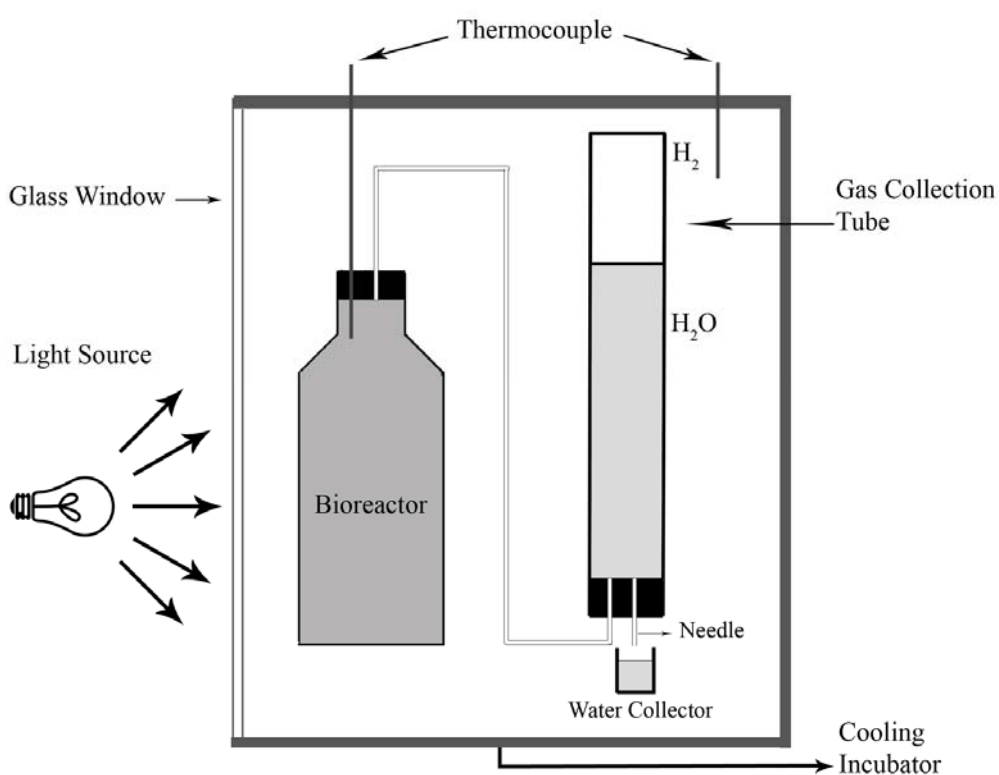


Figure 2.1- The schematic diagram of experimental set up



Figure 2.2- The photograph of the experimental set up for hydrogen production experiments

2.4 Experimental Procedure

For hydrogen production experiments bacterial inoculum was prepared. Stock bacteria which is in at 30% glycerol and stored at -80°C had to be activated. Stock bacteria were inoculated to plates which contained solid media in a sterile cabin. The agar plates were placed in an incubator (30°C) under the light intensity between 2000-2500 lux for cell growth. The growth of bacteria took approximately one week. A single colony was selected from the grown bacteria and inoculated to 1.5 ml sterile eppendorf tube which contains liquid growth medium. At the mid logarithmic phase (around OD_{660} 1.0) bacterial culture was scaled up to 50 ml by passaging. The bacteria was inoculated 10% (v/v) into the liquid growth media. The proliferation of bacteria up to mid logarithmic phase usually took 1-3 days.

Bacterial culture (5 ml) was injected to 45 ml liquid hydrogen production media with a sterile syringe. After inoculation, argon gas (>99 % purity) was flushed into the bottles for 5 minutes for replacement of the air and to make the environment

anaerobic. All these steps were carried out in sterile cabin to avoid the contamination.

2.5 Analyses

Liquid samples were taken from the photobioreactor periodically. Cell concentration, pH, gas composition and organic acid composition were analysed. Volume of hydrogen was calculated from the volume of gas and percentage of hydrogen in the gas. Millimoles of hydrogen, n , was calculated by use of the ideal gas law, $PV = nRT$, by taking P as 1 atmosphere, V as the volume of hydrogen (in milliliters), $R = 0.08205$ liter-atm/mole-°K and T as the incubator temperature in °K. Millimoles of hydrogen, n , was divided by the volume of the medium (0.05 liter) to find millimoles of hydrogen per liter of the medium (mmole/L).

2.5.1 Cell Concentration

The cell concentration measurements were performed by measuring optical density at specified wavelength. The absorbance of bacterial culture was determined by visible spectrophotometer (Shimadzu UV-1201) at 660 nm wavelength. Fresh medium was used as blank. The absorbance values were converted to dry cell weight values using the calibration curve (Uyar, 2008). The calibration curve of dry cell weight versus OD_{600} is shown in Appendix B

2.5.2 pH Analysis

pH measurements were performed by the aid of a pH meter (Mettler Toledo 3311) which was calibrated with standart solutions of 4.0, 7.0 and 9.21 pH before measurements.

2.5.3 Gas Composition Analysis

Gas samples were taken from the top of the gas collection tube. The composition of the evolved gas was analyzed by a Gas Chromatograph (GC), (Agilent Technologies 6890N). The column used in GC was Supelco Carboxen 1010. The Gas Chromatography device had a thermal conductivity detector. Argon was used as a carrier gas. The flow rate of argon was 26 mL/min. The temperatures of oven, injector and detector were 140 °C, 160 °C and 170 °C, respectively.

Before gas composition analysis, Gas Chromatography device was calibrated with pure H₂, air and CO₂. Gas samples (100 µL) were taken from gas collection tubes using a gas-tight syringe (Hamilton, 22 GA 500µL gas tight No. 1750). The software used in Gas Chromatography was Agilent Chemstation ver.B.01.01 (Agilent Technologies). A sample gas chromatogram is given in Appendix C.

2.5.4 Organic Acid Analysis

Samples taken from photobioreactors were centrifuged for 10 minutes at 13600 rpm to precipitate the bacteria. Supernatant was taken into a syringe and then filtered through 45µm nylon filters (Millipore, 13 mm) to remove impurities that may exist in the solution. Filtered liquid samples which contain organic acids were analysed by High Performance Liquid Chromatography (HPLC).

Two HPLC systems were used for analysis. One was Shimadzu 10A series and the other one was Shimadzu LC 20A- Prominence Series. The analyses were done by an Alltech IOA-1000 (300 mm x 7.8 mm) HPLC column. 20 µL samples were injected to the system with an autosampler (Shimadzu SIL-10AD) and the detection of organic acids was determined by an UV detector (Shimadzu FCV-10AT) at 210 nm. The oven temperature was kept at 66°C. As a mobile phase 0.085 M H₂SO₄ was used. Flow rate of mobile phase was adjusted to 0.4 ml/min.

In this study, the organic acids which were analysed are acetic acid, lactic acid, formic acid, propionic acid and butyric acid. For all organic acids calibration curves were constructed manually for different concentrations of pure organic acid standards. The determination of concentration of organic acids from peak areas which were recorded automatically were done by the calibration curves. A sample HPLC chromatogram and a sample calibration curve are given in Appendix D.

CHAPTER 3

RESULTS AND DISCUSSION

The main objective of this study was to investigate the effects of light intensity and temperature on hydrogen production by *Rb. capsulatus*, cell growth, changes in pH and consumption or production of organic acids. Quantities of biomass and hydrogen produced, pH and concentrations of acetic acid, lactic acid, formic acid, butyric acid and propionic acid were periodically determined as given in Section 3.5. Kinetic analyses of cell growth, hydrogen production and consumptions of organic acids were made by use of different models. The variables used were the light intensity and the temperature. The experiments were conducted at 20, 30 and 38°C incubator temperatures under different light intensities ranging between 1500 to 7000 lux.

3.1 The Medium Temperature Affected by Light Intensity

Experiments were made under 1500, 2000, 3000, 4000, 5000, 6000 and 7000 lux light intensities at incubator temperatures of 20, 30 and 38°C. Culture medium temperature was measured in each experiment by immersing a temperature probe into the reactor. The photobioreactors were kept in the incubator until the culture temperature reached a constant value. Culture medium temperatures determined for different light intensities, when incubator temperatures were set to 20, 30 and 38°C are given in Table 3.1

Table 3-1. The maximum photobioreactor temperatures measured under different light intensities at 20, 30 and 38°C incubator temperatures and change in temperature expressed as percentage of the incubator temperature

		20°C	% increase at 20°C	30°C	% increase at 30°C	38°C	% increase at 38°C
lux	1500	21	5	30	0	40	5
	2000	22	10	31	3	40	5
	3000	22	10	32	7	41	8
	4000	24	20	32	7	42	11
	5000	24	20	34	13	42	11
	6000	27	35	43	43	NA	NA
	7000	29	45	56	87	NA	NA

The results indicate that the actual culture temperature values are higher than the incubator temperatures for all light intensities. The difference between the culture temperature and the incubator temperature, ΔT , increase with light intensity for all incubator temperatures. ΔT values for 1500, 2000, 3000, 4000 and 5000 lux light intensities are smaller than those at higher light intensities and are close to each other. ΔT values for 6000 and 7000 lux light intensities are significant, however, and ΔT values for 30°C are significantly higher than those for 20°C incubator temperatures. No measurements were made at 38°C incubator temperature under 6000 and 7000 lux light intensities in view of the expected high ΔT values. Culture temperatures being higher than incubator temperatures should not be unexpected in view of the heating effect of light. It appears from the results that this is not the only factor and factors like cell concentration and changes and in the medium seem to affect ΔT . The heating effect of light has been very well demonstrated by Uyar (2008). He placed two photobioreactors of identical dimensions with one filled with distilled water and the other with bacteria of concentration of 0.6 gdw/l outdoor for 24 hours and recorded the air temperature and temperatures of the reactors continuously. He found temperature of the reactor containing distilled water to follow a pattern similar to air temperature but temperature of the reactor containing

bacteria followed a different pattern. He found temperature of the reactor containing distilled water reached more than 44°C under sunlight while the highest air temperature was 40°C. However, in the reactor containing the bacteria highest temperature was measured as 55°C. Based on his results, Uyar concluded that the difference is mainly due to heat generated by the bacteria. The difference between incubator and culture temperatures has not been reported in literature. Temperature values mentioned in all the following discussions mean the set incubator temperature. However it is worth to know that the actual culture temperatures may be different as indicated above.

3.2. The Effect of Light Intensity and Temperature on Cell Growth

Cell growth curves are known to consist of 4 phases; lag phase, exponential or logarithmic phase, stationary phase and death phase, as schematically shown in Figure 3.1. In the lag phase there is adaptation of bacteria to the environment with no cell division taking place. In this phase the cells increase their metabolic activities by synthesizing enzymes and proteins and prepare themselves to cell division. The duration of lag phase depends on physiological factors such as inoculum age, medium composition, temperature and light intensity. Cell doubling takes place in the exponential phase. The rate of cell division is constant in this phase and depends on the incubation conditions. The logarithm of cell numbers gives a straight line and the slope of this straight line is the specific growth rate of the organism. No cell growth takes place in the stationary phase due to the depletion of nutrients and essential metabolites and the cell concentration remains constant. Death phase starts after the stationary phase where the cell concentration decreases due to depletion of nutrients and other factors like formation of toxic or inhibitory by-products.

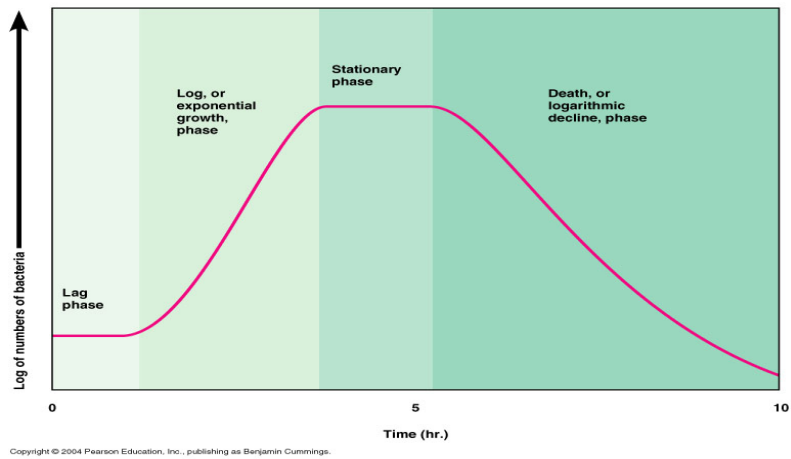


Figure 3.1 The schematic cell growth curve
 (<http://www.microscopesblog.com/2009/11/bacterial-growth.html>)

Cell growth data for 20, 30 and 38°C for different light intensities are given in graphical form in Figures 3.2, 3.3 and 3.4, respectively, where amount of biomass measured in gram dry weight per liter (gdw/L) are plotted against time measured in hours.

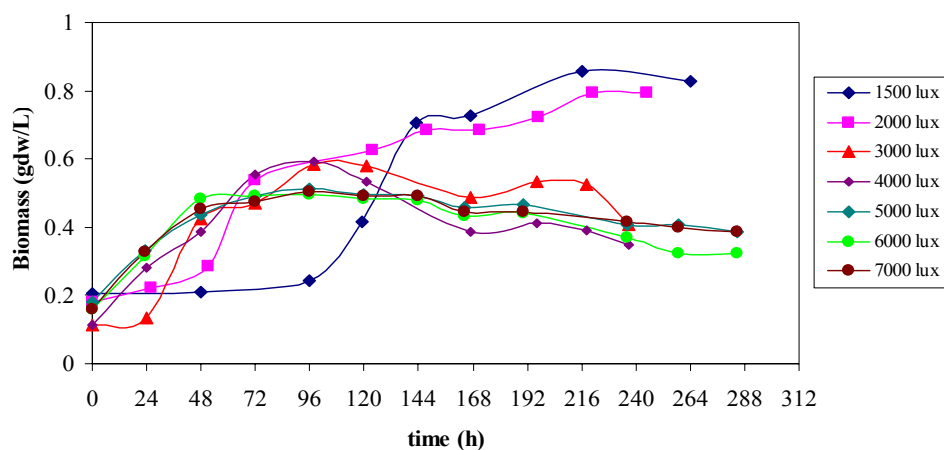


Figure 3.2- Cell growth for different light intensities at 20°C

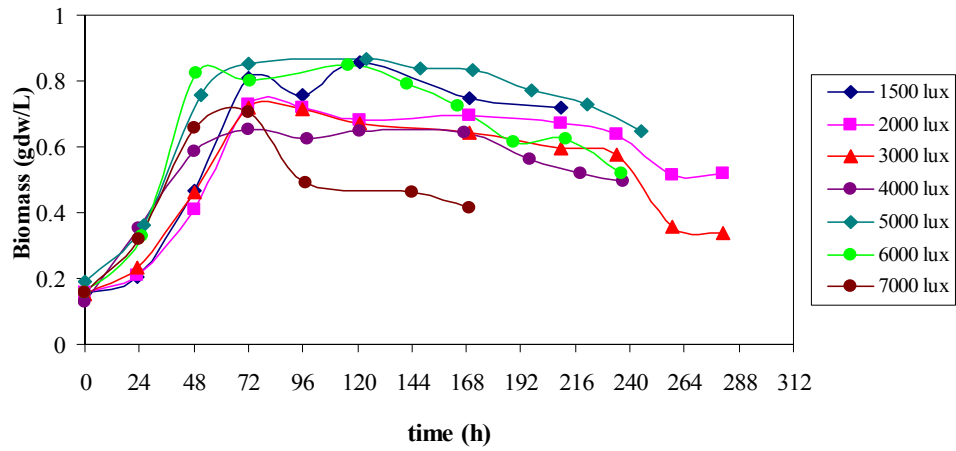


Figure 3.3- Cell growth for different light intensities at 30°C

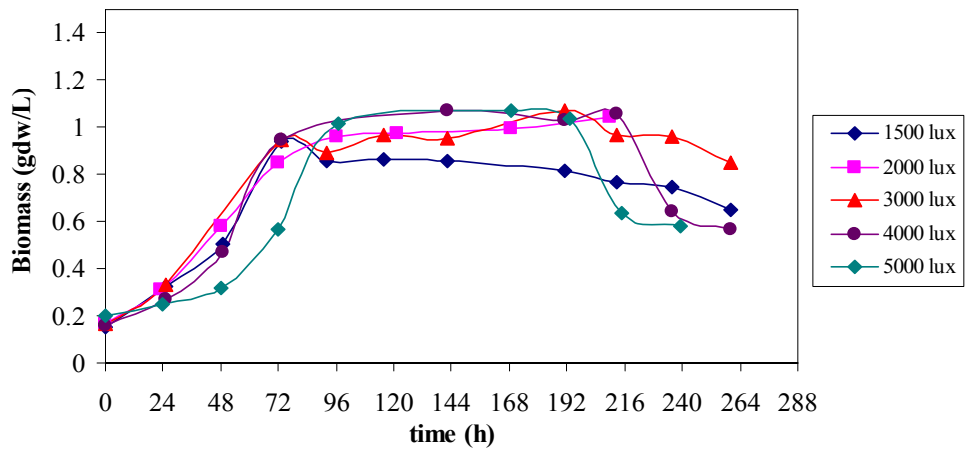
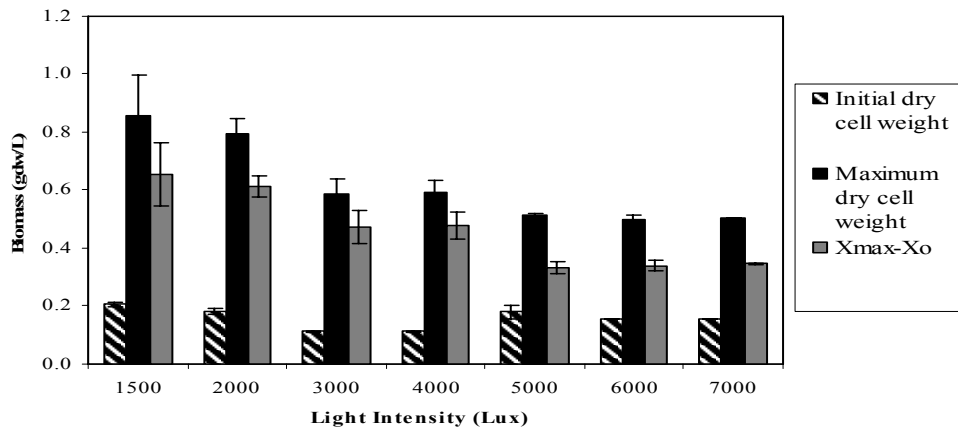
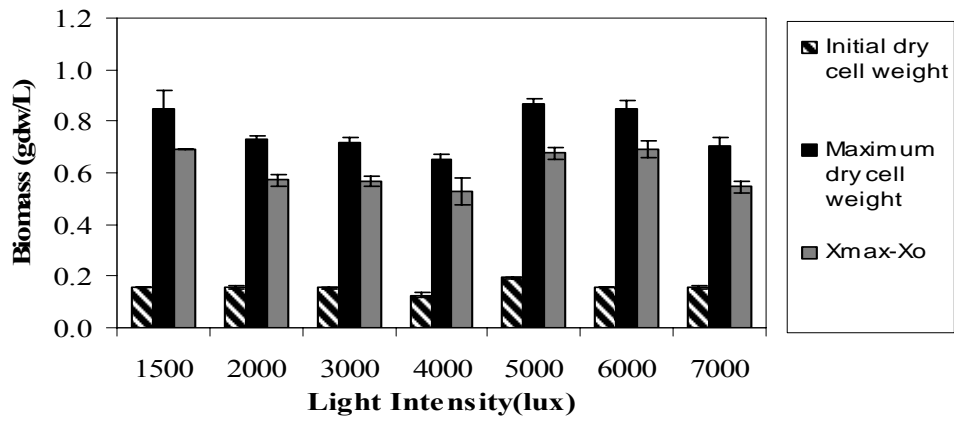


Figure 3.4- Cell growth for different light intensities at 38°C

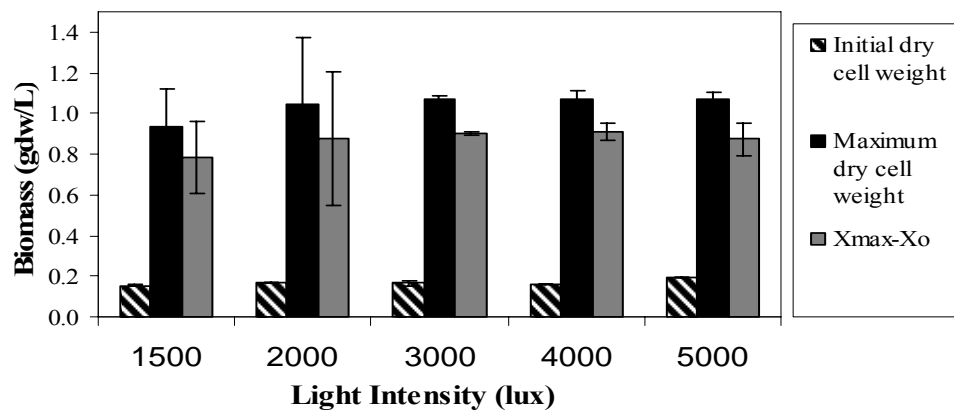
Initial and maximum cell concentrations and differences between the maximum cell concentrations and the initial cell concentrations for different light intensities at 20, 30 and 38°C are given graphically in Figures 3.5(a), 3.5(b) and 3.5(c), respectively.



(a)



(b)



(c)

Figure 3.5 Initial and maximum dry cell weights and their differences at (a) 20°C, (b) 30°C and (c) 38°C

As expected, in accord with the schematic curve shown in Figure 3.1, the results presented in Figures 3.2-3.4 show that the cell growth take place up to a certain time and cease beyond; quantity of biomass is seen to decrease with time for elongated times in some of the runs indicating death of cells. A lag period is seen in some of the conditions.

The cell growth results for 20°C shown in Figure 3.2 indicate presence of lag phases at 1500, 2000 and 3000 lux light intensities. The lag period seen to be 96 hours under 1500 lux light intensity decreases to less than 48 hours at 2000 lux light intensity and to 24 hours at 3000 lux light intensity. No lag phase is seen at 4000 lux and higher light intensities. These results indicate duration of lag phase to decrease with increase in light intensity.

The cell growth curves for 30°C in the early times for 1500, 2000 and 3000 lux light intensities are very close to each other in which after a lag phase of about 24 hours maximum biomass values are reached at about 72 hours when the stationary phase starts. No lag phase is observed to be present at 4000 lux and higher light intensities for 30°C incubator temperature similar to the case of 20°C. Eroğlu et al. (2008) found lag time at lower light intensity to be longer than that at higher light intensity.

Lag phase is not seen in the growth curves for 38°C shown in Figure 3.4 probably because of very short duration of the lag phase. Quantity of biomass is seen to change almost linearly with time for 1500, 2000 and 3000 lux. Cell growth is seen to be slow at 4000 lux light intensity and even slower at 5000 lux in the first 48 hours. However, the cell growth takes place faster after 48 hours.

As seen from the schematic growth curve in Figure 3.1 and the experimental growth curves in Figures 3.2 – 3.4, growth principally takes place in the exponential phase.

Rate of growth is expressed by the equation

$$\frac{dX}{dt} = \mu.X \quad (3.1)$$

in the exponential phase where X is the bacterial concentration, t is the time, and μ is the specific growth rate. Integrating this equation gives

$$X = X_0 .e^{-\mu.t} \quad (3.2)$$

Rearranging Equation (3.2) the experimental specific growth rate for a definite interval becomes:

$$\mu = \frac{\ln\left(\frac{X_2}{X_1}\right)}{(t_2 - t_1)} \quad (3.3)$$

Equation 3.3 is useful to analyze the effects of incubation conditions on rate of growth but only the exponential phase is considered here.

Growth is seen to take place with a very slow rate initially from the growth curves. Growth continues with a fast rate later and finally reaches an asymptotic value before the death phase. The shape of growth curve with the death phase excluded therefore resembles the letter S. Such curves are called sigmoidal curves. Mathematical models (equations) have been developed to analyze the variation of a quantity with time sigmoidally. Such equations which include the lag, the exponential and the stationary phases are useful to analyze growth systematically. One such model is the logistic model which has been developed by Verhulst (1838) as stated by Tsoularis and Wallace (2002) and Wachenheim et al. (2003) and used extensively to describe microbial growth in food and culture media. (Fujikawa, 2004, Gibson et al., 1987, Nath et al., 2008, Eroğlu et al., 2004, Uyar, 2008; Eroğlu et al., 2008, Androga,2009,

Koku et al., 2003). The cell growth of *Rb. sphaeroides* O.U. 001 (Uyar, 2008; Eroğlu, 2008, Nath et al., 2008) and *Rb. capsulatus* DSM 1710 (Androga, 2009) have been shown to fit to the logistic model in previous studies. Based on this, the logistic equation was used to model the growth in the present study.

The growth rate is expressed as:

$$\frac{dX}{dt} = k_c X \left(1 - \frac{X}{X_{\max}} \right) \quad (3.4)$$

in the logistic model where k_c is the apparent specific growth rate (h^{-1}), X is the dry cell weight (gdw/L) and X_{\max} is the maximum dry cell weight (gdw/L). Equation 3.4 differs from Equation 3.1 by the term $\left(1 - \frac{X}{X_{\max}} \right)$. The maximum dry cell weight has been called as the saturation point by Wachenheim et al. (2003) and as carrying capacity by Fujikawa et al. (2004). Wachenheim et al. (2003) stated that the saturation point could consist of many interacting factors, including nutrient availability, crowding, behavioral changes etc. The rate of growth increases due to X and decreases due to the term $\left(1 - \frac{X}{X_{\max}} \right)$ in Equation 3.4 as X increases. At very small X values the rate of growth is very small. As X approaches X_{\max} the term $\left(1 - \frac{X}{X_{\max}} \right)$ approaches zero and rate of growth approaches zero. Integrating Equation (3.4), Equation (3.5) is obtained:

$$X = \frac{X_{\max}}{\left[1 + \exp(-k_c \cdot t) \left(\frac{X_{\max}}{X_0} - 1 \right) \right]} \quad (3.5)$$

where X_0 is the initial bacterial concentration (g/L).

The experimental growth data presented in Figures (3.2) – (3.4), for times from 0 to the start of the death phase, were fitted to the logistic model using a program (Curve

Expert 1.3) for fitting curves. Curves fitted to the logistic model together with the experimental data for different light intensities for 20, 30 and 38°C are shown in Appendix E; the curve for 20°C and 2000 lux is given in Figure 3.6 as an example.

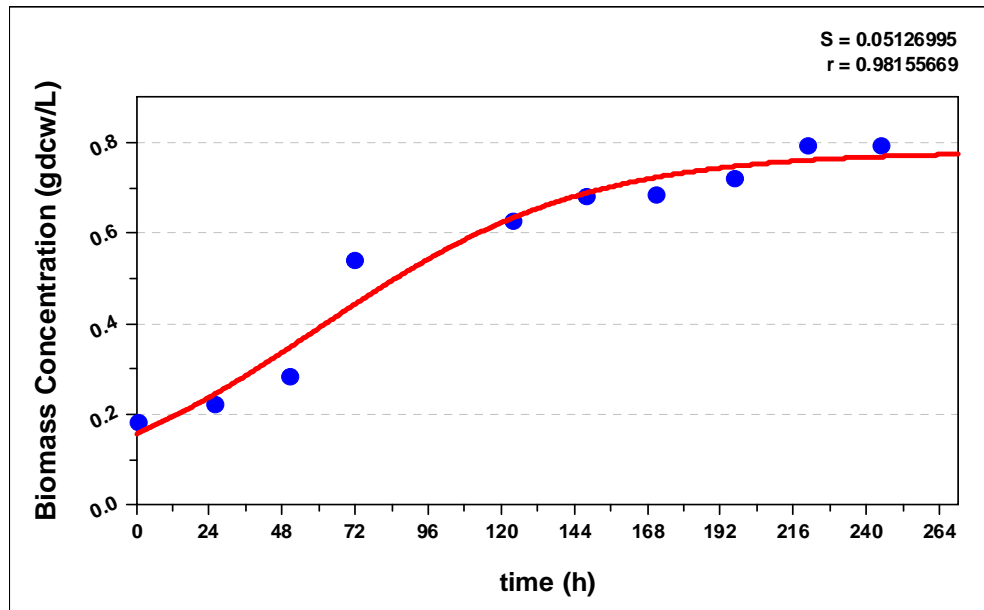


Figure 3.6 - The logistic growth model at 20°C and 2000 lux

Maximum values of the specific growth rate, μ_{max} , calculated by using Equation 3.3, initial and maximum experimental bacterial concentrations, $X_{0,e}$ and $X_{max,e}$, respectively, shown in Figure 3.5 are tabulated together with the initial bacterial concentration obtained by the logistic model, $X_{0,m}$, maximum bacterial concentration obtained by logistic model, $X_{max,m}$, specific growth rate constant obtained by logistic model, k_c , and extent of the fit, r , for 20, 30 and 38°C in Tables 3.2, 3.3 and 3.4, respectively.

Table 3.2- Comparison of experimental and logistic model constants of *Rb. capsulatus* at 20°C and different light intensities

Light Intensity (lux)	1500	2000	3000	4000	5000	6000	7000
r	0.949	0.982	0.979	0.984	0.997	0.992	0.998
$X_{o,e}$	0.206	0.182	0.113	0.113	0.180	0.158	0.158
$X_{o,m}$	0.070	0.160	0.069	0.116	0.180	0.145	0.157
$X_{max,e}$	0.859	0.795	0.585	0.591	0.513	0.497	0.505
$X_{max,m}$	0.920	0.782	0.591	0.577	0.503	0.493	0.495
μ_{max}	0.015	0.011	0.028	0.026	0.018	0.023	0.022
k_c	0.022	0.023	0.053	0.050	0.053	0.070	0.064

Table 3.3- Comparison of experimental and logistic model constants of *Rb. capsulatus* at 30°C and different light intensities

Light Intensity (lux)	1500	2000	3000	4000	5000	6000	7000
r	0.974	0.971	0.973	0.998	0.987	0.961	0.855
$X_{o,e}$	0.158	0.158	0.153	0.127	0.193	0.156	0.160
$X_{o,m}$	0.073	0,081	0.092	0.115	0.129	0.05	0.111
$X_{max,e}$	0.858	0.729	0.721	0.655	0.868	0.847	0.706
$X_{max,m}$	0.816	0.710	0.700	0.648	0.862	0.800	0.579
μ_{max}	0.019	0.025	0.023	0.032	0.027	0.034	0.030
k_c	0.059	0.057	0.059	0.074	0.066	0.100	0.088

Table 3.4- Comparison of experimental and logistic model constants of *Rb. capsulatus* at 38°C and different light intensities

Light Intensity (lux)	1500	2000	3000	4000	5000
r	0.989	0.998	0.988	0.987	0.973
$X_{o,e}$	0.118	0.169	0.166	0.162	0.197
$X_{o,m}$	0.064	0.144	0.07	0.08	0.086
$X_{max,e}$	0.938	1.044	1.071	1.070	1.071
$X_{max,m}$	0.915	1.022	0.99	1.067	1.092
μ_{max}	0.027	0.026	0.024	0.027	0.024
k_c	0.066	0.045	0.057	0.054	0.040

r: extent of the fit

$X_{o,e}$: Experimental initial bacterial concentration, (gdw/L)

$X_{o,m}$: Initial bacterial concentration obtained by logistic model, (gdw/L)

$X_{max,e}$: Experimental maximum bacterial concentration, (gdw/L)

$X_{max,m}$: Maximum bacterial concentration obtained by logistic model, (gdw/L)

μ_{max} : Specific growth rate constant obtained by exponential model, (1/h)

k_c : Specific growth rate constant obtained by logistic model, (1/h)

Growth data are seen to fit well to the logistic model with extent of the fit values close to 1 as seen from Tables 3.2 to 3.4. Initial cell concentration values determined by the model, $X_{o,m}$, are seen to be slightly different from the experimental values, $X_{o,e}$, while the maximum cell concentration values of the model, $X_{max,m}$, are very close to the experimental values, $X_{max,e}$. Nath and Muthukumar (2008) also found that both X_0 and X_{max} values determined by the logistic model are quite similar the experimental values.

From examination of the maximum and initial cell concentration values given in Figure 3.5 and Tables 3.2 – 3.4 the following results may be given. $X_{\max,e}$ and also $(X_{\max,e} - X_{o,e})$, which may be used as a measure of growth, decreases with increase in light intensity up to 5000 lux and then remains unchanged at 6000 and 7000 lux light intensities for 20°C.

At 30°C a decrease in $X_{\max,e}$ and also $(X_{\max,e} - X_{o,e})$ is seen with increase in light intensity up to 4000 lux. $X_{\max,e}$ and also $(X_{\max,e} - X_{o,e})$ values are seen to increase at 5000 and 6000 lux light intensities followed by a decrease at 7000 lux light intensity for 30°C. $X_{\max,e}$ and also $(X_{\max,e} - X_{o,e})$ appears not to be affected significantly with light intensity for 38°C incubator temperature. Growth is seen to increase with increase in incubator temperature at all light intensities.

A general trend of the effect of light intensity on growth does not exist. Sasikala et al. (1991) found light intensity not to affect the final biomass of *Rb. sphaeroides* O.U. 001. Kim et al. (2006) in their study with *Rb. sphaeroides* KD131 found growth to decrease with increase in light intensity at 30°C. Similarly, Akköse (2008) found growth at 3500 lux light intensity to be higher than that at 6500 lux light intensity. Nath and Das (2009), on the other hand, found growth to be highest at the highest light intensity. Li et al. (2009) in their study conducted with *Rb. sphaeroides* ZX-5 in the 2000 – 9000 lux light intensity range at 30°C, found growth to decrease with light intensity up to 5000 lux, increase at 5000 and 6000 lux light intensities and decrease after 7000 lux light intensity which is similar to the findings in the present study at 30°C.

$X_{\max,e}$ and also $(X_{\max,e} - X_{o,e})$ values given in Figure 3.5 and Tables 3.2 – 3.4 indicate that growth increases with increase in temperature for all light intensities. Although the effect of temperature on growth is clear in the present study, a general agreement of the effect of temperature on growth, also, does not exist in the literature. Sasikala et al. (1991) found growth to increase with increase in temperature in the 20 – 30°C range. They found growth at 30 and 35°C to be close and found growth to decrease

with temperature after 35°C up to 45°C. They also found no growth taking place at temperatures below 20°C and above 45°C. He et al. (2006) studied growth at 26, 30 and 34°C. They found maximum growth to occur at 34°C and minimum growth at 30°C with growth taking place at 26°C in between.

As stated before, incubator temperature was controlled in the present study and medium temperatures measured were higher than the incubator temperature independent of temperature and light intensity. Differences between the medium and incubator temperatures (ΔT values) were small at low light intensities but significantly high at the higher light intensities. The cell growth results presented above indicate that growth increases with increase in temperature for all light intensities and decreases with increase in light intensity in the low light intensity range at 20 and 30°C incubator temperatures. The effect of light intensity on growth in the low light intensity range may be considered to be only the effect of light intensity as medium temperature is almost constant in this range. It would be more appropriate, however, to consider the effect of light intensity on growth at the higher light intensities to be the compound effect of both the light intensity and temperature as medium temperature increases with increase in light intensity in this range. Based on this reasoning, it may be considered that increase in light intensity decreases growth while increase in temperature increases growth. In the low light intensity range, then, as medium temperature is almost constant, increase in light intensity decreases growth. In the high light intensity range, on the other hand, increase in light intensity decreases growth while growth increases due to increase in the medium temperature. The net effect of the two opposing effects depends on the magnitudes of the effects of increased light intensity and increased medium temperature on growth. 38°C temperature appears to be quite high so that growth is high when the effect of light intensity on growth is not significant.

Specific growth rate, μ , appearing in equation (3.1) and/or apparent specific growth rate, k_c , appearing in equation (3.4) may be used as criteria for rate of growth. The values of μ_{\max} and k_c are different as their definitions are different. Variation of

μ_{\max} and/or k_c , given in Tables 3.2 - 3.4, with increase in light intensity at a given incubator temperature shows scatter but indicates increase in growth rate with increase in light intensity which is in accord with the results of Obeid et al. (2009) who have worked at 30°C in the 6000 - 50000 lux range and Carlozzi (2009) who has worked in the 36 - 830 W/m² range. Variation of μ_{\max} and/or k_c values with temperature for a given light intensity indicates rate of growth to increase with increase in incubator temperature from 20 to 30°C but to decrease with increase in incubator temperature from 30 to 38°C. He et al. (2006) found rate of growth to increase with temperature in their study conducted at 26, 30 and 34°C temperatures. The effect of temperature on rate of growth at temperatures exceeding 34°C was not encountered in the literature.

3.3. Variation of pH at Different Temperatures and Light Intensities

Variation of pH during growth of *Rb. capsulatus* at different light intensities for temperatures of 20, 30 and 38°C are given in Figures 3.7, 3.8 and 3.9, respectively. pH values encountered for all light intensities and incubator temperatures in the present study are seen to be in the 6.0 to 8.5 range. That growth has taken place in all of the runs of the present study is in accord with the results of Sasikala et al. (1991) who found growth of *Rb. sphaeroides* to take place in the pH range of 6.0 to 9.0. No growth was observed for pH values of 5.5 and below in the same study. They also found optimum pH to be 7.0 for hydrogen production.

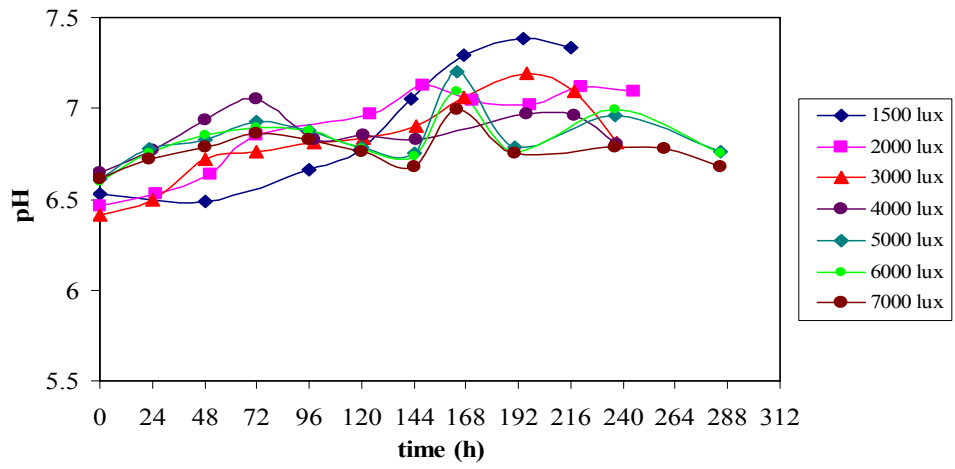


Figure 3.7- Variation of pH with time for different light intensities at 20°C

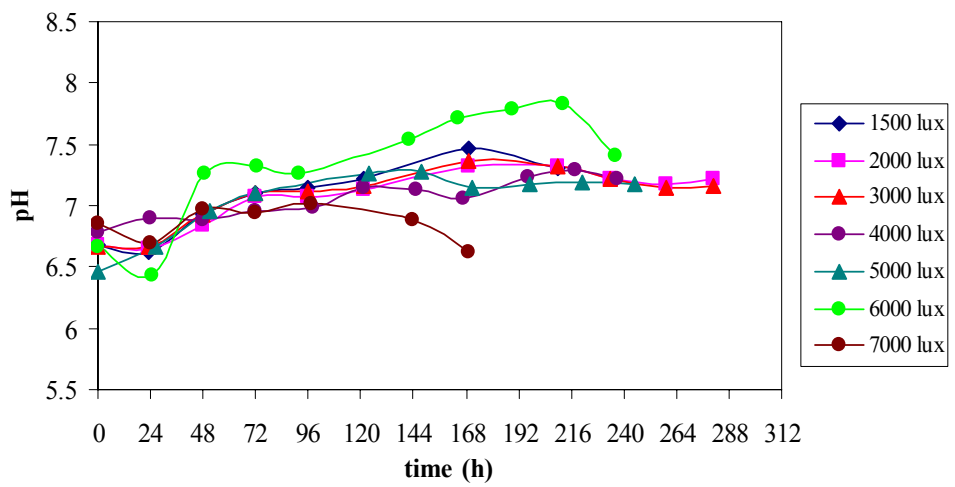


Figure 3.8- Variation of pH with time for different light intensities at 30°C

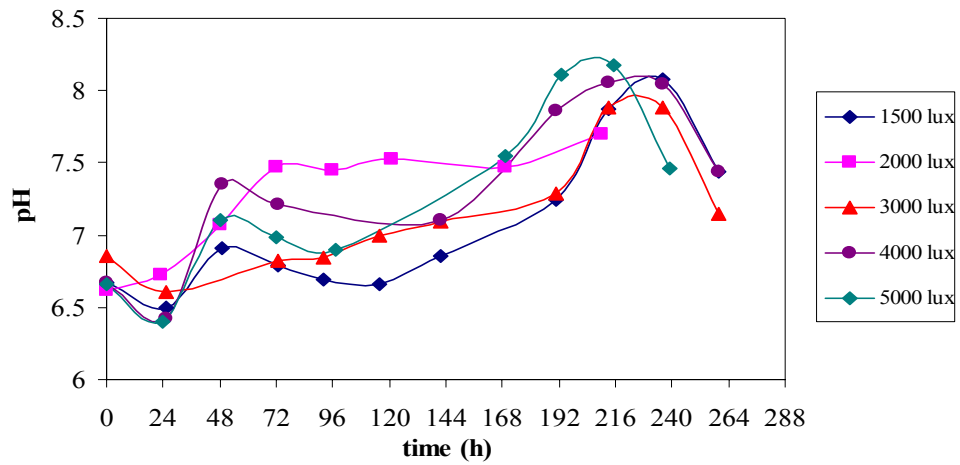


Figure 3.9- Variation of pH with time for different light intensities at 38°C

pH values for all light intensities for 20 and 30°C incubator temperatures are in the 6.5 to 7.5 range. pH is seen to have increased up to 8.0 at 38°C incubator temperature. Akköse (2008) observed pH to be highest when growth was maximum. Highest pH and highest growth were found at 38°C incubator temperature in the present study which is in accord with the observations of Akköse (2008). Sasikala et al. (1991) found decay in growth (decrease in quantity of biomass) for pH values exceeding 7.5 under 4000 lux light intensity. pH values higher than 7.5 were observed for 38°C incubator temperature in the present study, as seen from Figure 3.9, when decay in growth took place as can be seen from Figure 3.4. This result is in accord with the results of Sasikala et al. (1991).

3.4. The Effect of Light Intensity and Temperature on Hydrogen Production

Hydrogen production for 20, 30 and 38°C for different light intensities are given in graphical form in Figures 3.10, 3.11 and 3.12, respectively, where millimoles of hydrogen collected are plotted against time measured in hours. The results are given millimoles since the volume of gases is affected by temperature. Millimoles of hydrogen were calculated by use of the ideal gas law.

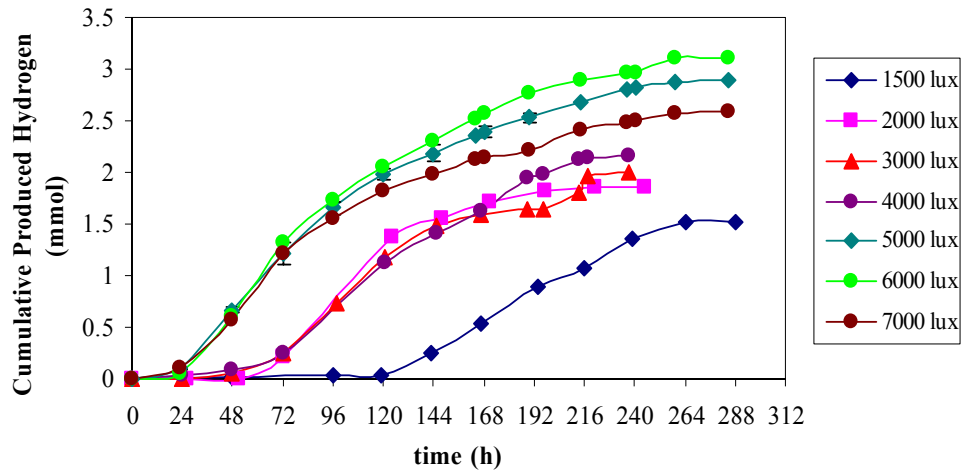


Figure 3.10- Cumulative Hydrogen Production for different light intensities at 20°C

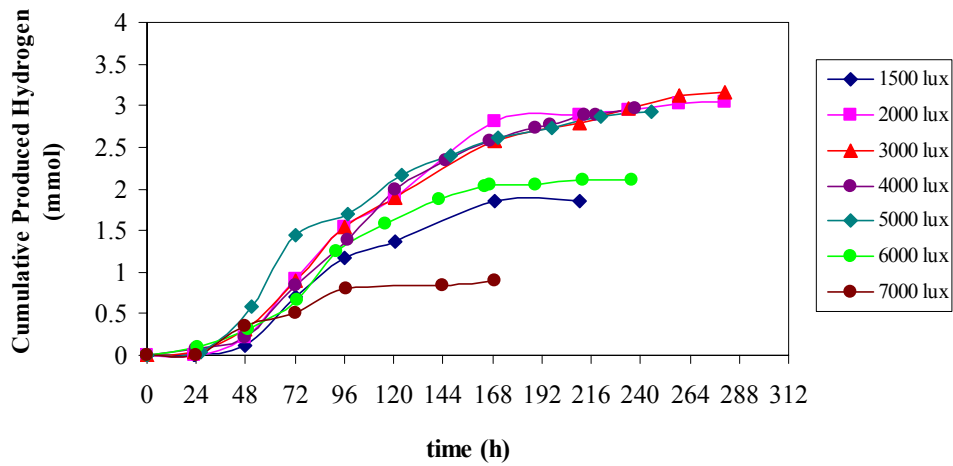


Figure 3.11- Cumulative Hydrogen Production for different light intensities at 30°C

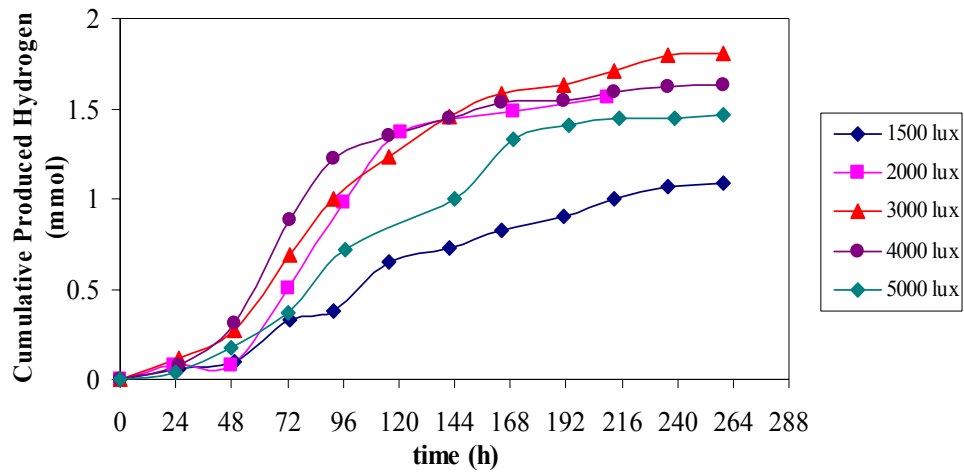


Figure 3.12- Cumulative Hydrogen Production for different light intensities at 38°C

The results indicate that hydrogen has been produced at all temperatures and light intensities; the amount of hydrogen changed, however. A lag phase appears to be present in all conditions. Total amounts of hydrogen produced at different temperatures and light intensities are given in Figure 3.13 as a summary.

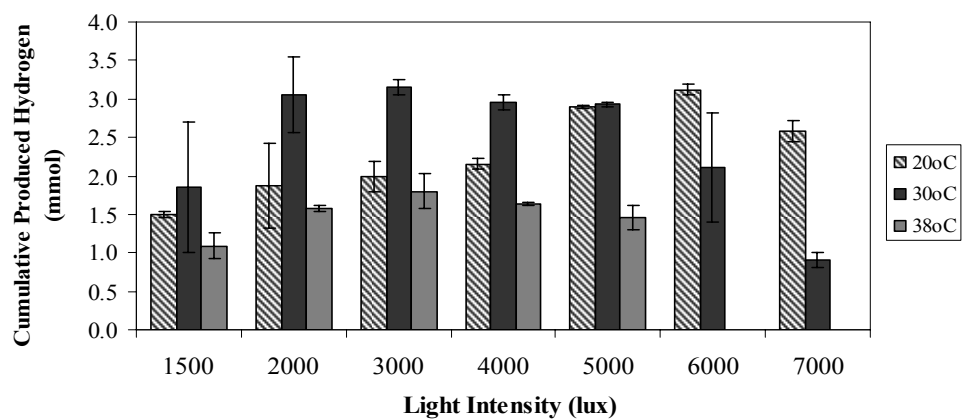


Figure 3.13 Total amount of hydrogen produced at different incubator temperatures and light intensities

The results show that maximum hydrogen production has taken place at 30°C for 1500 - 4000 lux. These results are in agreement with the results of Sasikala et al. (1991) who found optimum temperature range for hydrogen production by *Rb. sphaeroides* O.U. 001 to be 30 to 40°C. Uyar (2008) reported hydrogen production does not take place at 42 and 48 °C but takes place at 31 - 37 °C. Ünlü et al. (2009) obtained highest expression levels of both *nif* H and *nif* A genes by *Rb. sphaeroides* O.U.001 at 30°C. Hydrogen production for 5000 lux at 20°C is about the same as that at 30°C incubator temperature while cumulative hydrogen values for 6000 and 7000 lux at 20°C are higher than those at 30°C as in the present study high cumulative hydrogen values have generally been obtained at around 30°C. Cumulative hydrogen values for 6000 and 7000 lux at 20°C are higher than those at 30°C, however, in the present study. Medium temperatures for 20°C incubator temperature at these light intensities were close to 30°C while those at 30°C incubator temperature were higher than 40°C. The reason for high hydrogen production at 20°C may therefore be due to medium temperatures being close to 30°C.

The results for 20°C given in Figures 3.10 and 3.13 show that the lowest hydrogen production has taken place for 1500 lux; the lag phase is 120 hours at this light intensity which is the longest one among others. Hydrogen production for 2000, 3000 and 4000 lux have lag phases of about 48 hours. Hydrogen production at 5000 lux is higher than those at lower light intensities and the highest at production occurs at 6000 lux. A decrease in hydrogen production is seen for 7000 lux. Lag phases for 5000, 6000 and 7000 lux are about 24 hours or less. These results indicate that duration of lag phase decreases with increase in light intensity at 20°C. Hydrogen production increases with increase in light intensity up to 6000 lux but decreases for 7000 lux.

The results at 30°C, given in Figures 3.11 and 3.13, show that hydrogen production for 2000, 3000, 4000 and 5000 lux are close to each other (around 3 mmol total) and significantly higher than that at 1500 lux (around 1.5 mmol total). A decrease in hydrogen production is observed at 6000 lux and a further decrease is seen at 7000

lux. Decrease in hydrogen production for 7000 lux is so significant that hydrogen production for this light intensity is lower than even that for 1500 lux. Duration of lag phase is seen to be less than 48 hours for all light intensities. Increase in light intensity appears to decrease the duration of lag phase which is similar with the lag phase duration results to the case of 20°C.

The lowest hydrogen production was observed for 1500 lux at 38°C as seen from Figures 3.12 and 3.13. An increase in hydrogen production is seen to have taken place with increase of light intensity from 1500 to 2000 lux. Amount of hydrogen produced at 3000 lux is slightly higher than that produced at 2000 lux while hydrogen produced at 4000 lux and 5000 lux is slightly lower than that at 3000 lux. Amount of hydrogen produced at 38°C is lower than that of other temperatures. Therefore, changes in the amount of hydrogen produced with light intensity are not so significant. Increase in light intensity appears to decrease duration of lag phase again.

Hydrogen produced for all light intensities at 20°C are larger than those at 38°C and the difference between the amounts of hydrogen produced is very significant for 5000 lux. Highest hydrogen production has taken place at 30°C for light intensities up to 5000 lux. On the other hand the hydrogen produced at 20°C for 6000 and 7000 lux are larger than those at 30°C. Duration of lag phase is the longest at 20°C incubator temperature.

In general, the effect of light intensity on hydrogen production is as follows: Hydrogen production at 1500 lux light intensity is low. Hydrogen production increases with increase in light intensity up to a certain value and decreases beyond this value. The effect of light intensity on hydrogen production is slight in the 2000 to 4000 lux range at 20°C and in the 2000 to 5000 lux range at 30 and 38°C. Increase in light intensity decreases the duration of the lag phase.

Carlozzi (2009) found increased irradiation to increase the cumulative hydrogen in the study conducted with *Rp. palustris*. Sasikala et al. (1991) found that hydrogen production increased with increase in light intensity up to 5000 lux and that cumulative hydrogen did not change at higher light intensities. Hydrogen production was found to increase with increase in light intensity at low light intensities but to decrease with increase in light intensity at higher light intensities by Miyake (1982) and Kim et al (2006). Uyar et al. (2005) found total amount of hydrogen produced not to be related with light intensity. Decrease in cumulative hydrogen at high light intensities was observed by Macler et al. (1979). Akköse (2008) found cumulative hydrogen at 6500 lux light intensity was one half of that at 3500 lux light intensity and suggested that high light intensities may have inhibitory effect on hydrogen production. In view of the results of the present study and those of the investigators referred to above, it may be concluded that cumulative hydrogen increases with increase in light intensity at low light intensities and decreases with increase in light intensity beyond a certain light intensity and that hydrogen production is only slightly affected by light intensity in a certain range at medium light intensities.

Decrease in hydrogen production with light intensity may be due to photoinhibition. Photoinhibition is decrease of photosynthetic activity due to injure of the photosynthetic apparatus caused by strong illumination. (Yordanov and Velikova, 2000; Demmig-Adams and Adams, 1992; Horton et al., 1994) Decrease in hydrogen production with increase in light intensity, photoinhibition, at high light intensities has been found in the studies of Akköse (2008), Kim et al. (2006) and Li et al. (2009). Significant decrease in hydrogen production beyond 5000 lux at 30°C and beyond 6000 lux at 20°C may be due to photoinhibition. The reason for decrease in hydrogen production with increase in light intensity at 30°C may also be related with significantly higher medium temperature compare to incubator set temperature at high light intensities, however.

If decrease in hydrogen production with increase in light intensity, which is observed after 6000 lux at 20°C, 5000 lux at 30°C and 3000 lux at 38°C, is attributed to

photoinhibition then it may be argued that photoinhibition starts at higher light intensities at lower incubator temperatures. Use of higher light intensities at lower ambient temperatures (outdoor temperature under outdoor conditions and incubator temperature under indoor conditions) seems to be favorable to increase hydrogen production which may be of practical interest.

3.4.1 Modeling of Hydrogen Production Results

Hydrogen production curves given in Figures 3.10 – 3.12 resemble the schematic curve shown in Figure 3.14 and indicate that quantity of hydrogen produced increases very slowly with time from 0 (the beginning of measurement after inoculation) up to a certain time value λ and then increases rapidly almost at a constant rate and finally reaches an asymptotic value with no further increase. Kinetic models (mathematical equations) have been developed to analyze the variation of a quantity, H, with time by a curve similar to that given in Figure 3.14. Of the several models the Modified Gompertz Model is stated to be the widely used and the most suitable one (Mu et al., 2007, Nath et al., 2008, Wang and Wan, 2009) to describe the progress of hydrogen production.

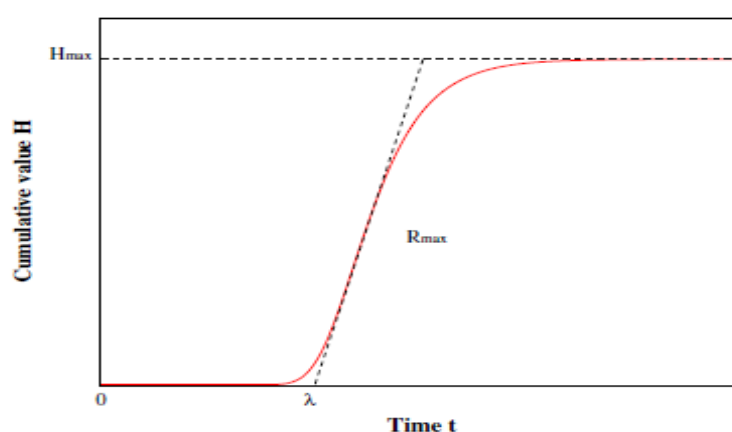


Figure 3.14- A schematic curve for the Modified Gompertz Model (Wang and Wan, 2009)

The equation for the Modified Gompertz Model is:

$$H = H_{\max} \exp \left\{ -\exp \left[\frac{R_{\max}}{H_{\max}} e (\lambda - 1) + 1 \right] \right\} \quad (3.7)$$

where, H and H_{\max} are the instantaneous and the maximum cumulative hydrogen values in millimole per liter culture, respectively, R_{\max} is the maximum hydrogen production rate (slope of the straight line cutting the time axis at λ , the lag time in hours) in millimole per liter culture per hour.

In this study the experimental hydrogen production data presented in Figures 3.10 – 3.12 were fitted to the modified Gompertz model using a program (Curve Expert 1.3) for fitting curves. Curve fitted to the Modified Gompertz Model together with the experimental data for 20°C and 2000 lux is shown as an example in Figure 3.15; curves for other temperatures and light intensities are given in Appendix F. Values of the maximum cumulative hydrogen ($H_{\max,m}$), maximum hydrogen production rate ($R_{\max,m}$) and lag time (λ_m) obtained by the Modified Gompertz Model are tabulated for different incubator temperatures in Tables 3.5- 3.7. In the same tables experimental values of these quantities, $H_{\max,e}$, $R_{\max,e}$ and λ_e , determined from the hydrogen production curves given in Figures 3.10 – 3.12 are also shown. In these tables r is the extent of the fit which indicates the similarity between experimental results and the model. An r value closer to 1 indicates better fit.

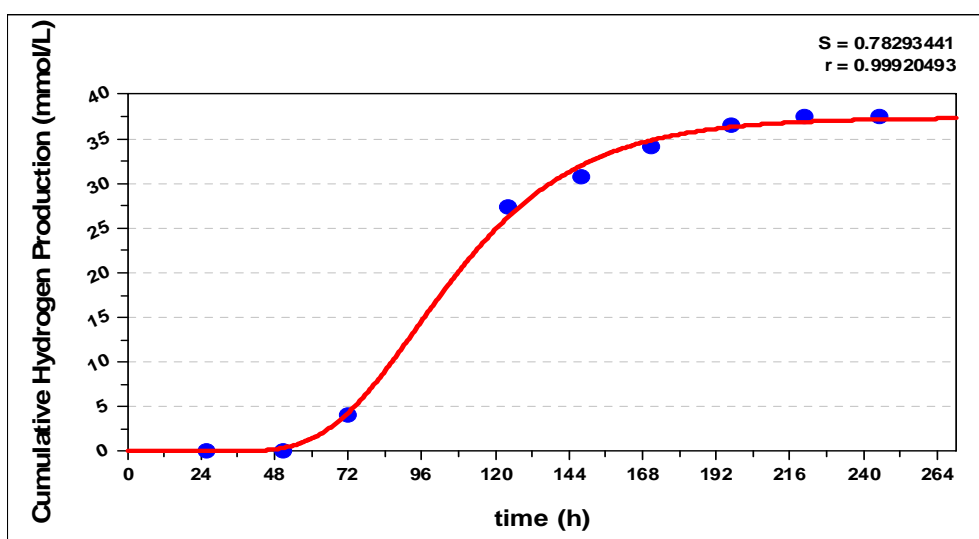


Figure 3.15- Comparison of hydrogen production data with Modified Gompertz Model at 20°C and 2000 lux

Table 3.5- Comparison of the Modified Gompertz Model parameters with the experimental values obtained at 20°C and different light intensities

Light Intensity (lux)	1500	2000	3000	4000	5000	6000	7000
r	0.999	0.999	0.997	0.999	0.997	0.996	0.995
$H_{\max,e}$	30.0	37.4	39.9	43.3	57.8	62.4	51.6
$H_{\max,m}$	33.4	37.4	39.4	47.9	57.9	62.9	50.9
$R_{\max,e}$	0.22	0.39	0.34	0.30	0.43	0.48	0.44
$R_{\max,m}$	0.27	0.48	0.36	0.34	0.40	0.44	0.37
λ_e	118	54	56	47	17	21	19
λ_m	128	65	57	59	17	20	15

Table 3.6- Comparison of the Modified Gompertz Model parameters with the experimental values obtained at 30°C and different light intensities

Light Intensity (lux)	1500	2000	3000	4000	5000	6000	7000
r	0.997	0.998	0.998	0.999	0.994	0.999	0.992
H _{max,e}	37.0	59.1	63.2	59.1	58.7	42.6	18.1
H _{max,m}	37.8	60.6	62.9	60.6	58	43.5	18.0
R _{max,e}	0.44	0.56	0.51	0.48	0.49	0.43	0.22
R _{max,m}	0.43	0.55	0.47	0.51	0.50	0.45	0.26
λ _e	42	40	36	38	23	36	21
λ _m	42	42	35	42	25	38	26

Table 3.7- Comparison of the Modified Gompertz Model parameters with the experimental values obtained at 38°C and different light intensities

Light Intensity (lux)	1500	2000	3000	4000	5000
r	0.997	0.998	0.999	0.998	0.997
H _{max,e}	21.8	31.4	36.1	32.5	29.0
H _{max,m}	22.9	31.2	36.9	31.7	31.5
R _{max,e}	0.16	0.38	0.29	0.43	0.22
R _{max,m}	0.14	0.46	0.30	0.43	0.22
λ _e	36	44	27	33	34
λ _m	32	50	29	33	37

r	:	extent of the fit
H	:	cumulative hydrogen produced (mmol/L)
$H_{\max,e}$:	maximum cumulative hydrogen production obtained from experimental results (mmol/L)
$H_{\max,m}$:	hydrogen cumulative hydrogen production obtained by Modified Gompertz Model (mmol/L)
$R_{\max,e}$:	maximum hydrogen production rate obtained from experimental results (mmol/L.h)
$R_{\max,m}$:	maximum hydrogen production rate obtained from Modified Gompertz Model (mmol/L.h)
λ_e	:	lag time obtained from experimental results(h)
λ_m	:	lag time obtained from Modified Gompertz Model (h)
e	:	constant (2.718282)

The model parameters are very close to the experimental values and the extent of fit is close to 1. The Modified Gompertz Model well defines the hydrogen production by *Rb. capsulatus* at all temperatures and light intensities.

Maximum cumulative hydrogen, $H_{\max,e}$, (which is very close to $H_{\max,m}$) was discussed above. A significant increase in maximum hydrogen production rate, R_{\max} from 1500 to 2000 lux followed by a less significant decrease in rate from 2000 to 3000 lux is seen at all incubator temperatures. Rate appears not to be appreciably affected at the higher light intensities except for the rates at 30°C for 7000 lux and at 38°C for 5000 lux for which the medium temperatures are much higher than the incubator temperatures. Excluding R_{\max} at 30°C for 7000 lux, R_{\max} values at 30°C are appreciably higher than those at 20°C while R_{\max} values at 20°C are slightly higher than those at 38°C at any light intensity. The results, therefore, indicate that maximum rate of hydrogen production for 1500 lux is low and imply that maximum rate is not significantly affected by light intensity at the higher light intensities at all temperatures. Maximum rate of hydrogen production is highest at 30°C and lowest at

20°C at any light intensity. Incubator temperature of 30°C and light intensity of 2000 lux seems to be the optimum conditions for maximum hydrogen production rate.

Lag time values at 20°C show lag time to decrease with increase in light intensity. A decrease in lag time with increase in light intensity is seen for 30°C also; the influence of light intensity on lag time at 30°C is not as high as it is at 20°C. Lag time values at 38°C appear not to be significantly affected by light intensity. Lag time values at any light intensity at 30°C are smaller than those at 20°C which are not much different from the lag times at 38°C.

3.4.2 Substrate Conversion Efficiency, Yield, Molar Productivity, Light Conversion Efficiency and Product Yield Factor Determinations

In addition to cumulative amount of hydrogen produced and the maximum rate of production, substrate conversion efficiency, yield, molar productivity, light conversion efficiency and product yield factor are very important parameters for analysis of hydrogen production. In this section these parameters are defined and determined values are presented.

Substrate conversion efficiency is defined as,

$$\frac{\text{number of moles of hydrogen produced}}{\text{stoichiometric number of moles of hydrogen that would be produced from full use of the initial substrates}} \quad (3.6)$$

Initially, acetic acid (40 mM) and lactic acid (7.5 mM) were used as substrates in this study where the reactions for hydrogen formation are given as:



respectively. Based on the stoichiometry of reactions 3.7 and 3.8 substrate conversion efficiencies were calculated by using the experimental data. The calculated substrate conversion efficiencies for different temperatures and light intensities are given in Figure 3.16.

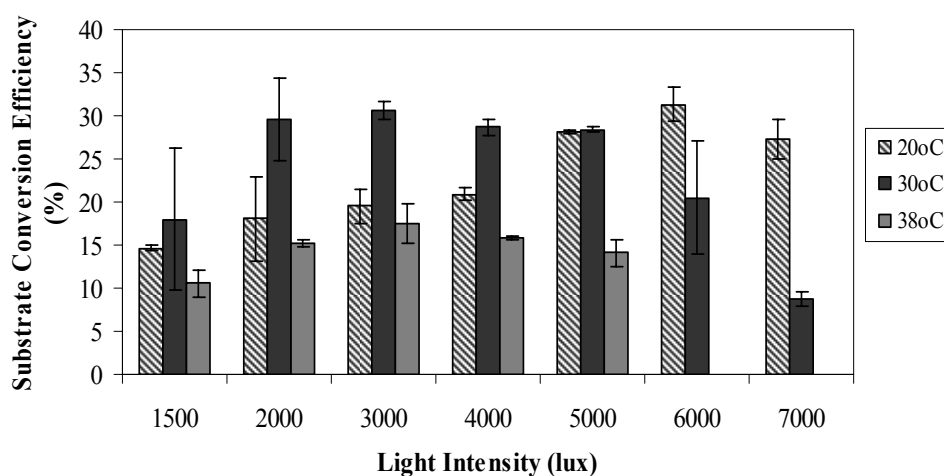


Figure 3.16 – Substrate Conversion Efficiency Results for Different Light Intensities and Temperatures

Initial amounts of acetate and lactate were kept same for all experiments. Cumulative hydrogen quantities given in Figure 3.13 and substrate conversion efficiencies given in Figure 3.16 accordingly differ by a constant factor, the denominator of Equation (3.6) hence they are proportional. Explanations and discussions given above for cumulative hydrogen production therefore apply equally for substrate conversion efficiency also. Li et al. (2009) found substrate conversion efficiency at 30°C increased with increase in light intensity between 2000 and 5000 lux but slightly decreased above which is similar to the findings of this study. He et al. (2006) found substrate conversion efficiency values with *Rb. capsulatus* to be maximum at 30°C.

Stevens et al. (1984) found that three of the tested *Rb. capsulatus* strains (B100, ST410 and ST 407) showed better acetate conversion efficiencies at 20°C while the other three strains showed optimal acetate conversion efficiencies at higher temperatures. This result indicates that the type of strain also affect substrate conversion efficiency.

Molar Productivity is defined as:

$$\frac{\text{cumulative millimoles of hydrogen produced}}{\text{volume of culture(L)} * t(\text{hour})} \quad (3.9)$$

where t is the duration of hydrogen production time from the end of the lag phase, λ , to the end of the hydrogen production. As such molar productivity is molar rate of production of hydrogen. Molar productivity values for different temperatures and light intensities are given in Figure 3.17.

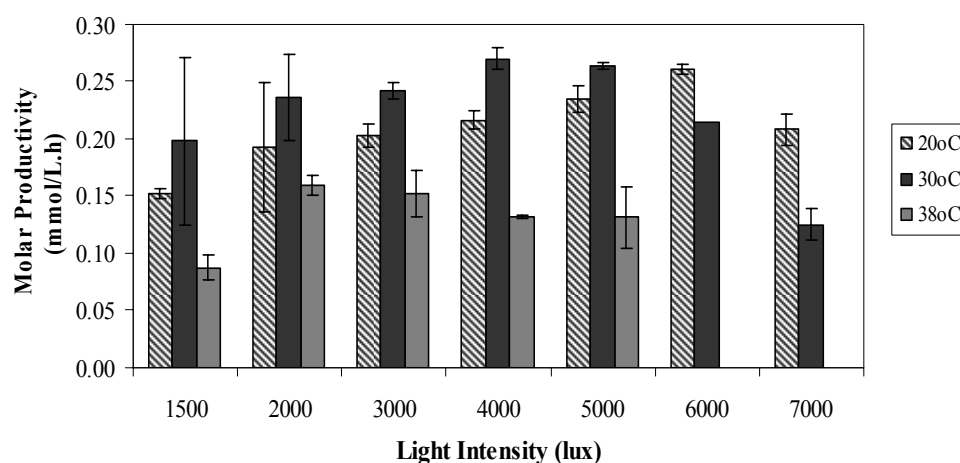


Figure 3.17 – Molar Productivity Values at Different Light Intensities and Temperatures

Molar productivity (rate) of hydrogen production values given in Figure 3.17 indicate an increase in rate up to a certain light intensity followed by a decrease at higher light intensities. The light intensity up to which rate increases is 6000 lux at 20°C, 4000 lux at 30°C and 2000 lux at 38°C. The effect of light intensity in increasing the rate of hydrogen production seems to be stronger at lower temperatures. Increase in hydrogen production rate with increase in light intensity has been observed by Obeid et al. (2009), Nakada et al. (1993), Klemme et al. (1993) and Akköse (2008). Uyar et al. (2007), Kondo et al. (2002) and Hillmer and Gest (1977) found rate to increase up to a certain light intensity and then remain constant. Ding et al. (2009) investigated the effects of light intensity on hydrogen production by *Rp. faecalis* in the 2000 to 10000 lux range and found the rate at 6000 lux to be the maximum. Hydrogen evolution rate was concluded to be low at high light intensities by Arık (1995). Increase in rate with increase in light intensity in a certain light intensity range found in the present study is in accordance with these results.

Molar rate at any light intensity up to 5000 lux is highest at 30°C and lowest at 38°C. These results indicate that 30°C is the optimum temperature from the standpoint of overall hydrogen production rate. This is in accordance with the studies of He et al. (2006) who found hydrogen production rate with *Rb. capsulatus* to be maximum at 30°C, Özgür et al. (2010) who found higher productivity by *Rb. capsulatus* YO3 mutant strain at 33°C and Arık (1995) who found hydrogen production rate at 31°C to be higher than that at 36°C. Hydrogen production rates at 20°C at 6000 and 7000 lux are higher than those at 30 °C. Medium temperatures at 20 °C for 6000 and 7000 lux are 27.5 °C and 29.5 °C while those at 30 °C are 43 and 56, respectively. The medium temperatures for 20 °C incubator temperature are close to the optimum temperature of 30 °C. This could be the reason for higher rates at 20 °C for 6000 and 7000 lux light intensities.

Yield values, calculated from the definition given below, for different temperatures and light intensities are given in Figure 3.18. As will be mentioned later, all of the lactate and most of the acetate were consumed by the bacteria during the runs.

Accordingly the denominator of Equation 3.6 does not change significantly between the runs. The trend in Figure 3.18, therefore, is not very different from that in Figure 3.13 or 3.16.

$$\text{Yield} = \frac{\text{mass of hydrogen produced (g)}}{\text{total mass of substrates (acetate and lactate) utilized}} \quad (3.10)$$

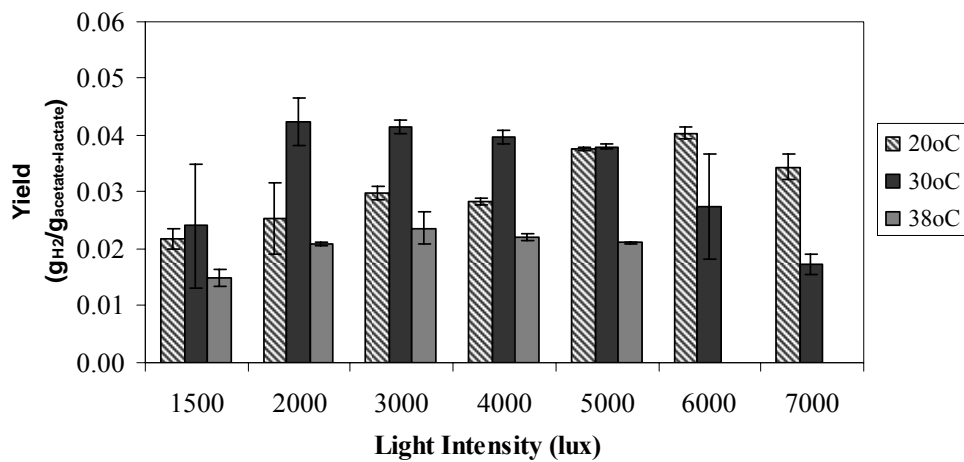


Figure 3.18- Hydrogen Yield Values for Different Light Intensities and Temperatures

Yield is seen to increase with light intensity up to a certain value and then decrease at higher light intensities for all incubator temperatures. Yield is the highest at 30°C (except for 6000 and 7000 lux light intensities). He et al (2006) found the highest yield at 30°C and Özgür et al. (2010) found the highest yield at 33°C. As for average rate, 30°C seems to be optimum temperature for yield also. Yield values at 20°C for 6000 and 7000 lux are higher than those at 30°C. The reason for this could be the medium temperature for 20°C incubator temperature to be close to the optimum temperature of 30°C as stated above. Increase in yield up to a certain light intensity followed by a decrease at higher light intensities was found by Ding et al (2009) and

Godhamshetty et al. (2008). Also Akköse (2008) found yield at 6500 lux to be smaller than that at 3500 lux.

Light conversion efficiency, η , is defined as the ratio of the total energy value (heat of combustion) of the hydrogen that has been produced to the total energy input to the photobioreactor by light radiation and is calculated by:

$$\eta(\%) = \frac{33.6 \times \rho_{H_2} \times V_{H_2}}{I \times A \times t} \times 100 \quad (3.11)$$

where V_{H_2} is the volume (L) of produced H_2 , ρ_{H_2} is the density (g/L) of the produced hydrogen gas, I is the light intensity (W/m^2), A is the irradiated area (m^2) and t is the duration of hydrogen production from the end of the lag phase, λ , to the end of the run. Incident light intensity was used in the calculations instead of the actual absorbed light intensity since the runs were carried out in batch mode, where the cell concentrations and thus the absorbed light intensities vary throughout the process. (Uyar et. al., 2007) Light conversion efficiencies for different light intensities and temperatures are summarized in Figure 3.19

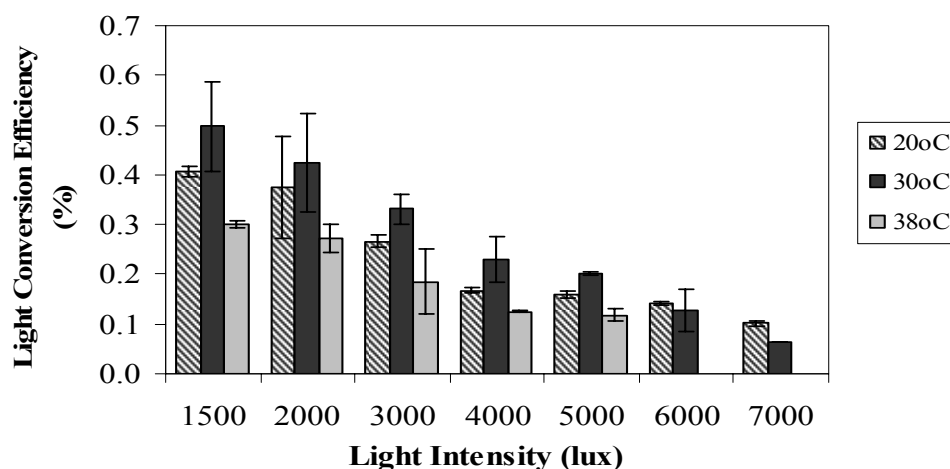


Figure 3.19- Light Conversion Efficiencies for Different Light Intensities and Temperatures

Light conversion efficiencies given in Figure 3.19 show a steady decrease with increase in light intensity at any temperature. Light conversion efficiencies for all light intensities other than 6000 and 7000 lux at 30°C are the highest while those at 38°C are the lowest. Decrease in light conversion efficiency with increase in light intensity has been found by several investigators (Uyar et al., 2007 , Akköse, 2008; Nath and Das, 2009; Barbosa et al., 2001; Miyake et al., 1987; Koku et al., 2002; Yang et al., 2005; Shi and Yu, 2005). Das and Veziroğlu (2008) concluded that the light conversion efficiency is inversely proportional with light intensity. The statement that light energy bioconversion by photosynthetic microorganisms is much lower under high light intensities is a very common statement (Liu et al., 2006). Low light conversion efficiency at high light intensities is due to the supply of energy in excess of the capability of the hydrogen producing nitrogenase enzyme (Nath and Das, 2005).

Product yield factor, defined as the ratio of cumulative hydrogen produced in millimoles to the maximum dry cell weight in grams, values for different light intensities and temperatures are given in Figure 3.20.

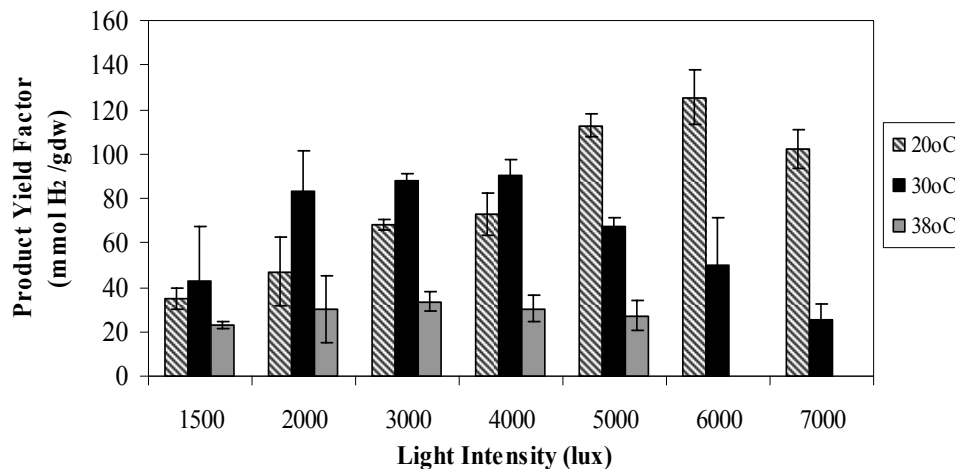


Figure 3.20- Product Yield Factor Values for Different Light Intensities and Temperatures

Product yield factors given in Figure 3.20 show an increase with increase in light intensity up to a certain value and to decrease beyond at any temperature. The light intensity value up to which product yield factor increases is 6000 lux at 20°C, 4000 lux at 30°C and 3000 lux at 38°C. The smallest product yield factor values were obtained at 38°C at any light intensity. Variation of product yield factor with light intensity is very small also at this temperature. This is a normal result in view of the fact that hydrogen production was the lowest while growth was the highest at 38°C for all of the tested light intensities as stated above. Product yield factor values at 30°C are higher than those at 20°C for low light intensities while the opposite is true at 5000, 6000 and 7000 lux light intensities. Hydrogen production values at 20°C for 6000 and 7000 lux were higher than those at 30°C while growth values for these two light intensities at 20°C are smaller than those at 30°C. Accordingly product yield factors for 6000 and 7000 lux light intensities at 20°C are higher than those at 30°C. Hydrogen production value for 5000 lux at 30°C was found to be higher than that at 20°C. In spite of this product yield factor for this light intensity at 20°C is higher than

that at 30°C. This arises from the fact that growth at 30°C for 5000 lux is higher than that at 20°C.

Both cell growth and hydrogen formation take place during photofermentative hydrogen production. As hydrogen is produced by the cells, increase in number of cells is expected to increase the produced hydrogen. Both of cell growth and hydrogen formation processes, however, use the same substrates. From this point of view cell growth and hydrogen formation may be considered competitive. Competitive nature of the two processes has been well recognized (Koku et al., 2002). So an excessive cell growth may be considered unfavorable for high hydrogen production. Product yield factor defined above may be taken as a measure of the relative values of hydrogen production and cell growth. Increase in product yield factor may be considered to be the result of the use of higher amount of substrate for hydrogen formation. The results indicate that 30°C is the optimum temperature for product yield factor for light intensities up to 4000 lux while 20°C is better for higher light intensities.

3.5 Organic Acid Consumption and Production

Lactate and acetate are carbon sources. Concentrations of these substrates decrease with time as they are consumed during photofermentation. Meanwhile formic acid, butyric acid and propionic acid are produced as side products. Concentrations of all these organic acids were determined periodically. In this section consumption and production of the organic acids during the growth and hydrogen production will be presented.

3.5.1 Lactic Acid Consumption

Variation of the concentration of lactic acid with time is shown for different light intensities in Figures 3.21- 3.23 at 20°C, 30°C and 38°C.

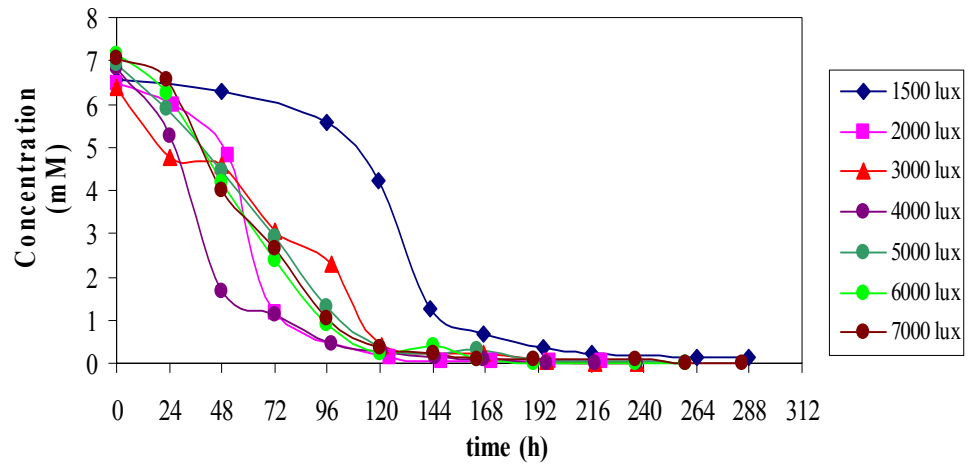


Figure 3.21- Lactic Acid Consumption at different light intensities and 20°C

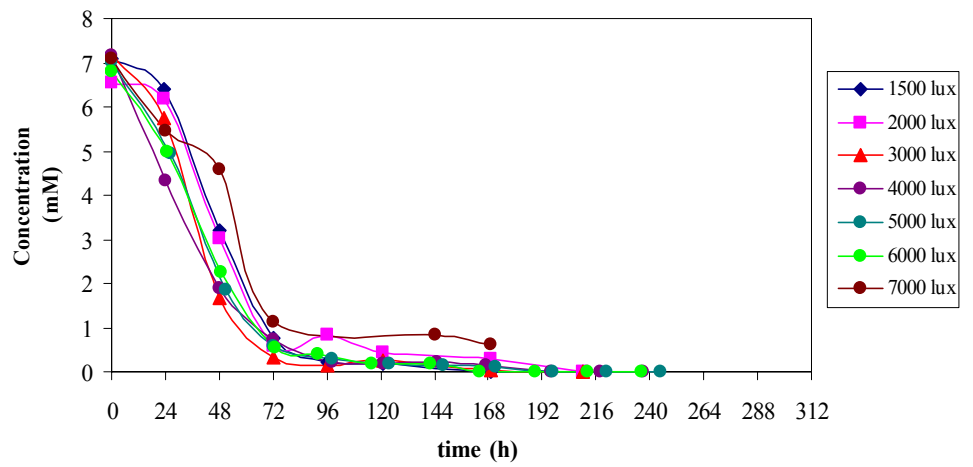


Figure 3.22- Lactic Acid Consumption at different light intensities and 30°C

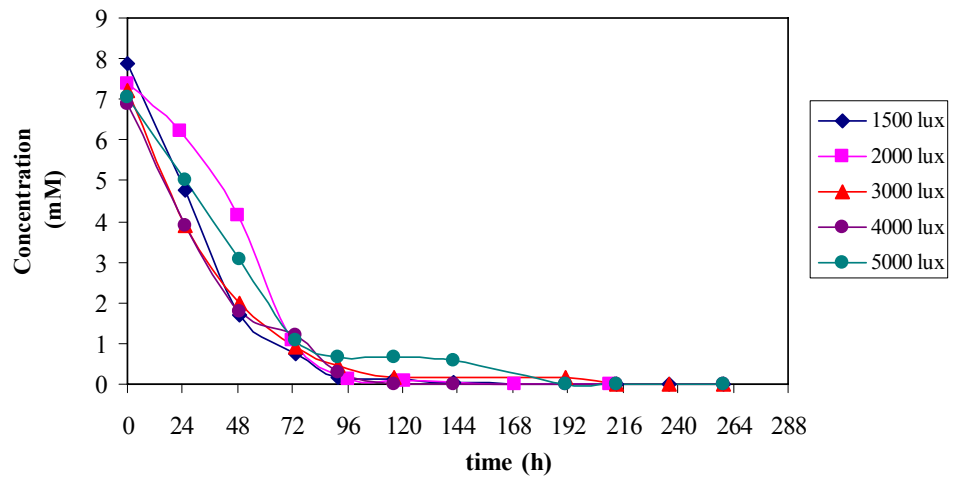


Figure 3.23- Lactic Acid Consumption at different light intensities and 38°C

Integration method is widely used in the kinetic analysis of several chemical processes in which the rate defined as the time derivative of the concentration of a reactant or product is expressed as a function of the concentration(s) of reactant(s) and product(s). Concentration(s) of the product(s) is (are) not taken into account in irreversible processes when the rate equation becomes simpler. If rate of consumption of a reactant, S , is related to some power, n , of the concentration, C , of that reactant the rate equation takes the form

$$-\frac{dC}{dt} = k \cdot C^n \quad (3.13)$$

where k is the rate constant and n is the order. A function of concentration, $f(C)$, which varies linearly with time, is obtained by integration of equation (3.13). The rate equations and the corresponding functions of concentration for zeroth, first and second processes are as given in Table 3.8.

Table 3.8- Differential and the integrated forms of the 0th, 1st and 2nd order rate equations

Order, n	Rate Equation	f(C)
0	$-\frac{dC}{dt} = k$	$C - C_0 = -k(t - t_0) \quad (3.14)$
1	$-\frac{dC}{dt} = k.C$	$\ln \frac{C}{C_0} = -k(t - t_0) \quad (3.15)$
2	$-\frac{dC}{dt} = k.C^2$	$\frac{1}{C} - \frac{1}{C_0} = k(t - t_0) \quad (3.16)$

where C_0 is the concentration at time = t_0 . $f(C)$, calculated for each order by using concentration versus time data presented graphically in Figures 3.21 – 3.23, were plotted against time by taking $t_0 = 0$ and C_0 as the initial concentration and equations of best fitting lines were determined. The rate constants (k_0 for $n = 0$, k_1 for $n = 1$ and k_2 for $n = 2$) and the coefficient of determination values (R^2) of the best fitting lines for different light intensities at 20, 30 and 38°C are given in Tables 3.19, 3.10 and 3.11, respectively. The extent of the fit values indicate best fit for any light intensity at all temperatures when $n = 1$. Based on this lactate consumption is concluded to follow first order kinetics.

Table 3.9- Extent of the fits and rate constants for lactic acid consumption at 20°C

		Zero th Order (n=0)		First Order (n=1)		Second Order (n=2)	
		k₀	R²	k₁	R²	k₂	R²
Light Intensity (lux)	1500	0.0256	0.83	0.0134	0.86	0.0197	0.65
	2000	0.0371	0.76	0.0273	0.91	0.1310	0.78
	3000	0.0351	0.86	0.0223	0.89	0.1180	0.40
	4000	0.0538	0.59	0.0264	0.98	0.0423	0.76
	5000	0.0394	0.75	0.0219	0.95	0.6470	0.55
	6000	0.0511	0.89	0.0231	0.91	0.3260	0.53
	7000	0.0356	0.64	0.0230	0.95	0.1270	0.40

Table 3.10- Extent of the fits and rate constants for lactic acid consumption at 30°C

		Zero th Order (n=0)		First Order (n=1)		Second Order (n=2)	
		k₀	R²	k₁	R²	k₂	R²
Light Intensity (lux)	1500	0.0676	0.90	0.0306	0.92	0.0373	0.82
	2000	0.0478	0.72	0.0209	0.87	0.0170	0.87
	3000	0.0580	0.56	0.0320	0.91	0.0817	0.67
	4000	0.0554	0.50	0.0272	0.92	0.0385	0.86
	5000	0.0529	0.57	0.0273	0.94	0.0400	0.85
	6000	0.0602	0.75	0.0288	0.94	0.0355	0.80
	7000	0.0465	0.75	0.0153	0.88	0.0075	0.87

Table 3.11- Extent of the fits and rate constants for lactic acid consumption at 38°C

		Zero th Order (n=0)		First Order (n=1)		Second Order (n=2)	
		k₀	R²	k₁	R²	k₂	R²
Light Intensity (lux)	1500	0.0721	0.64	0.0381	0.97	0.1482	0.48
	2000	0.0478	0.61	0.0337	0.93	0.3075	0.68
	3000	0.0536	0.26	0.0248	0.85	0.0327	0.76
	4000	0.0798	0.89	0.0294	0.93	0.0217	0.59
	5000	0.0447	0.57	0.0228	0.77	0.1335	0.29

The equation $\ln \frac{C}{C_0} = -k(t - t_0)$ for n = 1 in Table 3.9 can be converted to

$$C = C_0 \exp[-k(t - t_0)] \quad (3.17)$$

C versus t curves were plotted by taking t₀ as zero, C₀ as the initial lactate concentration and k as the values given in Tables 3.10 – 3.12 together with the experimental data points for different light intensities and temperatures. The curve for 30°C and 4000 lux is given in Figure 3.24 as an example. Curves for other temperatures and light intensities are given in Appendix G.

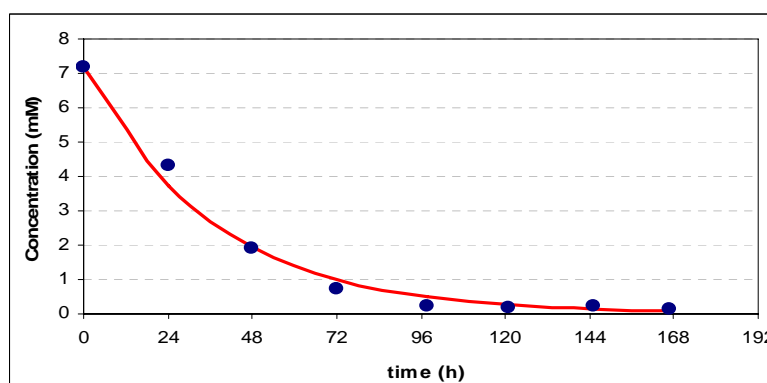


Figure 3.24- First Order Kinetics for Lactic Acid consumption at 30°C 4000 lux

The experimental data points are seen to fit reasonably good to the best fitting curves. The fit seems to be better in the later parts while the fit is not as good for earlier times when the data points lie above the curves. This indicates consumption of lactate in earlier times to be less than that predicted by the model curve. This may be due to presence of lag phases in both the growth and the hydrogen production in earlier times.

Figures 3.21 – 3.23 indicate consumption of lactic acid at any temperature not to be strongly affected by light intensity. A clear trend is not seen for variation of rate constant (k_1) with light intensity in Tables 3.10 – 3.12 which may be taken as an indication that the effect of light intensity on rate of consumption of lactate is not large. This is in agreement with the results of Wakayama et al. (2000) who found that rate was unaffected by the cycle period in their study on the effect of light dark cycle on lactate consumption. Kitajima et al. (1998) in their study on hydrogen production in photobioreactors of different depths of the reactor (increased depth decreases light intensity) found lactate to be entirely consumed within some days in all of the reactors.

The effect of temperature on rate is generally analyzed by the Arrhenius equation in which rate constant is taken to vary exponentially with temperature:

$$k = k' \exp\left(-\frac{E}{R T}\right) \quad (3.18)$$

where k' is a constant, E is activation energy, R is the universal gas constant and T is temperature in °K. Best fitting straight lines were determined from plots of $\ln k_1$ given in Tables 3.10 – 3.12 versus the reciprocal of the medium temperatures given in Table 3.1. The curve for 4000 lux is given in Figure 3.25 as an example.

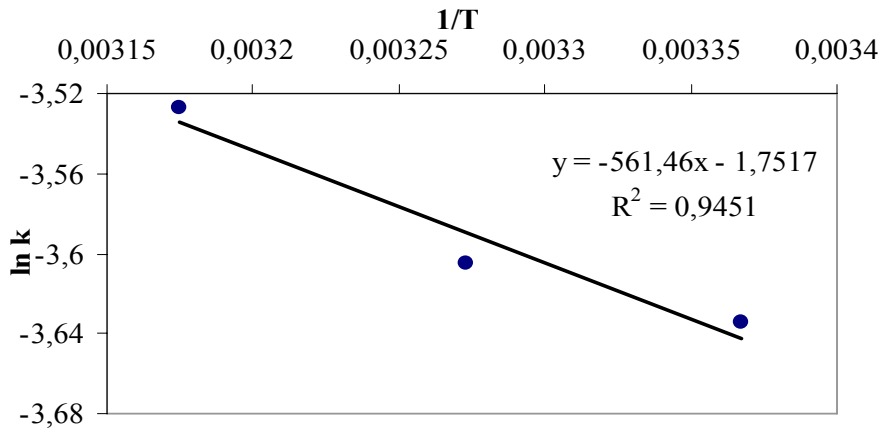


Figure 3.25- Variation of $\ln k_1$ with reciprocal of temperature for lactate consumption at 4000 lux

The fit of data points to the best fitting lines were not as good as that shown in Figure 3.25 but all lines had negative slopes in accord with the expected increase in rate constant with increase in temperature. Activation energies for different light intensities and temperatures are given in Table 3.12. In spite of poor fit of data to the Arrhenius equation the calculated activation energies are seen to decrease with increase in light intensity.

Table 3.12 Activation energies for lactic acid consumption under different light intensities

		Activation Energy (J/mol)
Light Intensity (lux)	1500	41897
	2000	8101
	3000	4992
	4000	4668
	5000	2231

Half life, time in which the concentration of a substance being consumed reaches one half of the initial concentration, is also commonly used in kinetic analyses. Half life, $t_{1/2}$, for a first order process is:

$$t_{1/2} = \ln 2/k \quad (3.19)$$

Half life periods calculated by equation 3.18 by taking k_1 values given in Tables 3.9 – 3.11 are tabulated in Table 3.13. A trend is difficult to find from Table 3.13 but half life periods are seen to be short. This is an expected result in view of the fact that almost complete consumption of lactate takes place in times less than 120 hours as can be seen from Figures 3.21-3.23.

Table 3.13- Half-life for lactate consumption, hours.

		Temperature (°C)		
		20	30	38
Light Intensity (lux)	1500	52	23	18
	2000	25	33	21
	3000	31	22	28
	4000	26	25	24
	5000	32	25	30
	6000	30	24	
	7000	30	45	

3.5.2 Acetic Acid Consumption

Variation of the concentration of acetic acid expressed as mM with time measured in hours is shown for different light intensities in Figures 3.25, 3.26 and 3.27 at 20°C, 30°C and 38°C, respectively.

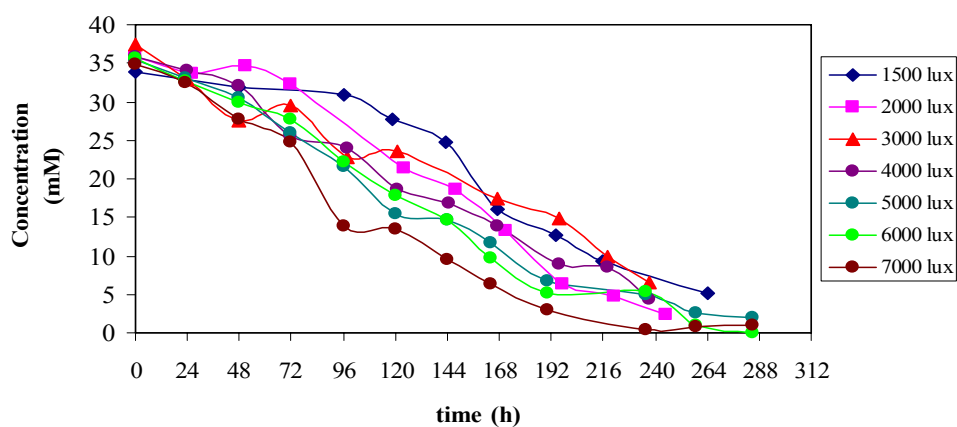


Figure 3.26 Acetic Acid Consumption at different light intensities and 20°C

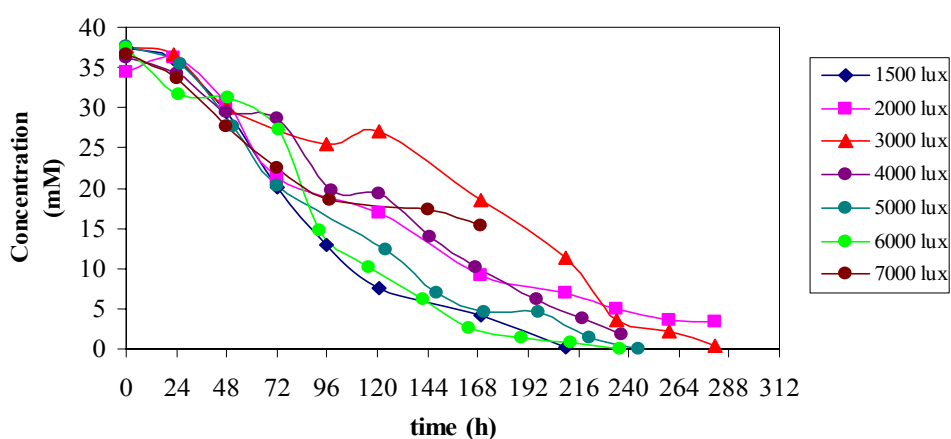


Figure 3.27- Acetic Acid Consumption at different light intensities and 30°C

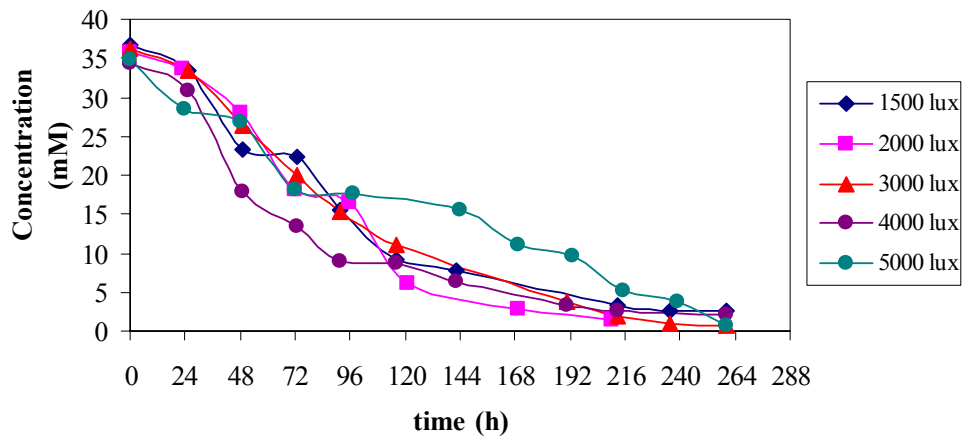


Figure 3.28- Acetic Acid Consumption at different light intensities and 38°C

Concentration versus time curves for acetic acid are different from those for lactic acid. It was stated above that almost complete consumption of lactic acid was complete in a short time. This is not the case for acetic acid. Acetic acid is consumed slowly at longer period of time. This implies lactate to be the preferred substrate in the system. The results indicate that lactate is used first during which acetate is not very extensively.

Similar to the kinetic analyses for lactic acid, $F(C)$ defined by equations 3.14, 3.15 and 3.16 were calculated by using the concentration versus time data for acetic acid and plotted against time by taking t_0 as the inoculation time and C_0 as the initial concentration. Equations of the best fitting lines and the coefficient of determination values (R^2) were determined. The coefficient of determination values indicated best fit for any light intensity at all temperatures when $n = 1$ for lactic acid. This is not the case for acetic acid. The coefficient of determination values indicated best fit when $n = 0$ for 13 runs and when $n = 1$ for the other 6 runs.

A shift in reaction order was considered to be a possibility. The data were divided into two groups and analyzed separately. One group was taken from $t = 0$ to $t = t^*$ and the second group from $t = t^*$ to the end of the run. Several possibilities for choice of t^* such as time for complete consumption of lactic acid, time for a certain percentage (such as 95%, 90% etc) consumption of lactic acid were tested. These trials indicated the group from $t = 0$ to $t = t^*$ fitted best to zero order while the group from $t = t^*$ to the end of the run fitted best to first order kinetics. Taking t^* as time for a certain percentage of consumption lactic acid gave good fits for some runs but the fit for the same percentage of consumption of lactic acid was not as good for the other runs. By trying almost all of the times where data exist, t^* giving the best fit (highest R^2) for both groups was found for each run. t^* values, concentrations of lactic and acetic acids at $t = t^*$, C_L^* and C_A^* , respectively, rate constants for zero order for times up to t^* , k_0 , and for first order for times beyond t^* , k_1 , are tabulated together with coefficient of determination, R^2 values in Tables 3.14, 3.15 and 3.16 for 20, 30 and 38°C, respectively. The values of the ratio of lactic acid concentration to acetic acid concentration at $t = t^*$, $\frac{C_L^*}{C_A^*}$, are also given in these tables.

Table 3.14 Kinetic Analysis for Acetate Consumption at 20°C

		0 th order		1 st Order					
		R^2	k_0	t^*	R^2	k_1	C_{lactate}	C_{acetate}	$C_{\text{lactate}}/C_{\text{acetate}}$
Light Intensity (lux)	1500	0.89	0.0418	143	0.96	0.0106	1.24	27.7	0.045
	2000	0.97	0.1282	72	0.93	0.0139	1.19	26.3	0.045
	3000	0.93	0.1268	121	0.99	0.0131	0.41	23.5	0.0072
	4000	0.97	0.1277	98	0.97	0.009	0.44	24.0	0.018
	5000	0.97	0.1351	96	0.97	0.012	1.29	21.5	0.06
	6000	0.99	0.1373	96	0.89	0.0116	0.91	22.2	0.041
	7000	0.98	0.1418	72	0.92	0.0182	2.67	24.7	0.110

Table 3.15 Kinetic Analysis for Acetate Consumption with shift in order at 30°C

		0 th order			1 st Order				
		R ²	k ₀	t*	R ²	k ₁	C _{lactate}	C _{acetate}	C _{lactate} /C _{acetate}
Light Intensity (lux)	1500	0.85	0.1455	48	0.99	0.0167	3.20	29.4	0.100
	2000	0.92	0.1478	121	0.98	0.0105	0.42	9.14	0.046
	3000	0.99	0.1221	210	0.96	0.0428	0.00	11.32	0
	4000	0.94	0.1126	72	0.97	0.0125	0.74	28.69	0.026
	5000	0.89	0.1735	51	0.94	0.0147	1.85	27.72	0.067
	6000	0.89	0.1435	73	0.99	0.0251	0.54	27.28	0.020
	7000	0.98	0.1876	72	0.86	0.0042	1.12	22.83	0.049

Table 3.16 Kinetic Analysis for Acetate Consumption with shift in order at 38°C

		0 th order			1 st Order				
		R ²	k ₀	t*	R ²	k ₁	C _{lactate}	C _{acetate}	C _{lactate} /C _{acetate}
Light Intensity (lux)	1500	0.98	0.1886	73	0.96	0.0138	0,75	22,40	0.034
	2000	0.90	0.2113	72	0.99	0.0192	1.1	18.22	0.06
	3000	0.93	0.1852	49	0.93	0.0154	2.00	26.30	0.076
	4000	0.96	0.2728	72	0.96	0.0107	1.22	13.39	0.091
	5000	0.93	0.1513	144	0.95	0.0142	0.67	15.49	0.043

C versus t curves were plotted in accord with the equation $C = C_0 - k_0 t$ with C_0 as the initial acetate concentration for times up to t^* and in accord with the equation $C = C_0 \exp[-k_1(t - t^*)]$ with C_0 as the acetate concentration at $t = t^*$, C_A^* , for times beyond t^* together with the experimental data points. The curve for 20°C and 1500 lux is given in Figure 3.29 as an example. Curves for other temperatures and light intensities are given in Appendix H.

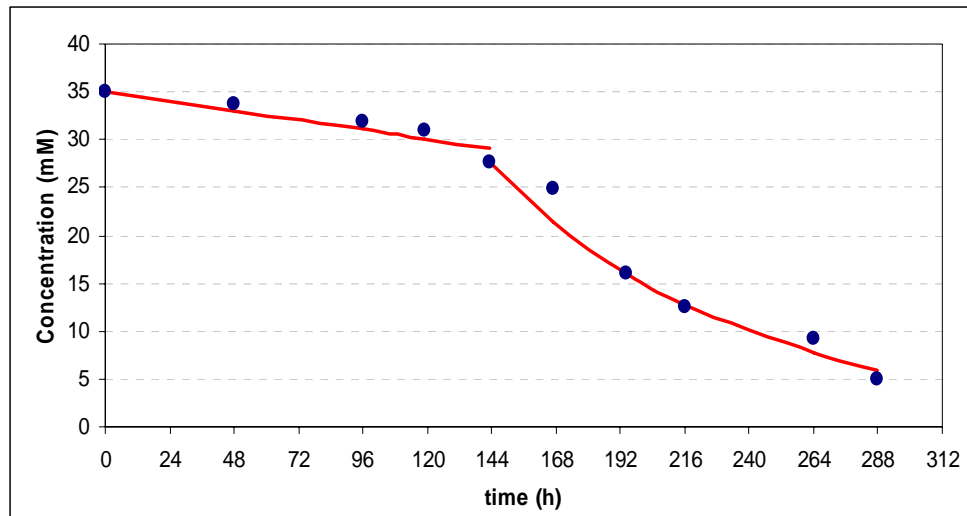


Figure 3.29- Comparison of model and experimental results of acetic acid consumption at 20°C and 1500 lux

The fit of experimental data points to the best fitting curves in Figures 3.28 and in Appendix H were much better than the fits to curves (not shown) by consideration of the zero or first order for the entire period. Based on this, consumption of acetic acid was concluded to obey zeroth order kinetics in the early period and first order kinetics after a certain time, t^* . The lactic acid concentrations at $t = t^*$, C_L^* values, are quite low whereas the acetic acid concentrations at these points, C_A^* values, are significant. It is not possible to find a critical value for C_L^* and/or C_A^* below or above which the order changes as these values are different for different runs. $\frac{C_L^*}{C_A^*}$ ratios differ for different runs also but they are small. It is difficult to find a critical value for $\frac{C_L^*}{C_A^*}$ ratio where the order changes however, it may be stated that the consumption rate of acetic acid is independent of its concentration ($n = 0$) when the

concentration of lactic acid is high. The consumption rate of acetic acid becomes proportional to its concentration ($n = 1$) after most of lactic acid is consumed.

Two different orders were reported in the study of Özgür et al. (2010) on hydrogen production with *Rb. capsulatus* DSM1710 by use of acetic acid as the carbon source. They found acetate to be consumed through first order kinetics for initial acetic acid concentrations of 30 mM or lower and through second order kinetics for 40mM or higher initial concentrations. They suggested that this might imply a shift in the metabolism of acetate depending on its initial concentration without giving further explanation. Uyar (2008) found in his study on hydrogen production that consumption of acetic acid did not fit to either first or second order when acetate was the sole substrate. In the same study by use of mixtures of acetate, malate and butyrate, acetic acid consumption was found to be different in absence or presence of the minor substrates. They reported good fit of their data on acetate consumption in presence of the minor substrate to first order rate equation until complete consumption of the minor substrate and to a different first order rate equation afterwards. They also found an increased rate of consumption of acetate when minor substrate was unavailable.

A specific trend is not apparent for variation of rate of consumption of acetic acid with light intensity in Figures 3.26 – 3.28. The same applies for variation of k_0 and k_1 in Tables 3.14 – 3.16. Based on this it may be concluded that the effect of light intensity on rate of consumption of acetic is not significant. Rate of consumption of acetic acid was found to increase with increase in light intensity in the study of Barbosa et al. (2001) who conducted their hydrogen production experiments at two different light intensities using separately *Rhodospseudomonas sp.*, *Rp. palustris* R1 and a non-identified strain. They have not conducted kinetic analyses but their data indicated the effect of light intensity on acetic acid consumption to be different for different strains especially in early times for *Rp. palustris* R1.

The effect of temperature on rate of consumption of acetic acid was analyzed separately for zero order and first order periods by the Arrhenius equation as previously done for lactic acid. The fit of data points to the best fitting $\ln k_0$ and $\ln k_1$ versus $1/T$ straight lines were not good as for the lactic acid mentioned above however the best fitting lines indicated increase in rate constants with increase in temperature as expected. Activation energies for different light intensities and temperatures are given in Table 3.17. The calculated activation energies show a decreasing trend with increase in light intensity. This was the case for lactic acid also. Light conversion efficiency is known to decrease with increase in light intensity as stated above. One reason for this is suggested to be supply of energy at high light intensities to be in excess of hydrogen production capacity of the nitrogenase enzyme (Nath and Das, 2009). It should be worth to investigate whether this excess energy has a role in decreasing activation energy.

Table 3.17 Activation energies for acetic acid consumption under different light intensities

		Activation Energy (J/mol)	
		0 th Order	1 st Order
Light Intensity (lux)	1500	65300	10400
	2000	20800	12700
	3000	14800	9000
	4000	33200	7300
	5000	5300	7600

3.5.3 Other Organic Acids

Acetic acid and lactic acid were used as substrates as stated before. These acids were consumed during the experiments. Analysis of the samples indicated formic acid, butyric acid and propionic acid were also formed. Concentration versus time graphs

of formic acid, butyric acid and propionic acid for different light intensities at 20, 30 and 38°C are given in Figures 3.30-3.32, 3.33-3.35 and 3.36-3.38 respectively.

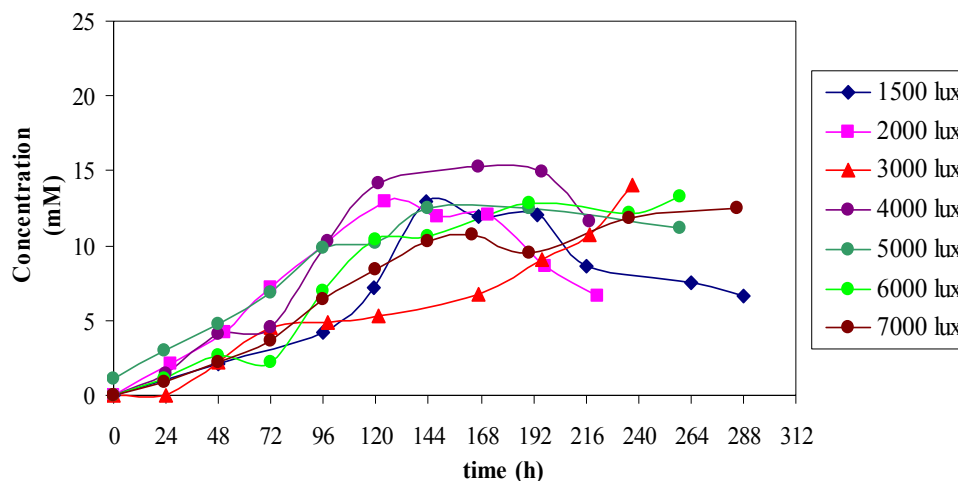


Figure 3.30- Variation of Formic Acid Concentration with time for different light intensities at 20°C

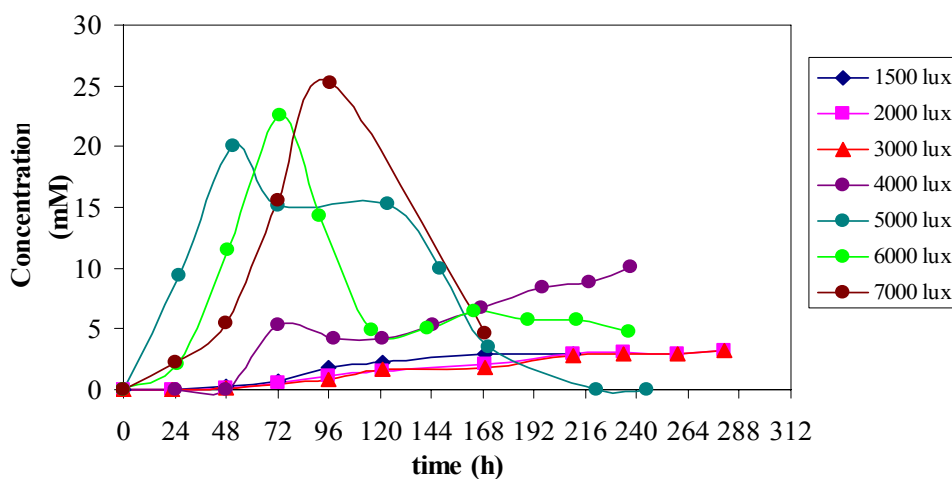


Figure 3.31- Variation of Formic Acid Concentration with time for different light intensities at 30°C

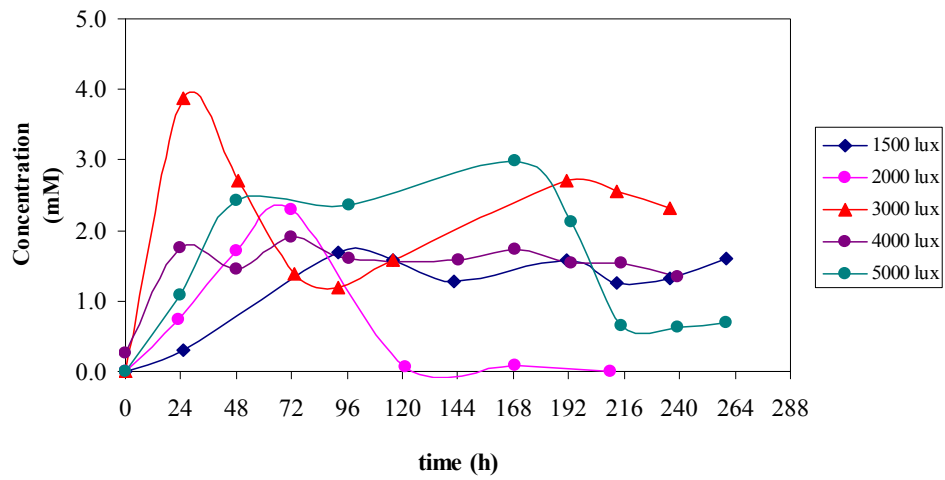


Figure 3.32- Variation of Formic acid Concentration with time for different light intensities at 38°C

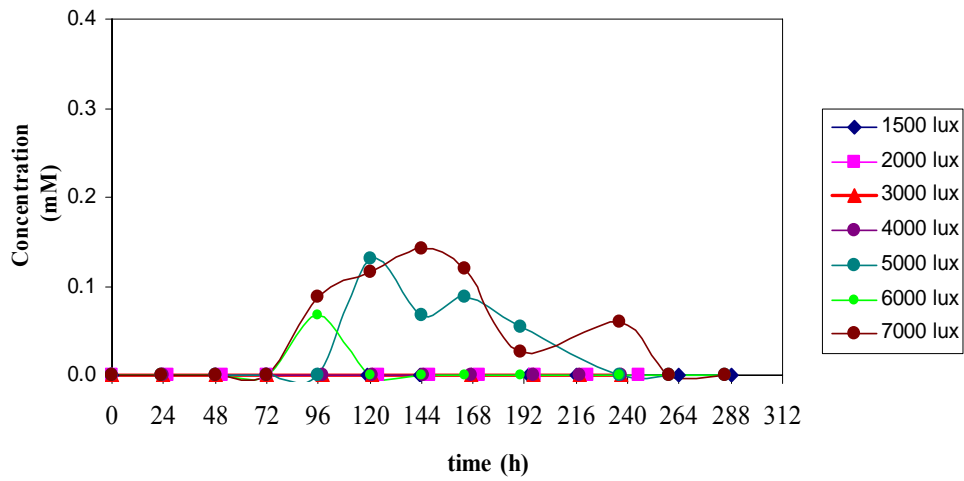


Figure 3.33- Variation of Butyric Acid Concentration with time for different light intensities at 20°C

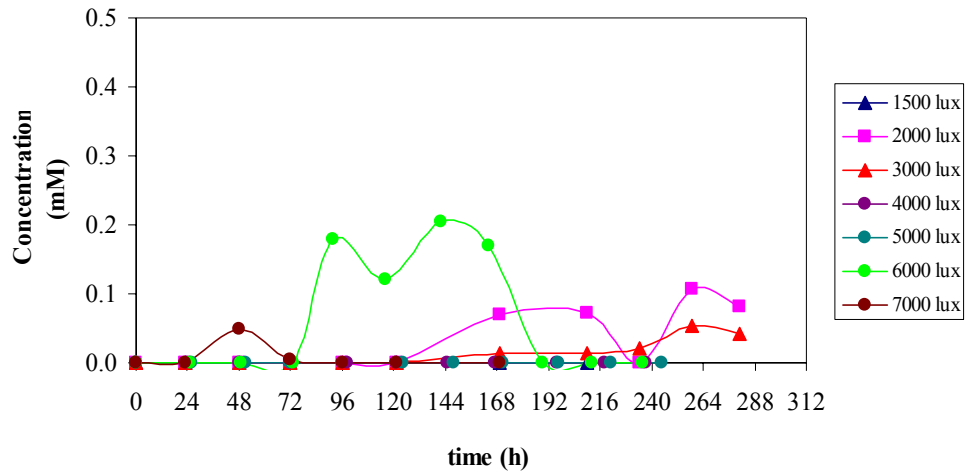


Figure 3.34- Variation of Butyric Acid Concentration with time for different light intensities at 30°C

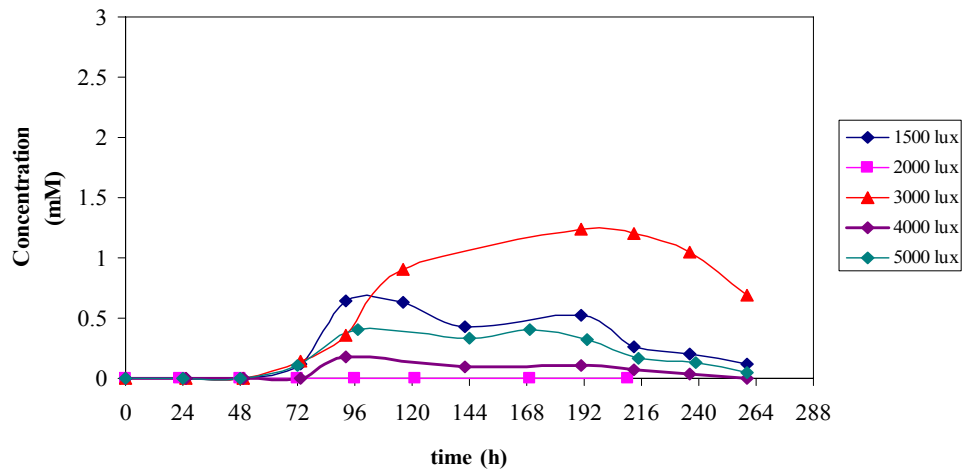


Figure 3.35- Variation of Butyric Acid Concentration with time for different light intensities at 38°C

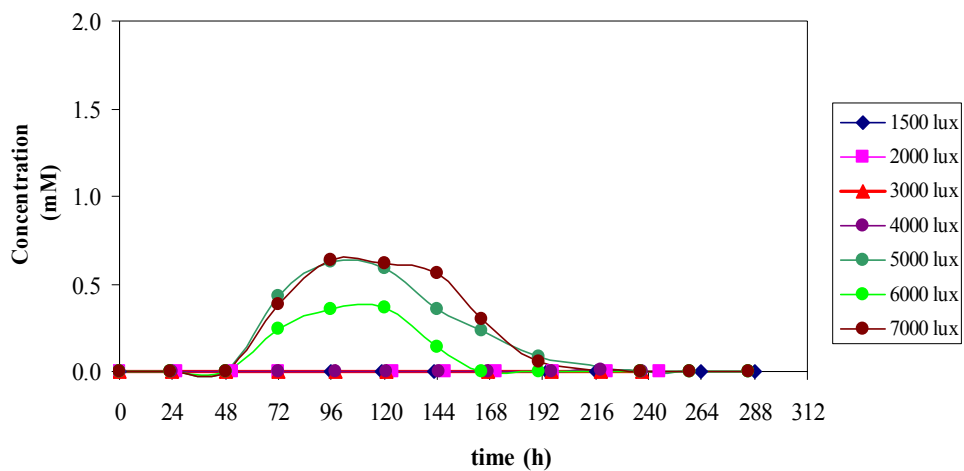


Figure 3.36- Variation of Propionic Acid Concentration with time for different light intensities at 20°C

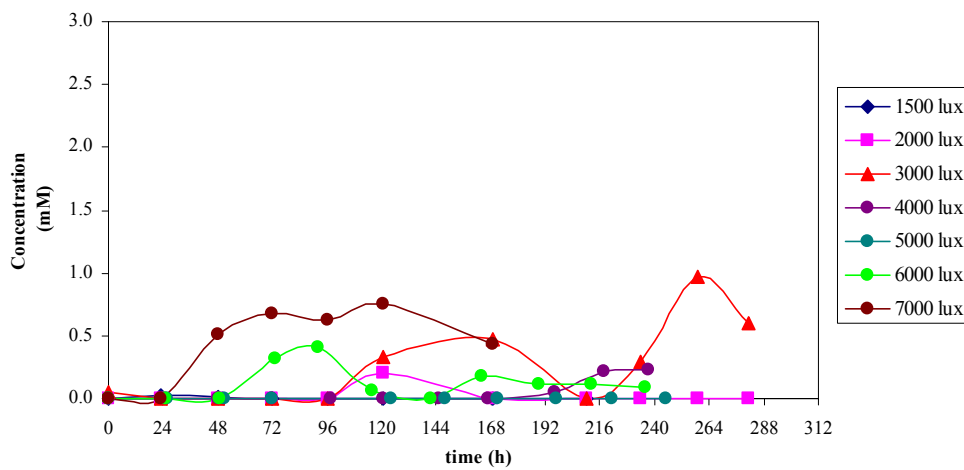


Figure 3.37- Variation of Propionic acid Concentration with time for different light intensities at 30°C

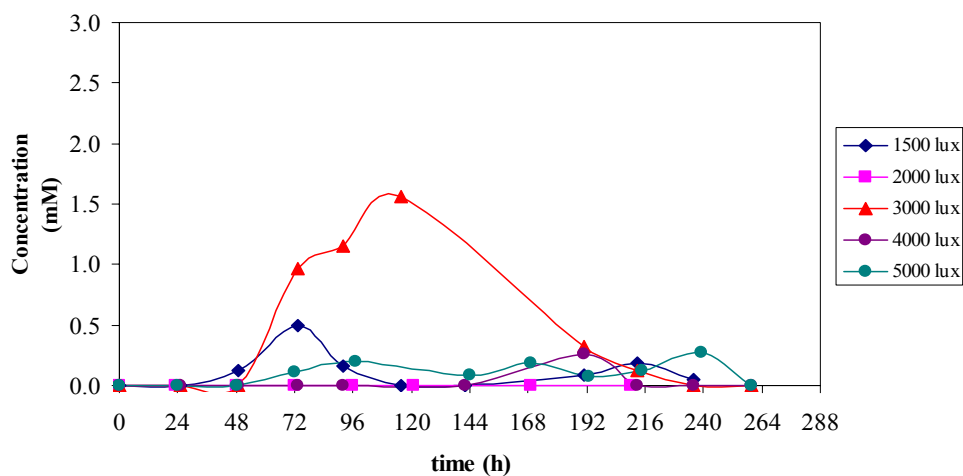


Figure 3.38- Variation of Propionic acid Concentration with time for different light intensities at 38°C

Figures 3.30- 3.38 indicate formic acid, butyric acid and propionic acid to have first formed and then consumed. Concentrations of propionic acid and especially butyric acid are quite low. Consequently, analysis of variations in the concentrations of these acids may not be meaningful.

However, change in concentrations of formic acid was significant. Formation of formic acid has been found in previous studies such as those of Tabanoğlu (2002), Androga (2009), Eroğlu et al. (2008) and Gurgun et al. (1976). The curves 3.30-3.32 indicate formic acid to form in the early periods when most of lactic acid is consumed as stated above. These results imply formic acid to form when lactic acid is present in the system.

It is known that reversible conversion of pyruvate and CoA results in formation of acetyl-CoA and formate and this is catalysed by pyruvate formate-lyase (PFL) enzyme (Becker et al., 1999). Pyruvate formate-lyase is known to exist in *Rs. rubrum* which is a PNS bacteria (Vignais et al., 1988). Haselkorn et al. (2001) in their study

of *Rb. capsulatus* genome stated that pyruvate-formate lyase and pyruvate-formate lyase activating enzyme are found in *Rb. capsulatus* also. In view of the simplified overall scheme of the carbon metabolism in PNS bacteria shown in Figure 1.8 lactate enters to scheme before acetate and results in formation of pyruvate. Based on this information formation of formic acid is expected to take place when lactate is present in the system which is in accord with the findings of the present study.

Formic acid concentration versus time curves shown in Figures 3.30-3.32. It is seen that formic acid formed at all temperatures and light intensities. And the highest amount of formic acid formation occurred at 30 ° C while the lowest formation was at 38°C. It is difficult to understand the effect of temperature on formic acid formation from these results. The highest amount of formic acid is observed at high light intensities of 5000, 6000 and 7000 lux at 30°C which is contrary to the findings of Eroğlu et al. (2008) ; Gurgun et. al. (1976) and Androga (2009) who have reported that formic acid formation occurred in the dark or low light intensities. Few studies have been encountered in literature on formation and consumption of formic acid during photofermentation. Studies on this subject would be useful to clarify the behaviour of formic acid during photofermentative hydrogen production.

CHAPTER 4

CONCLUSIONS

Effects of temperature and light intensity on photofermentative hydrogen production by *Rhodobacter capsulatus* DSM1710 by use of acetic and lactic acids as substrates were studied. Based on the results obtained and the related discussion given in the previous Chapter the followings are concluded:

- Temperature of the hydrogen production medium kept in an incubator under illumination is higher than the incubator temperature and the difference between these temperatures increases with increase in light intensity.
- Cell growth was found to take place under all of the experimental conditions. Growth, which fitted well to the logistic model, was found to increase with increase in temperature but to decrease with increase in light intensity. Increase in light intensity was found to shorten the lag phase.
- Hydrogen was produced under all of the experimental conditions. The results, which fitted well to the Modified Gompertz Model, indicated that hydrogen production increased with increase in light intensity up to 6000 lux at 20°C, up to 5000 lux at 30°C and up to 3000 lux at 38°C and decreased beyond these values. The effect of light intensity on hydrogen production was slight in the 2000-4000 lux range at 20°C and in the 2000-5000 lux range at 30°C and 38°C. Lowest amount of hydrogen was produced 38°C for all light intensities. Medium temperature of about 30°C was found to be optimum for cumulative hydrogen.

- Substrate conversion efficiency, molar productivity, yield and product yield factor were found to increase with increase in light intensity up to certain values and to decrease at higher light intensities. These quantities were lowest at 38°C. Medium temperature of about 30°C was found to be optimum for these quantities also. Light conversion efficiency was found to decrease steadily with increase in light intensity at all temperature.
- Almost all of lactic acid and most of acetic acid was consumed while formic, butyric and propionic acids were first formed and then consumed in the experiments. Lactic acid was found to be almost completely consumed by first order kinetics in early times. Consumption of acetic acid was found to follow zeroth order kinetics in the early times when lactic acid existed in the system but the order shifted to one later when most of lactic acid was consumed.
- Due to change of organic acid concentrations, pH of the medium changed during the experiments. pH values encountered for all light intensities and temperatures were in the 6.0-8.5 range

REFERENCES

Akköse, S., 2008, “Expression Analysis of nitrogenase Genes in *Rhodobacter sphaeroides* O.U.001 Grown Under Different Physiological Conditions” M.Sc.Thesis in Biology Department, Middle East Technical University, Ankara, Turkey

Akköse, S., Gündüz, U., Yücel, M., Eroğlu, I., 2009, “Effects of ammonium ion, acetate and aerobic conditions on hydrogen production and expression levels of nitrogenase genes in *Rhodobacter sphaeroides* O.U.001”, International Journal of Hydrogen Energy, **34**:8818-8827

Androga, D.D., 2009, “Biological Hydrogen Production on Acetate in Continues Panel Photobioreactors Using *Rhodobacter capsulatus*”, M.Sc.Thesis in Chemical Engineering Department, Middle East Technical University, Ankara, Turkey

Arık, T., 1995, “Production of Hydrogen by *Rhodobacter sphaeroides* O.U. 001” M.Sc.Thesis in Biotechnology Department, Middle East Technical University, Ankara, Turkey

Barbosa, M.J., Rocha, J.M.S., Tramper, J., Wijffels, R.H., 2001, “Acetate as a carbon source for hydrogen production by photosynthetic bacteria”, Journal of Biotechnology **85**:25–33

Basak, N., Das, D., “Microbial Biohydrogen Production by *Rhodobacter sphaeroides* O.U.001 in Photobioreactor”, Proceedings of the World Congress on Engineering and Computer Science 2007, October 24-26, 2007, San Francisco, USA

Basak, N., Das, D., 2007, “The prospect of purple non-sulfur (PNS) photosynthetic bacteria for hydrogen production: the present state of the art”, World J. Microbiol. Biotechnol., **23**:31–42

Becker, A., Fritz-Wolf, K., Kabsch, W., Knappe, J., Schultz, S., Wagner, A.F.V., 1999, "Structure and mechanism of the glycyl radical enzyme pyruvate formate-lyase" (http://hasyweb.desy.de/science/annual_reports/1999_report/part2/contrib/72/1348.pdf)

Biebl, H., Pfennig, N., 1981, "Isolation of members of the family Rhodospirillaceae In: The prokaryotes" Editors: Starr, M.P., Stolp, H., Trüper, H.G., Balows, A., Schlegel, H.G., New York: Springer-Verlag, 267-273

Carlozzi, P., 2009, "The effect of irradiance growing on hydrogen photoevolution and on the kinetic growth in *Rhodospseudomonas palustris* strain 42OL", International Journal of Hydrogen Energy, **34**:7949-7958

Chen, C.Y., Yang, M.H., Yeh, K.L., Liu, C.H., Chang, J.S., 2008, "Biohydrogen production using sequential two-stage dark and photo fermentation processes", International Journal of Hydrogen Energy, **33**:4755-4762

Chong, M.L., Sabaratnam, V., Shirai Y., Hassan, M.A., 2009, "Biohydrogen production from biomass and industrial wastes by dark fermentation", International Journal of Hydrogen Energy, **34**:3277-3287

Claassen, P.A.M., De Vrije, T., 2006, "Non-thermal production of pure hydrogen from biomass: HYVOLUTION", International Journal of Hydrogen Energy, **31**:1416 – 1423

Das, D., Veziroglu, T.N., 2001, "Hydrogen production by biological processes: a survey of literature", International Journal of Hydrogen Energy, **26**:13-28

Das, D., Veziroglu, T.N., 2008, "Advances in biological hydrogen production processes", International Journal of Hydrogen Energy, **33**:6046-6057

De Vrije, T., Mars, A.E., Budde, M.A.W., Lai, M.H., Dijkema, C., De Waard, P., Claassen, P.A.M., 2007, "Glycolytic pathway and hydrogen yield studies of the extreme thermophile *Caldicellulosiruptor saccharolyticus*", Appl. Microbiol. Biotechnol., **74**:1358–1367

- Demmig-Adams, B., W. W. Adams III, 1992, “Photoprotection and other responses of plants to high light stress”, *Ann. Rev. Plant Physiol. Plant Mol. Biol.*, **43**:599–626
- Ding, J., Liu, B.F., Ren, N.Q., Xing, D.F., Guo, W.Q., Xu, J.F., Xie, G.J., 2009, “Hydrogen production from glucose by co-culture of *Clostridium Butyricum* and immobilized *Rhodospseudomonas faecalis* RLD-53”, *International Journal of Hydrogen Energy*, **34**:3647-3652
- Eroğlu, E., Gündüz, U., Yücel, M., Turker, L., Eroğlu, I., 2004, “Photobiological hydrogen production by using olive mill wastewater as a sole substrate source”, *International Journal of Hydrogen Energy*, **29**:163 – 171
- Eroğlu, I., Tabanoğlu, A., Gündüz, U., Eroğlu, E., Yücel, M., 2008, “Hydrogen production by *Rhodobacter sphaeroides* O.U.001 in a flat plate solar bioreactor”, *International Journal of Hydrogen Energy*, **33**:531-541
- Favinger, J., Stadtwald, R., Gest, H., 1989, “*Rhodospirillum centenum*, sp. nov., a thermotolerant cyst-forming anoxygenic photosynthetic bacterium”, *Antonie Van Leeuwenhoek*, **55**: 291-296
- Fay, P., 1992, “Oxygen Relations of Nitrogen Fixation in Cyanobacteria”, *Microbiological Reviews*, **56**:340-373
- Fu, H., Burris, R.H., 1989, “Ammonium Inhibition of Nitrogenase Activity in *Herbaspirillum seropedicae*”, *Journal of Bacteriology*, **171**:3168-3175
- Fujikawa, H., Kai, A., Morozumi, S., 2004, “A new logistic model for *Escherichia coli* growth at constant and dynamic temperatures”, *Food Microbiology* **21**:501–509
- Gadhamshtetty, V., Sukumaran, A., Nirmalakhandan, N., Myint, M.T., 2008, “Photofermentation of malate for Biohydrogen production—A modeling approach”, *International Journal of Hydrogen Energy*, **33**:2138-2146
- Gibson, A.M., Bratchell, N., Robert, T.A., 1987, “The effect of sodium chloride and temperature on the rate and extent of growth of *Clostridium botulinum* type A in pasteurized pork slurry”, *Journal of Applied Bacteriology*, **62**: 479-490

Gurgun, V., Kirschner, G., Pfennig, N., 1976, "Fermentation of pyruvate by seven species of phototrophic purple bacteria". *Z Allg Mikrobiol*, **16**: 573-576

Hallenbeck, P.C., Benemann, J.R., 2002, "Biological hydrogen production; fundamentals and limiting processes", *International Journal of Hydrogen Energy*, **27**:1185-1193

Haselkorn, R., Lapidus, A., Kogan, Y., Vlcek, C., Paces, J., Paces, V., Ulbrich, P., Pecenkova, T., Rebrekov, D., Milgram, A., Mazur, M., Cox, R., Kyrpides, N., Ivanova, N., Kapatral, V., Los, T., Lykidis, A., Mikhailova, N., Reznik, G., Vasieva, O., Fonstein, M., 2001, "The *Rhodobacter capsulatus* genome", *Photosynthesis Research*, **70**: 43–52

He, D., Bultel, Y., Magnin, J.P., Willison, J.C., 2006, "Kinetic analysis of photosynthetic growth and photohydrogen production of two strains of *Rhodobacter capsulatus*", *Enzyme and Microbial Technology* **38**:253–259

Henson, B.J., Watson, L.E., Barnum, S.R., 2004, "The Evolutionary History of Nitrogen Fixation, as Assessed by NifD", *J. Mol. Evol*, **58**:390–399

Hillmer, P., Gest, H., 1977, "H₂ Metabolism in the Photosynthetic Bacterium *Rhodospseudomonas capsulata*: H₂ Production by Growing Cultures", *Journal of Bacteriology*, **129**:724-731

Hochman, A., Burris, R.H., 1981, "Effect of Oxygen on Acetylene Reduction by Photosynthetic Bacteria", *Journal of Bacteriology*, **147**:492-499

Holladay, J.D., Hu, J., King, D.L., Wang, Y., 2009, "An overview of hydrogen production Technologies", *Catalysis Today*, **139**: 244-260

Horton, P., A. V. Ruban, R. G. Walters, 1994, "Regulation of light harvesting in green plants", *Plant Physiol.*, **106**:415–420

Husted, E., Steinbüchel, A., Schlegel, H.G., 1993, "Relationship between the photoproduction of hydrogen and the accumulation of PHB in non-sulphur purple bacteria", *Appl Microbiol Biotechnol*, **39**:87-93

Imhoff, F.J., 1995, "Taxonomy and physiology of phototropic purple bacteria and green sulfur bacteria. Anoxygenic Photosynthetic Bacteria 2", 1-15

Imhoff, J.F., Truper, H.G., Pfennig, N., 1984, "Rearrangement of the Species and Genera of the Phototrophic Purple Nonsulfur Bacteria", *International Journal of Systematic Bacteriology*, **34**: 240-343

Kapdan, I.K., Kargi, F., 2006, "Bio-hydrogen production from waste materials", *Enzyme and Microbial Technology*, **38**:569–582

Kars, G., Gündüz, U., Rakhely, G., Yücel, M., Eroğlu, I., Kovacs, K.L., 2008, "Improved hydrogen production by uptake hydrogenase deficient mutant strain of *Rhodobacter sphaeroides* O.U.001", *International Journal of Hydrogen Energy*, **33**:3056-3060

Khatipov, E., Miyake, M., Miyake, J., Asada, Y., 1998, "Accumulation of poly- β -hydroxybutyrate by *Rhodobacter sphaeroides* on various carbon and nitrogen sources", *FEMS Microbiology Letters*, **162**:39-45

Kim, M.S., Baek, J.S., Lee, J.K., 2006, "Comparison of H₂ accumulation by *Rhodobacter sphaeroides* KD131 and its uptake hydrogenase and PHB synthase deficient mutant", *International Journal of Hydrogen Energy*, **31**:121-127

Kitajima, Y., El-Shishtawy, R.M.A, Ueno, T., Otsuka, S., Miyake, J., Morimoto, M., 1998, "Analysis of Compensation Point of Light Using Plane-Type Photosynthetic Bioreactor", *Biohydrogen*, edited by Zaborsky et al. Plenum Press

Klemme, H., 1993, "Photoproduction of hydrogen by purple bacteria: a critical evaluation of the rate limiting enzymatic steps", *Z. Naturforsch.*, **48**: 482–487

Koku, H., Eroğlu, I., Gunduz, U., Yucel, M., Turker, L., 2002, "Aspects of the Metabolism of Hydrogen Production by *Rhodobacter sphaeroides*", *International Journal of Hydrogen Energy*, **2**:1315-1329

Koku, H., Eroğlu, I., Gündüz, U., Yücel, M., Türker, L., 2003, "Kinetics of biological hydrogen production by the photosynthetic bacterium *Rhodobacter sphaeroides* O.U. 001", *International Journal of Hydrogen Energy*, **28**: 381-388

Kondo, T., Arakawa, S., Hirai, T., Wakayama, T., Hara, M., Miyake, J., 2002, "Enhancement of Hydrogen Production by a Photosynthetic Bacterium Mutant with Reduced Pigment", *Journal of Bioscience and Bioengineering*, **93**:145-150

Kotay, S.M, Das, D., 2007, "Biohydrogen as a renewable energy resource—Prospects and potentials", *International Journal of Hydrogen Energy*, doi: 10.1016/j.ijhydene.2007.07.031

Kothari, R., Buddhi, D., Sawhney, R.L., 2008, "Comparison of environmental and economic aspects of various hydrogen Production Methods", *Renewable and Sustainable Energy Reviews*, **12**: 553-563

Kovács, K.L., Maróti, G., Rákhelya, G., 2006, "A novel approach for biohydrogen production", *International Journal of Hydrogen Energy*, **31**:1460 – 1468

Li, X., Wang, Y.H., Zhang, S.L., Chu, J., Zhang, M., Huang, M.Z., Zhuang, Y.P., 2009, "Enhancement of phototrophic hydrogen production by *Rhodobacter sphaeroides* ZX-5 using a novel strategy-shaking and extra-light supplementation approach", *International Journal of Hydrogen Energy*, **34**:9677-9685

Liu, J., Bukatin, V.E., Tsygankov, A.A., 2006, "Light energy conversion into H₂ by *Anabaena variabilis* mutant PK84 dense cultures exposed to nitrogen limitations", *International Journal of Hydrogen Energy*, **31**:1591 – 1596

Macler, B.A., Pelroy, R.A., Bassham, J.A., 1979, "Hydrogen Formation in Nearly Stoichiometric Amounts from Glucose by a *Rhodospseudomonas sphaeroides* mutant", *Journal of Bacteriology*, **138**:446-452

Melis, A., 2002, "Green alga hydrogen production: progress, challenges and prospects", 2002, **27**:1217-1228

Miyake J., Tomizuka, N., Kawamura, S., 1982, Report of the Fermentation Research Institute, No:58

Miyake, J., Kawamura, S., 1987, "Efficiency of light energy conversion to hydrogen by the photosynthetic bacterium *Rhodobacter sphaeroides*", *International Journal of Hydrogen Energy*, **12**:147-149

Miyamoto, K., 1997, "Renewable biological systems for alternative sustainable energy production" FAO Agricultural Services Bulletin (edited by K. Miyamoto), Food and Agriculture Organization of the United Nation, pp:1-5

Mu, Y., Yu, H.Q., Wang, G., 2007, "A kinetic approach to anaerobic hydrogen-producing process", Water Research, **41**:1152-1160

Nakada, E., Kaji, Y., Aoyama, K., Nishikata, S., Asada, Y., Miyake, J., 1993, "Photosynthetic Bacterial Hydrogen Production Combined with a Fuel Cell for Light Energy", New Energy Systems and Conversions by Universal Academy Pres, 225-228

Nath, K., Das, D., 2004, "Improvement of fermentative hydrogen production: various Approaches" Appl. Microbiol. Biotechnol., **65**: 520–529

Nath, K., Das, D., 2009, "Effect of light intensity and initial pH during hydrogen production by an integrated dark and photofermentation process", International Journal of Hydrogen Energy, **34**:7497-7501

Nath, K., Kumar, A., Das, D., 2005, "Hydrogen production by *Rhodobacter sphaeroides* strain O.U.001 using spent media of *Enterobacter cloacae* strain DM11", Appl Microbiol Biotechnol, **68**: 533–541

Nath, K., Muthukumar, M., Kumar, A., Das, D., 2008, "Kinetics of two-stage fermentation process for the production of hydrogen", International Journal of Hydrogen Energy, **33**:1195 – 1203

Obeid, J., Magnin, J.P. Flaus, J.M., Adrot, O., Willison, J.C., Zlatev, R., 2009, "Modelling of hydrogen production in batch cultures of the photosynthetic bacterium *Rhodobacter capsulatus*", International Journal of Hydrogen Energy , **34**:180-185

Özgür, E., Uyar, B., Öztürk, Y., Yücel, M., Gündüz, U., Eroğlu, I., 2010, "Biohydrogen production by *Rhodobacter capsulatus* on acetate at fluctuating temperatures", Resources, Conservation and Recycling **54**:310–314

Öztürk, Y., Yücel, M., Daldal, F., Mandacı, S., Gündüz, U., Türker, L., Eroğlu, I., 2006, “Hydrogen production by using *Rhodobacter capsulatus* mutants with genetically modified electron transfer chains”, International Journal of Hydrogen Energy, **31**:1545 – 1552

Paschen, A., Drepper, T., Masepohl, B., Klip, W., 2001, “*Rhodobacter capsulatus* nifA mutants mediating nif gene expression in the presence of ammonium”, FEMS Microbiology Letters **200**:207-213

Pearl, R., Reed, L.J., 1920, “On the rate of growth of the population of the United States since 1790 and its mathematical representation”, Proc. Nat. Acad. Sci., **6**:275–288.

Pellerin, N.B., and Gest, H., 1983, “Diagnostic Features of the Photosynthetic Bacterium *Rhodospirillum rubrum*”, Current Microbiology, **9**: 339-344.

Pierrard, J., Ludden, P.W., Roberts, G.P., 1993, “Posttranslational Regulation of Nitrogenase in *Rhodobacter capsulatus*: Existence of Two Independent Regulatory Effects of Ammonium”, Journal of Bacteriology, **175**:1358-1366

Redwood, M.D., Macaskie, L.E., 2006, “A two-stage, two-organism process for biohydrogen from glucose”, International Journal of Hydrogen Energy, **31**:1514 – 1521

Riis, T., Hagen, E.F., Vie, P.J.S., Ulleberg, Ø., 2005, “Hydrogen Production – Gaps and Priorities” IEA Hydrogen Implementing Agreement (HIA) , 11 pages

Rocha, J.S., Barbosa, M.J., Wijffels, R.H., 2001, “Hydrogen Production by Photosynthetic Bacteria: Culture Media, Yields and Efficiencies”, In: J. Miyake, T. Matsunaga, A. San Pietro (Editors), Biohydrogen II - An Approach to Environmentally Acceptable Technology, Elsevier Science Ltd., UK, 3-32.

Sasikala, K., Ramana, C.H., Rao, P.R., 1991, “Environmental Regulation for Optimal Biomass Yield and Photoproduction of Hydrogen by *Rhodospirillum rubrum* O.U.001”, International Journal of Hydrogen Energy, **16**: 597-601

Sasikala, K., Ramana, C.V., Rao, P.R., Subrahmanyam, M., 1990, "Effect of Gas Phase on the Photoproduction of Hydrogen and Substrate Conversion Efficiency in the Photosynthetic Bacterium *Rhodobacter sphaeroides* O.U.001", *International Journal of Hydrogen Energy*, **15**: 795-797.

Shi, X.Y., Yu, H.Q., 2005, "Response surface analysis on the effect of cell concentration and light intensity on hydrogen production by *Rhodopseudomonas capsulata*", *Process Biochemistry*, **40**:2475-2481

Stevens, P., Vertonghen, C., De Vos, P., De Lep, J., 1984, "The Effects of Temperature and Light Intensity on Hydrogen Gas production by Different *Rhodopseudomonas capsulata* strains", *Biotechnology Letters* **6**:277-282

Su, H., Cheng, J., Zhou, J., Song, W., Cen, K., 2009, "Combination of dark- and photo-fermentation to enhance hydrogen production and energy conversion efficiency", *International Journal of Hydrogen Energy*, **34**:8846-8853

Tabanoglu, A., 2002, "Hydrogen production by *Rhodobacter sphaeroides* O.U.001 in a solar bioreactor", MSc. Thesis in Biotechnology, Middle East Technical University, Ankara.

Tao, Y., Chen, Y., Wu, Y., He, Y., Zhou, Z., 2007, "High hydrogen yield from a two-step process of dark- and photo-fermentation of sucrose", *International Journal of Hydrogen Energy*, **32**:200 – 206

Tsoularis, A., Wallace, J., 2002, "Analysis of logistic growth models", *Mathematical Biosciences* **179**:21–55

Tsuihiji, H., Yamazaki, Y., Kamikubo, H., Imamoto, Y., Kataoka, M., 2006, "Cloning and Characterization of *nif* Structural and Regulatory Genes in the Purple Sulfur Bacterium, *Halorhodospira halophila*", *Journal of Bioscience and Bioengineering*, **101-3**: 263-270

Ünlü, G., Sevinç, P., Gündüz, U., 2009, "Expression Analysis of *nif* A and *nif* H genes in *Rhodobacter sphaeroides* O.U.001 at different temperatures", presented in International Symposium on Biotechnology: Developments and Trends, BTEC 2009, METU, Ankara, Turkey

Uyar, B., 2008, “Hydrogen Production by Microorganisms in Solar Bioreactor”, Ph.D. Thesis in Biotechnology Engineering Department, Middle East Technical University, Ankara, Turkey

Uyar, B., Eroglu, I., Yücel, M., Gündüz, U., Türker, L., 2005, “ Effect of Light Intensity and Illumination Protocol on Biological Hydrogen Production by *Rhodobacter sphaeroides* O.U. 001”, presented in Proceedings International Hydrogen Energy Congress and Exhibition IHEC 2005, 13-15 July 2005 Istanbul, Turkey,

Uyar, B., Eroglu, I., Yücel, M., Gündüz, U., Türker, L., 2007, “Effect of light intensity, wavelength and illumination protocol on hydrogen production in photobioreactors”, International Journal of Hydrogen Energy, **32**:4670 – 4677

Valdez-Vazquez, I., Poggi-Varaldo, H.M., 2009, “Hydrogen production by fermentative consortia”, Renewable and Sustainable Energy Reviews, 13:1000–1013
Verhulst, P.F, 1838, “Notice sur la loi que la population suit dans son accroissement” ,Corr. Math. et Phys. Publ. par A. Quetelet. T **X**:113–121.

Vignais, P.M., Colbeau, A., Willison, J.C., Jouanneau, Y., 1985, “Hydrogenase, Nitrogenase, and Hydrogen Metabolism in Photosynthetic Bacteria”, Adv. Microbial Phys., **26**: 154-234

Vignais, P.M., Willison J.C., Jouanneau, Y., Colbeau, A., Magnin, J.P., Leclerc, M., Schatt, E., Edited by Bothe, H., de Bruijn, F.J., Newton, W.E., 1988, Proceedings of the 7th International Congress on Nitrogen Fixation, March 13-20, 1988, Köln, Germany

Wachenheim, D.E., Patterson, J.A., Ladisch, M.R., 2003, “Analysis of the logistic function model: derivation and applications specific to batch cultured microorganisms”, Bioresource Technology **86**:157–164

Wakayama, T., Nakada, E., Asada, Y., Miyake, J., 2000, “Effect of Light/Dark Cycle on Bacterial Hydrogen Production by *Rhodobacter sphaeroides* RV”, Applied Biochemistry and Biotechnology, **84-86**: 431-440

Waligórska, M., Seifert, K., Górecki, K., Moritz, M., Łaniecki, M., 2009, “Kinetic model of hydrogen generation by *Rhodobacter sphaeroides* in the presence of NH_4^+ ions”, *Journal of Applied Microbiology* **107**:1308–1318

Wang, J., Wan, W., 2009, “Kinetic models for fermentative hydrogen production: A review”, *International Journal of Hydrogen Energy*, **34**:3313-3323

Yordanov, I., Velikova, V., 2000, “ Photoinhibition of Photosystem 1” *Bulg. J. Plant Physiol.* , **26**: 70–92

Zwietering, M.H., Jongenburger, I., Rombouts, F.M., Van't Riet, K., 1990, “Modeling of the bacterial growth curve”, *Appl Environ Microbiol*” **56**:1875–1881

APPENDIX A

COMPOSITION OF THE GROWTH AND HYDROGEN PRODUCTION MEDIA

Table A.1 The constituents of the growth and hydrogen production medium per liter of solution.

Medium Composition	Growth Medium	Hydrogen Production Medium
KH ₂ PO ₄	3 g	3 g
MgSO ₄ .7H ₂ O	0.5 g	0.5 g
CaCl ₂ .2H ₂ O	0.05 g	0.05 g
Acetate	1.15 ml	2.29 ml
Lactate	0.56 ml	0.56 ml
Na-Glutamate	1.85 g	0.36 g
Vitamin Solution	0.1 ml	1 ml
Trace Element Solution	0.1 ml	0.1 ml
Fe-Citrate	0.5 ml	0.1 ml

Table A.2 The composition of 1 liter of vitamin solution

Composition	Amount
Thiamine chloride hydrochloride	500 mg
Niacin (Nicotinic Acid)	500 mg
D+ Biotin	15 mg

Table A.3 The composition of 1 liter of trace element solution

Composition	Amount
ZnCl ₂	70 mg
MnCl ₂ .4H ₂ O	100 mg
H ₃ BO ₃	60 mg
CoCl ₂ .6H ₂ O	200 mg
CuCl ₂ .2H ₂ O	20 mg
NiCl ₂ .6H ₂ O	20 mg
Na ₂ MoO ₄ .2H ₂ O	40 mg
HCl (25% v/v)	1 ml

Ferric Citrate Solution:

0.5 g Fe-citrate was dissolved in 100 ml distilled water and sterilized by autoclaving.

APPENDIX B

OPTICAL DENSITY-DRY WEIGHT CALIBRATION CURVE

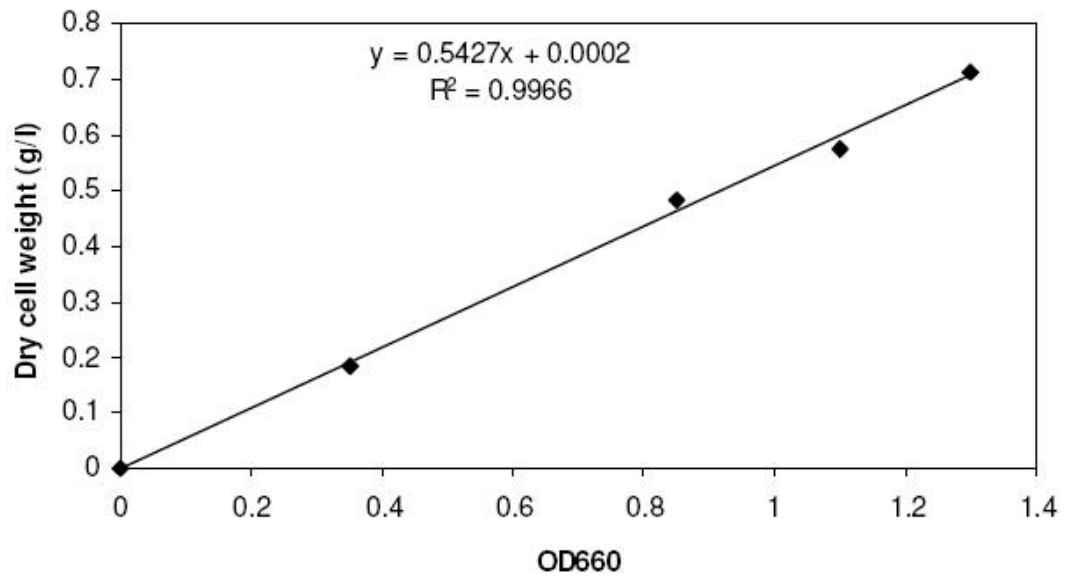
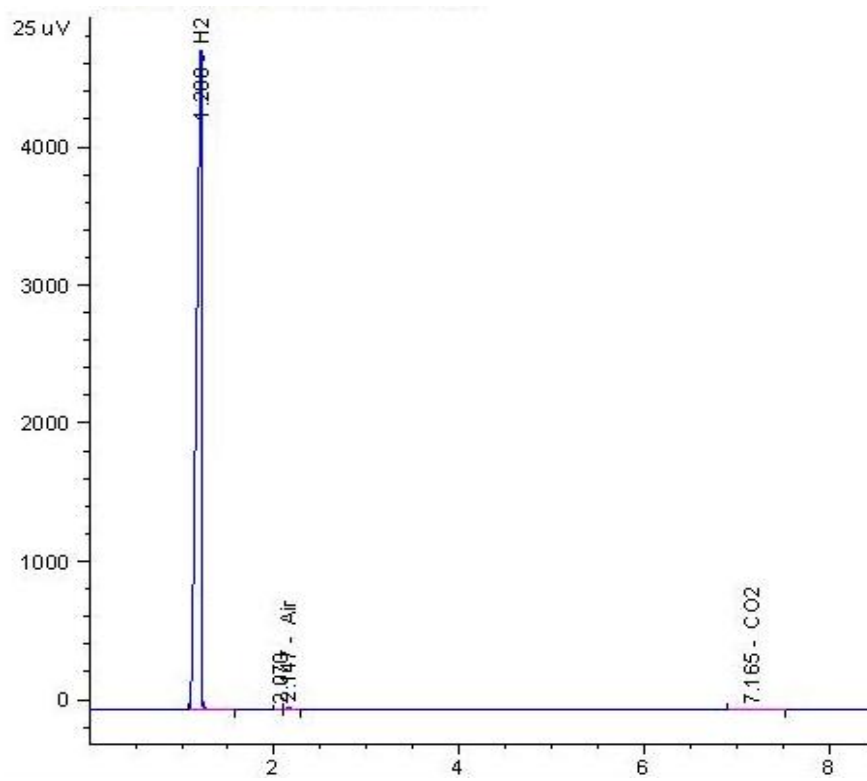


Figure B. Calibration curve and the regression trend line for *Rhodobacter capsulatus* (DSM 1710) dry weight versus OD660 (Uyar, 2008).

APPENDIX C

SAMPLE GAS CHROMATOGRAM



RetTime [min]	Type	Area [25 uV*s]	Amt/Area	Norm %	Grp	Name
1.208	BB	1.78157e4	5.36760e-3	92.790983	H2	H2
2.147	VB	104.16668	4.30476e-2	4.351104	Air	Air
7.165	BB	52.88443	5.56929e-2	2.857913	CO2	CO2

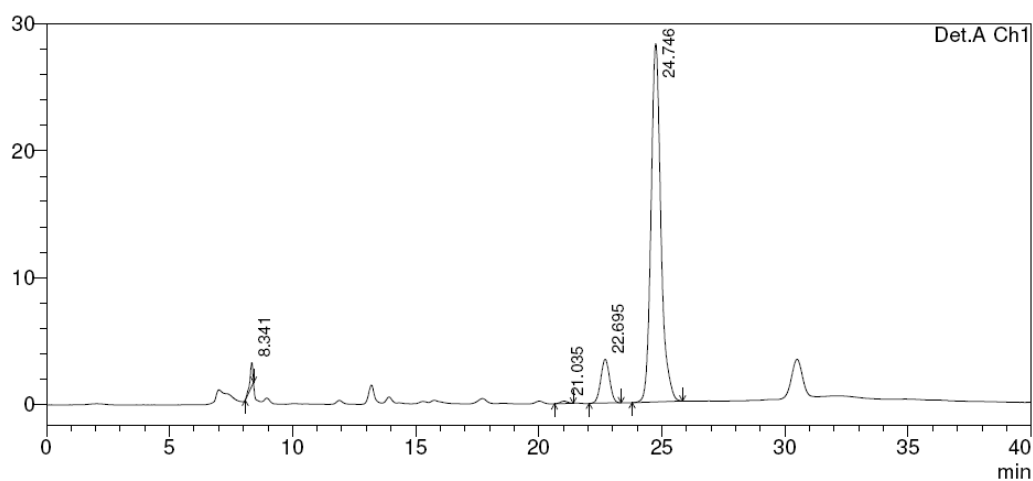
Totals : 100.000000

Figure C. Sample Gas Analysis Chromotogram

APPENDIX D

ORGANIC ACID ANALYSIS

D1. Sample HPLC Chromatogram



PeakTable

Detector A Ch1 210nm

Peak#	Ret. Time	Area	Height	Area %	Height %
1	8.341	14689	1859	1.654	5.516
2	21.035	3735	182	0.420	0.542
3	22.695	86422	3453	9.730	10.248
4	24.746	783359	28200	88.196	83.694
Total		888205	33695	100.000	100.000

Figure D.1 Sample HPLC analysis chromatogram. Peak 1 (mobile phase- H_2SO_4), Peak 2 (lactic acid), Peak 3 (Formic acid) and Peak 4 (acetic acid).

D2. Sample Acetic Acid Calibration Curve

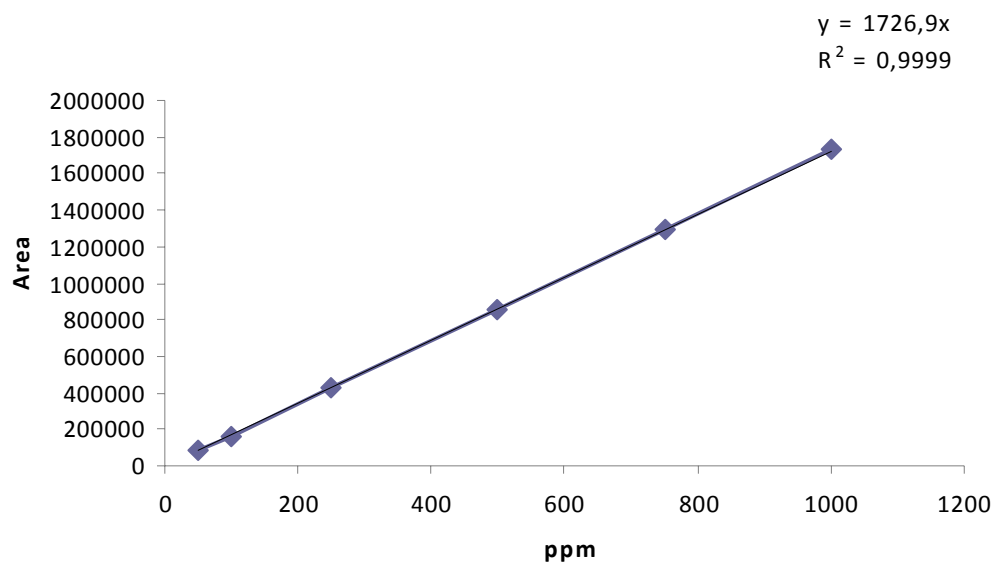


Figure D.2 Sample Acetic Acid Calibration Curve

APPENDIX E

LOGISTIC MODEL

E1-E6. Curves fitted to the logistic model together with the experimental data for different light intensities at 20°C

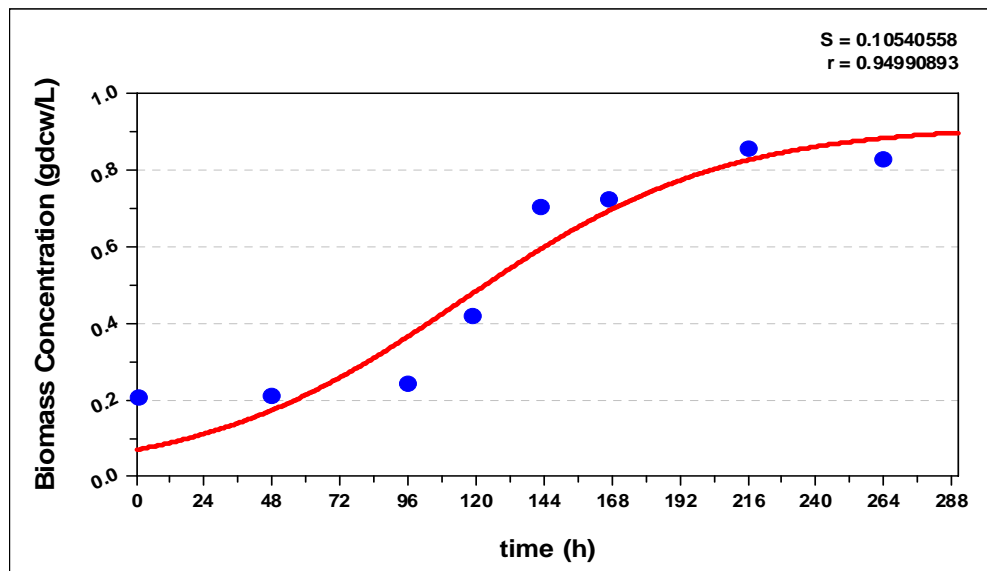


Figure E. 1 The logistic growth model at 20°C and 1500 lux

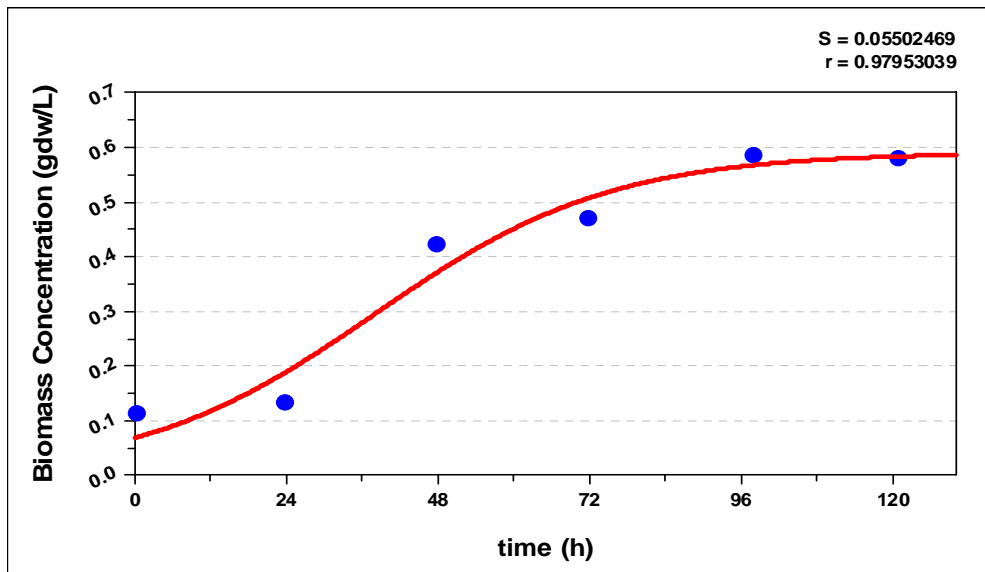


Figure E. 2 The logistic growth model at 20°C and 3000 lux

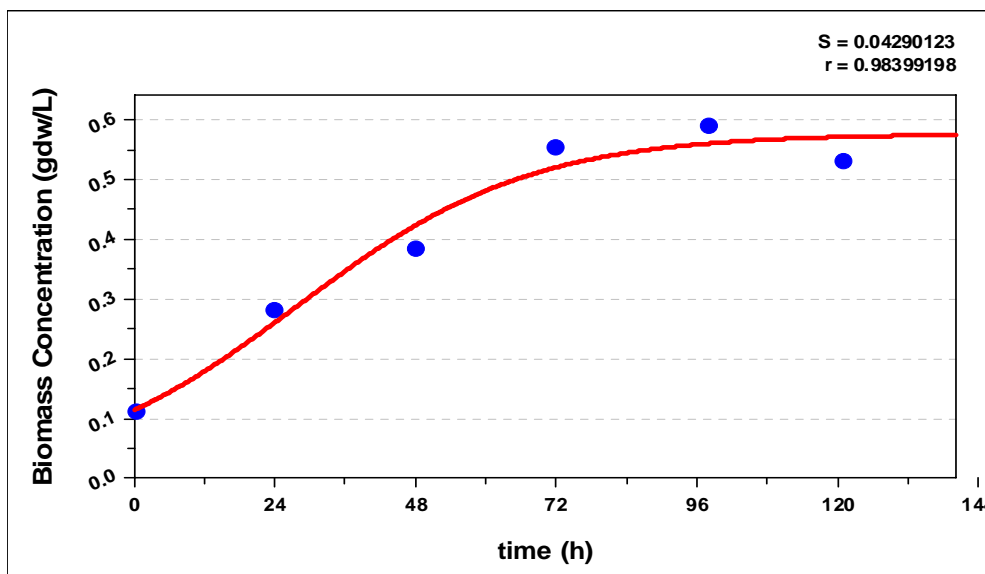


Figure E. 3 The logistic growth model at 20°C and 4000 lux

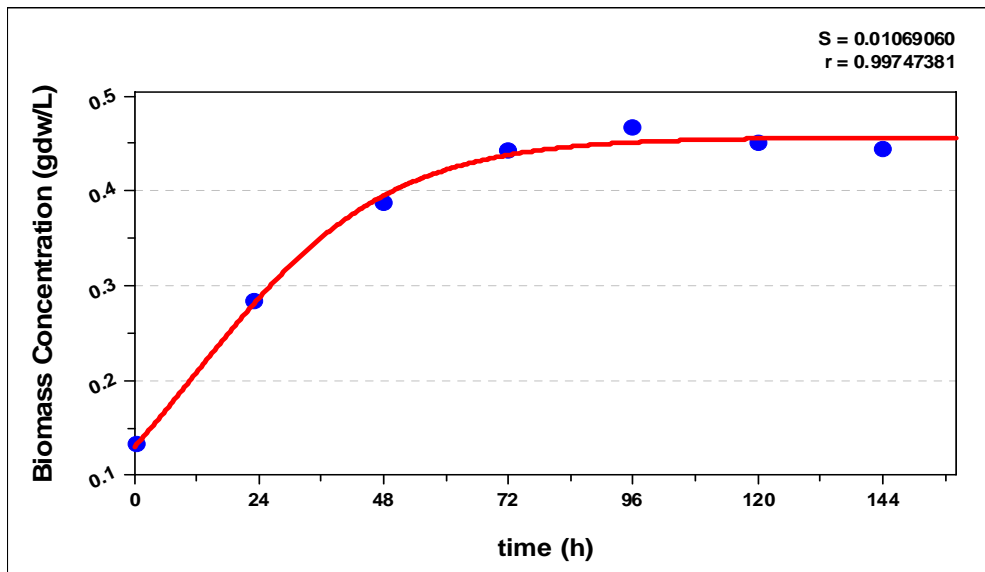


Figure E. 4 The logistic growth model at 20°C and 5000 lux

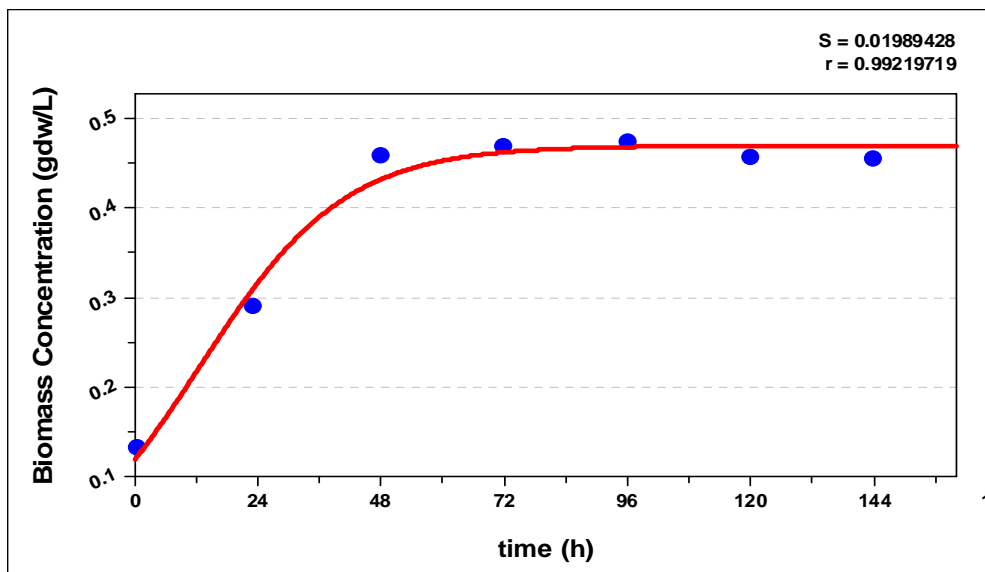


Figure E. 5 The logistic growth model at 20°C and 6000 lux

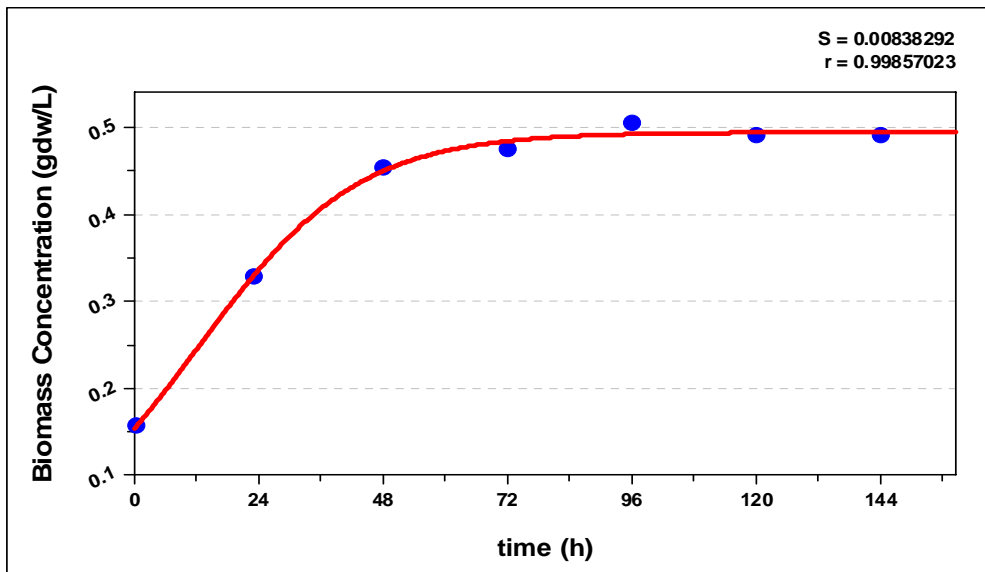


Figure E. 6 The logistic growth model at 20°C and 7000 lux

E7-E.13 Curves fitted to the logistic model together with the experimental data for different light intensities at 30°C

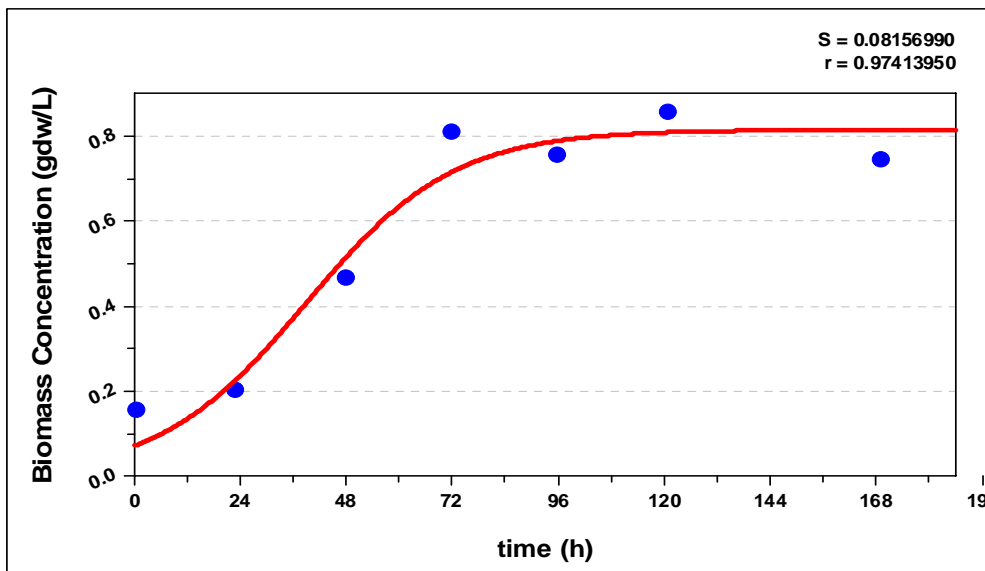


Figure E. 7 The logistic growth model at 30°C and 1500 lux

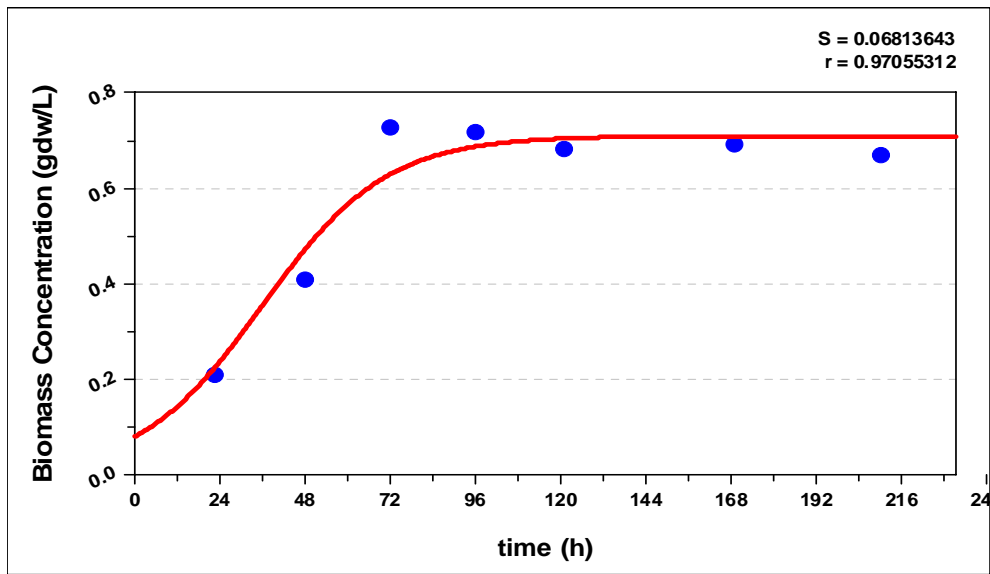


Figure E. 8 The logistic growth model at 30°C and 2000 lux

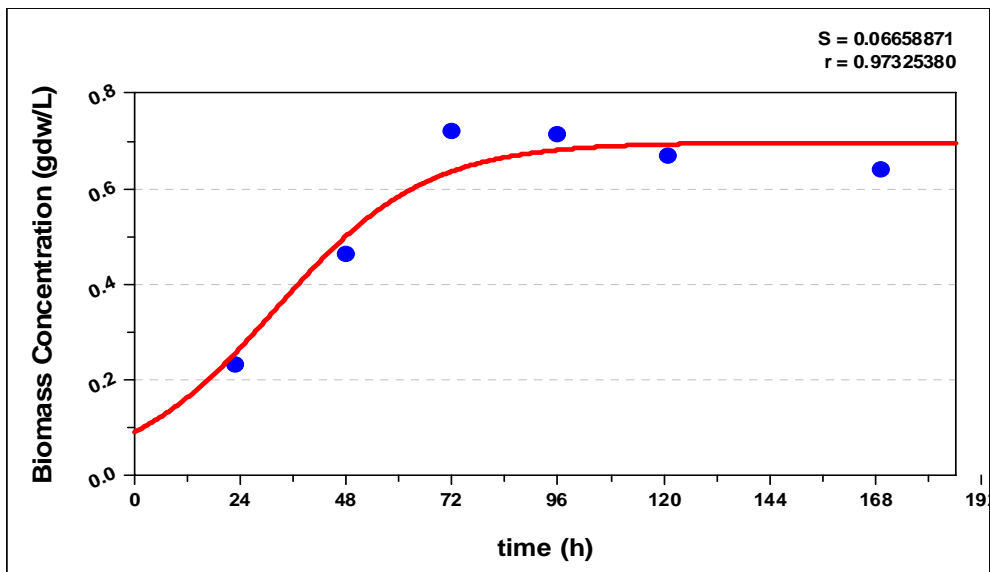


Figure E. 9 The logistic growth model at 30°C and 3000 lux

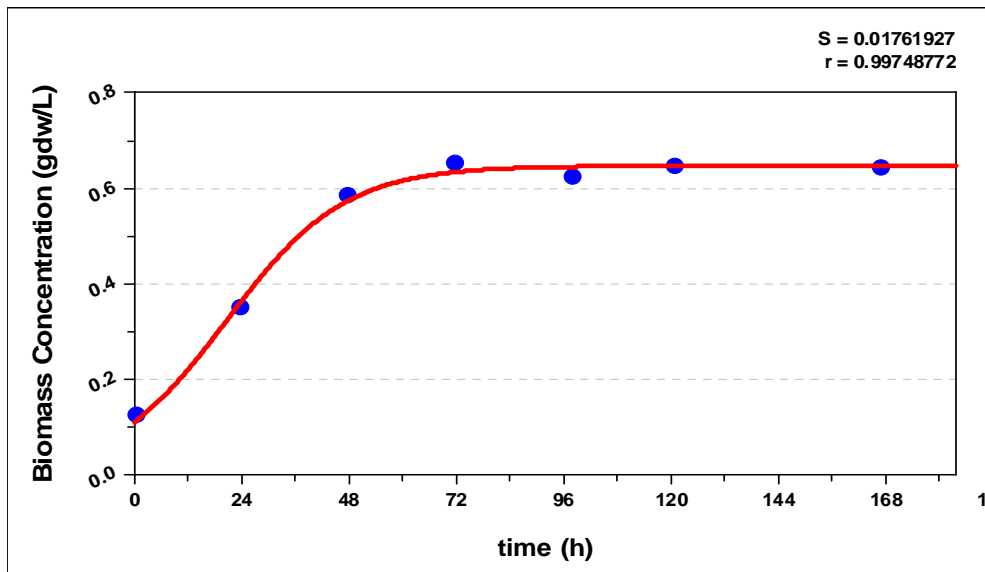


Figure E.10 The logistic growth model at 30°C and 4000 lux

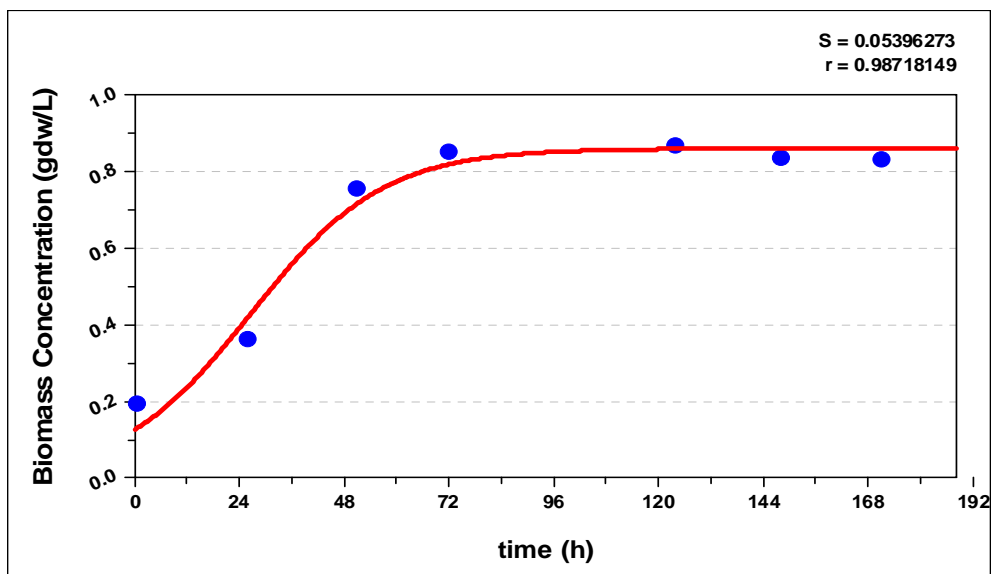


Figure E.11 The logistic growth model at 30°C and 5000 lux

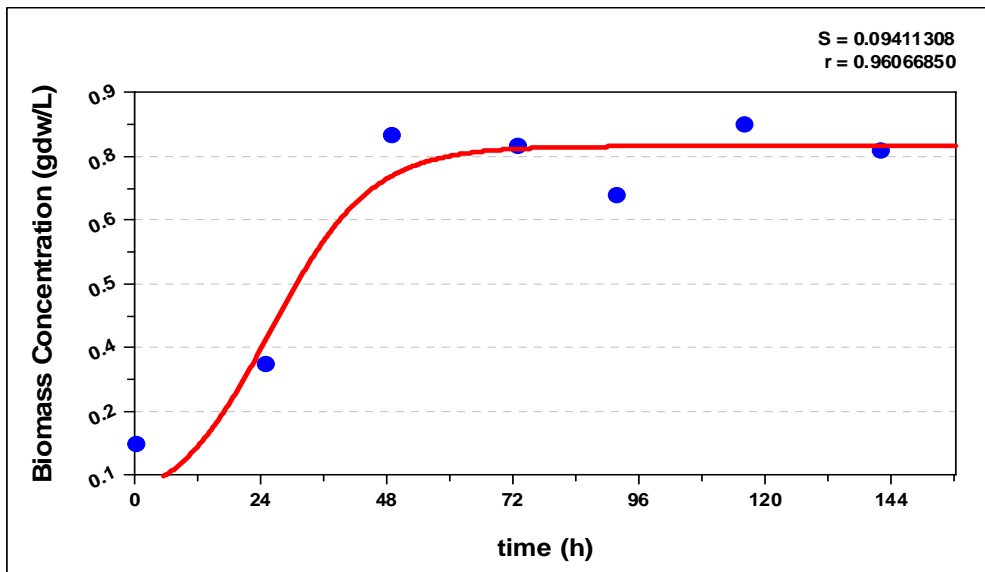


Figure E.12 The logistic growth model at 30°C and 6000 lux

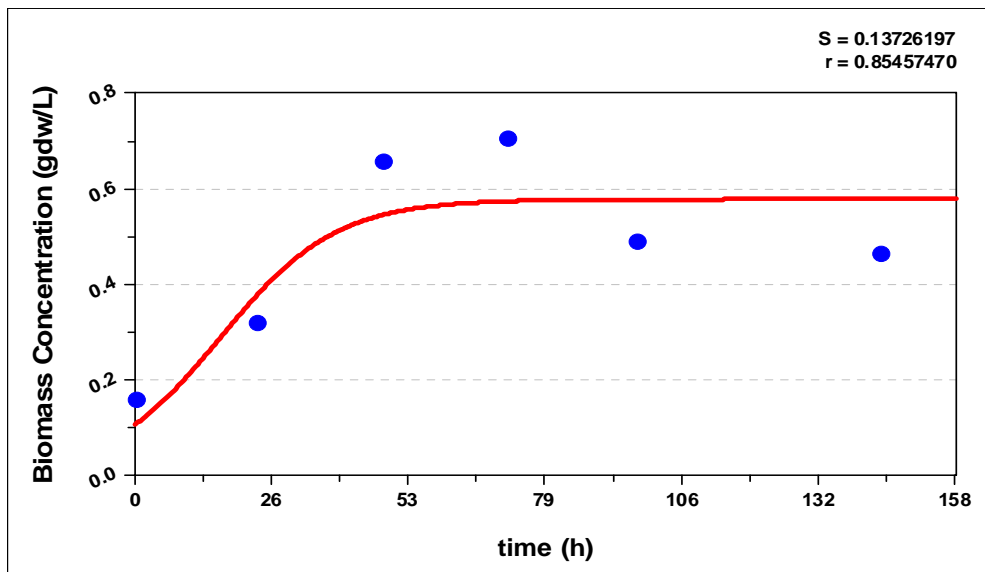


Figure E.13 The logistic growth model at 30°C and 7000 lux

E14-E .18 Curves fitted to the logistic model together with the experimental data for different light intensities at 38°C

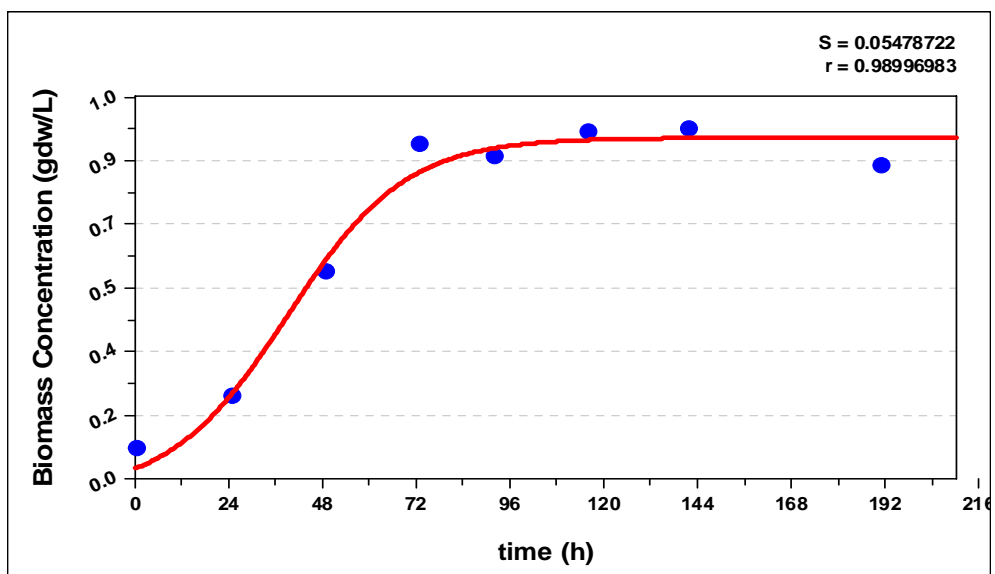


Figure E.14 The logistic growth model at 38°C and 1500 lux

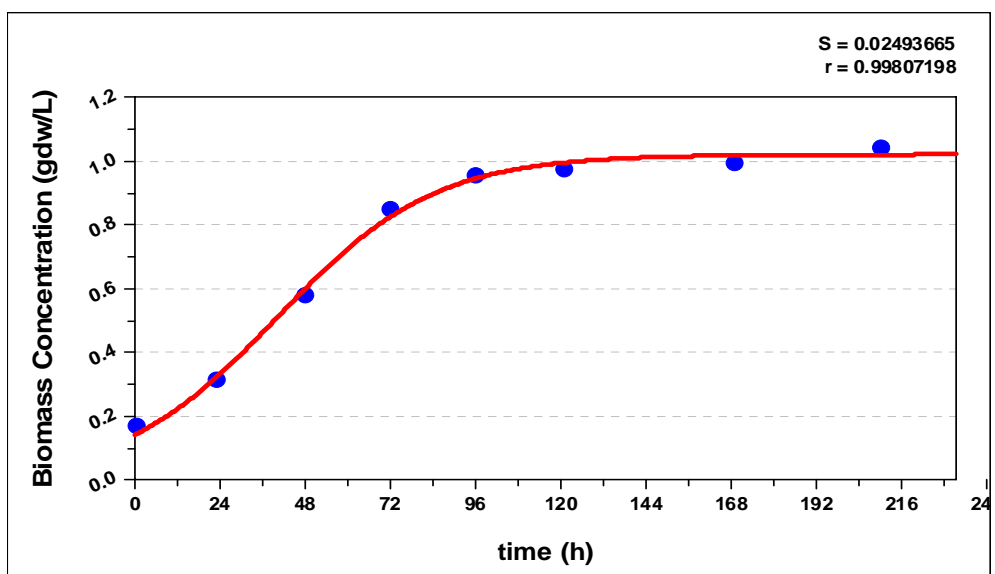


Figure E.15 The logistic growth model at 38°C and 2000 lux

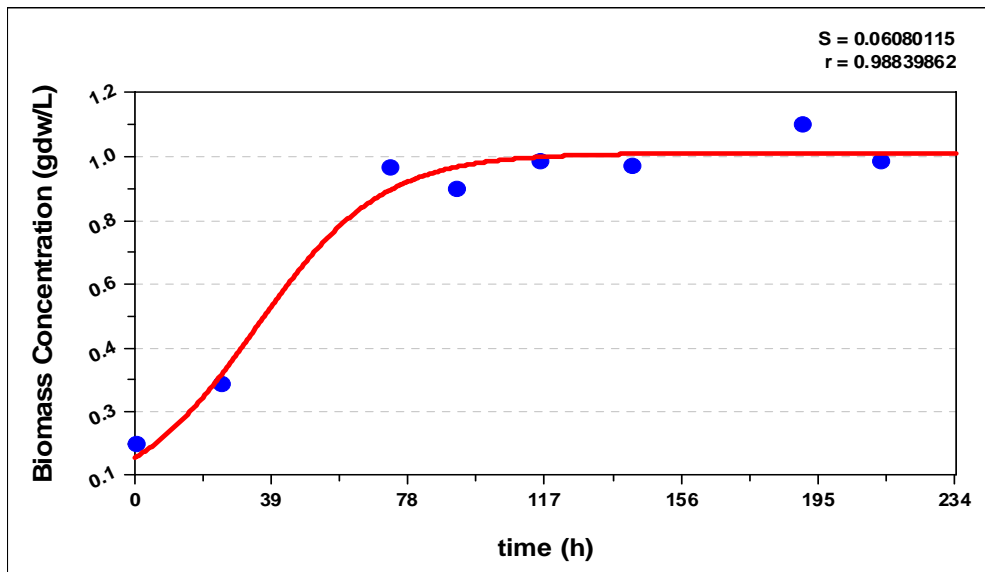


Figure E.16 The logistic growth model at 38°C and 3000 lux

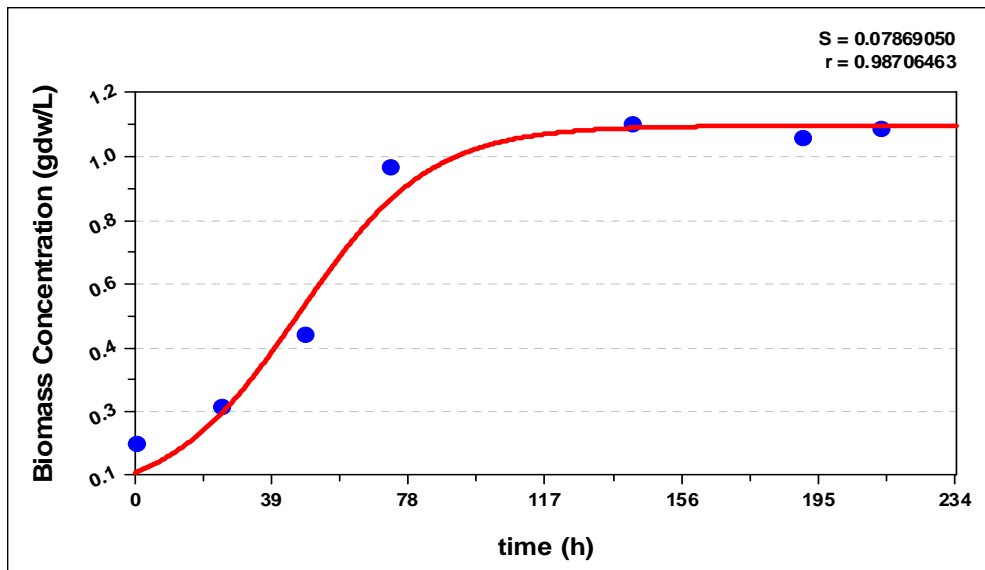


Figure E.17 The logistic growth model at 38°C and 4000 lux

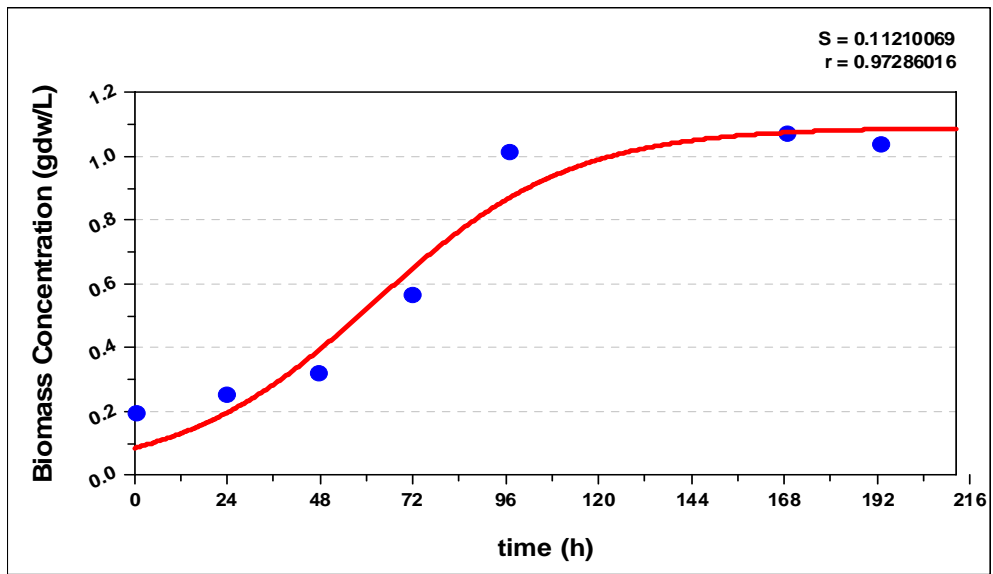


Figure E.18 The logistic growth model at 38°C and 5000 lux

APPENDIX F

MODIFIED GOMPERTZ MODEL

F1-F6. Curves fitted to the Modified Gompertz Model together with the experimental data for different light intensities at 20°C

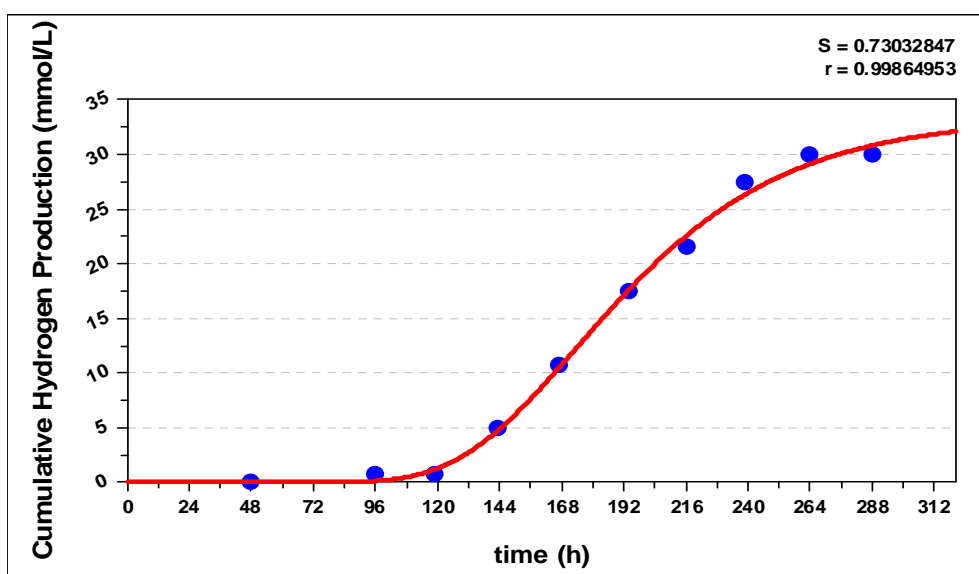


Figure F.1 The Modified Gompertz Model at 20°C and 1500 lux

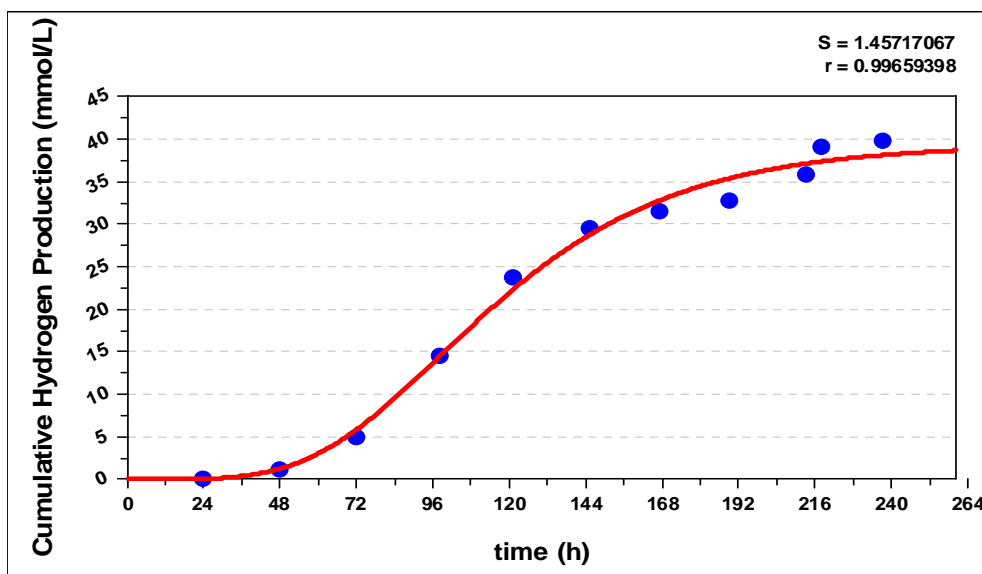


Figure F.2 The Modified Gompertz Model at 20°C and 3000 lux

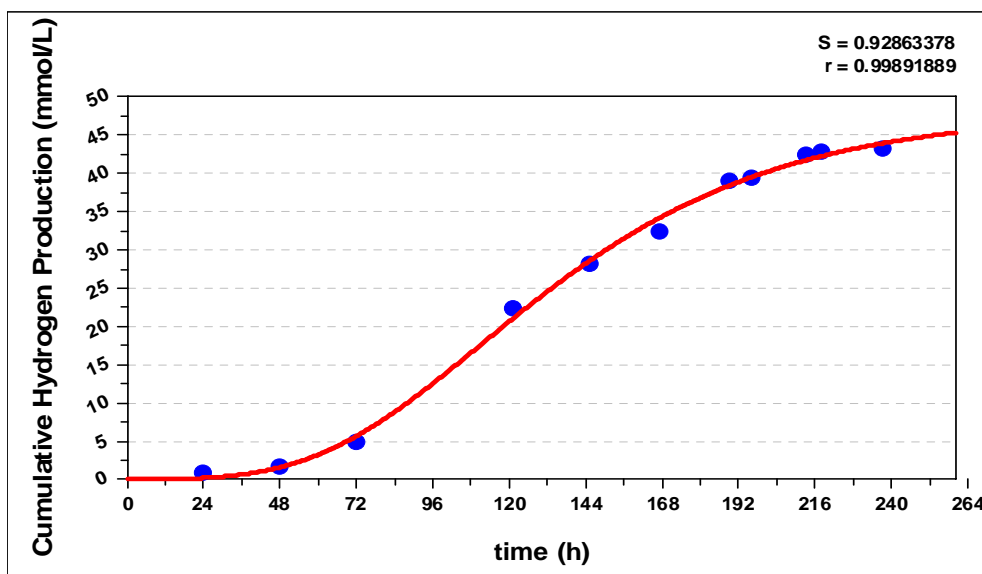


Figure F.3 The Modified Gompertz Model at 20°C and 4000 lux

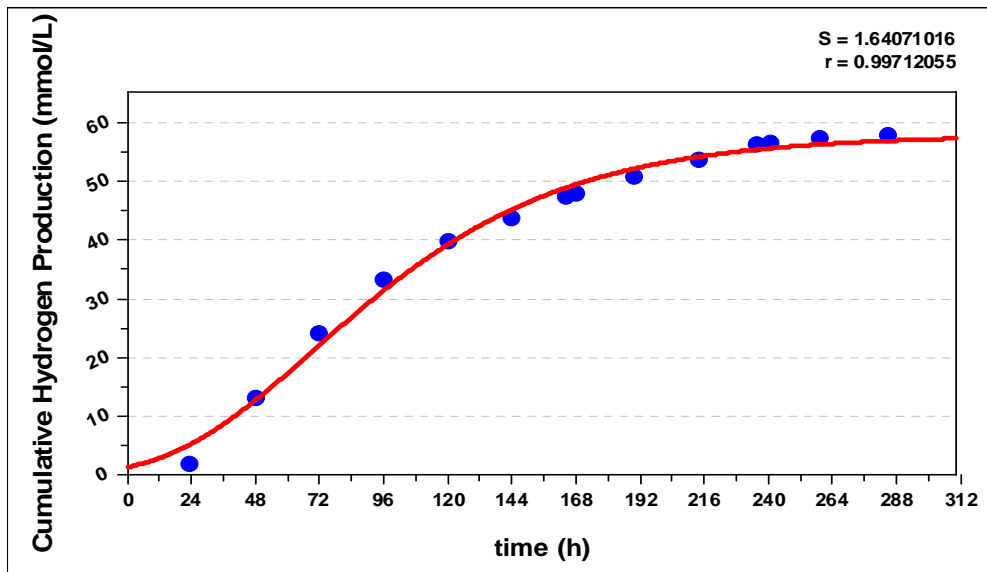


Figure F.4 The Modified Gompertz Model at 20°C and 5000 lux

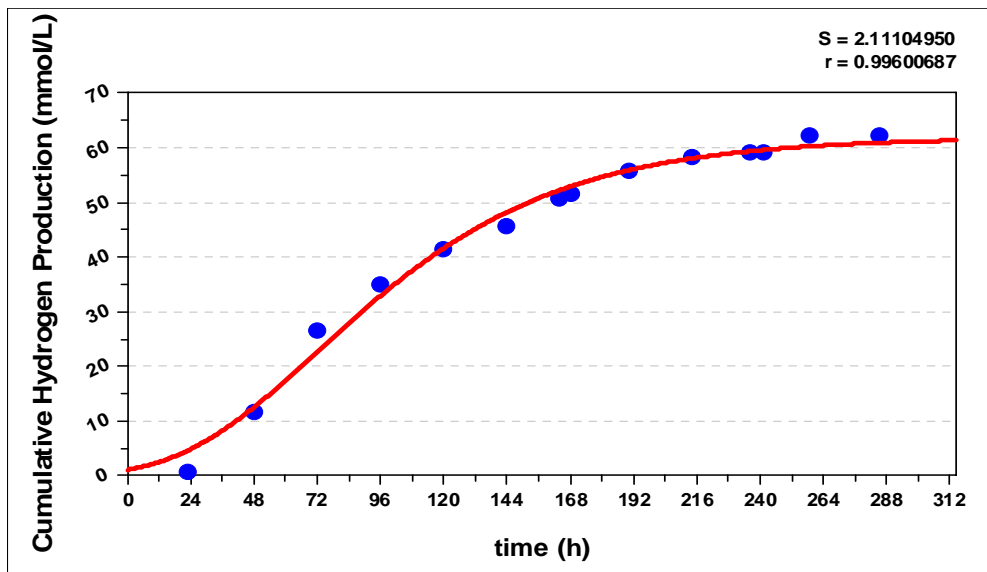


Figure F.5 The Modified Gompertz Model at 20°C and 6000 lux

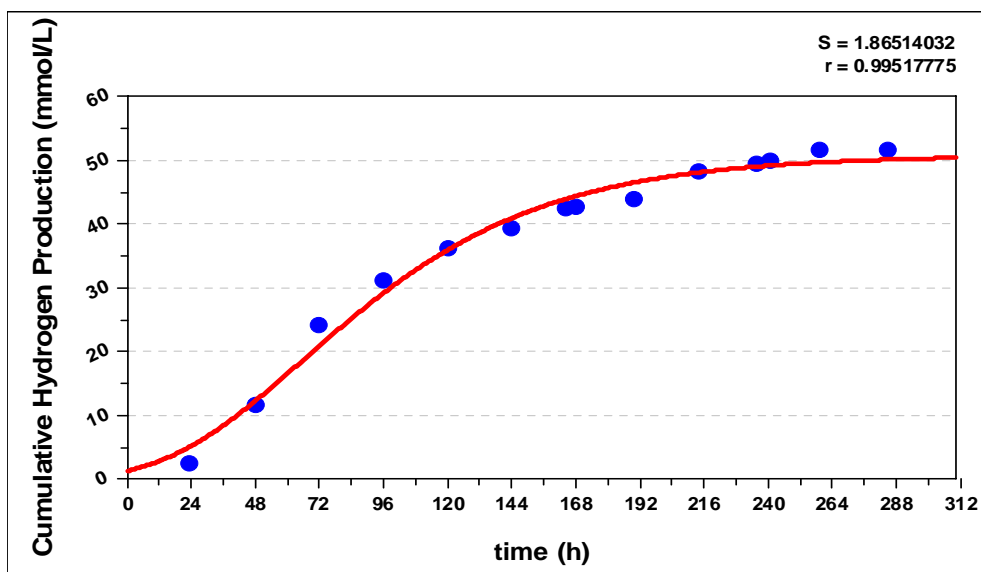


Figure F.6 The Modified Gompertz Model at 20°C and 7000 lux

F7-F13. Curves fitted to the Modified Gompertz Model together with the experimental data for different light intensities at 30°C

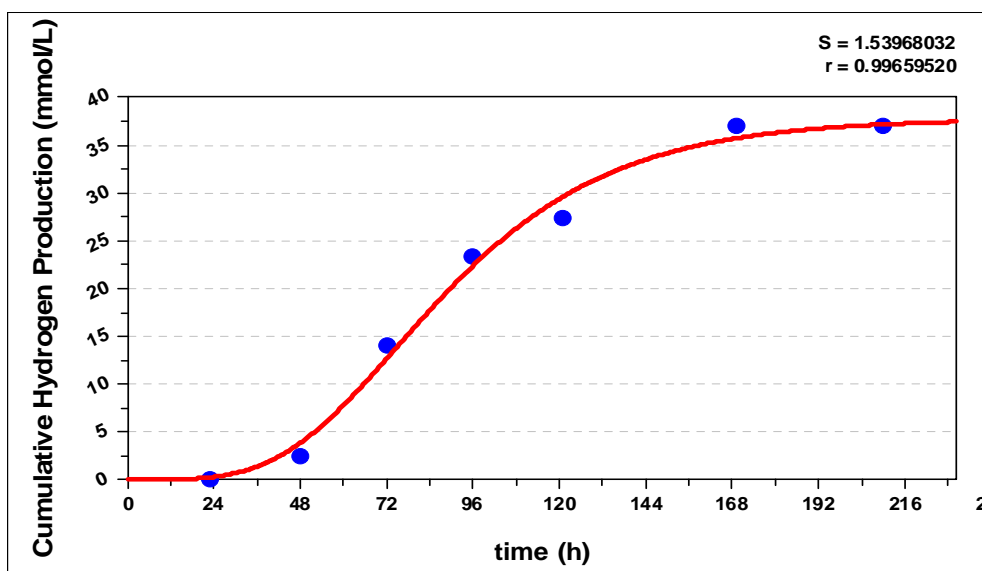


Figure F.7 The Modified Gompertz Model at 30°C and 1500 lux

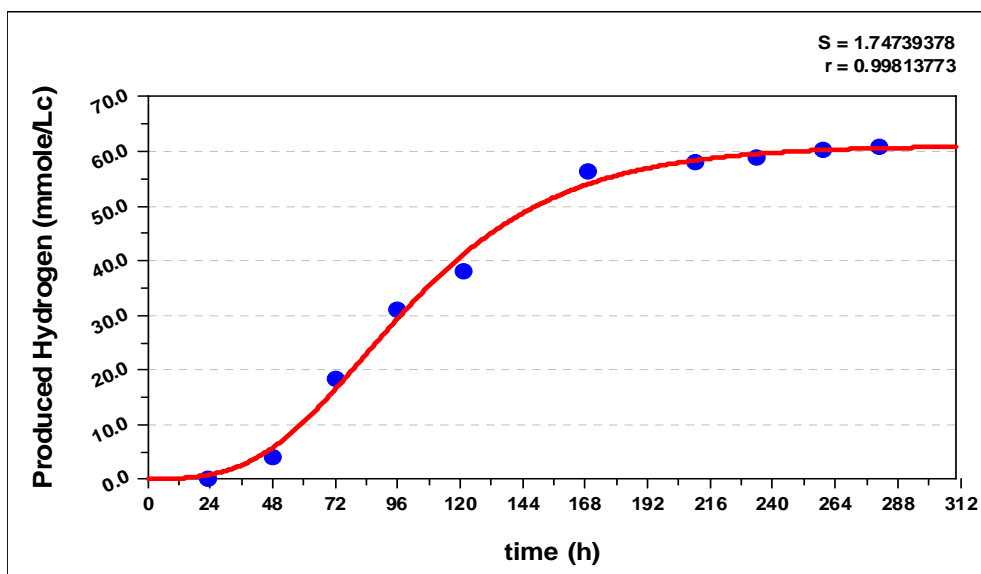


Figure F.8 The Modified Gompertz Model at 30°C and 2000 lux

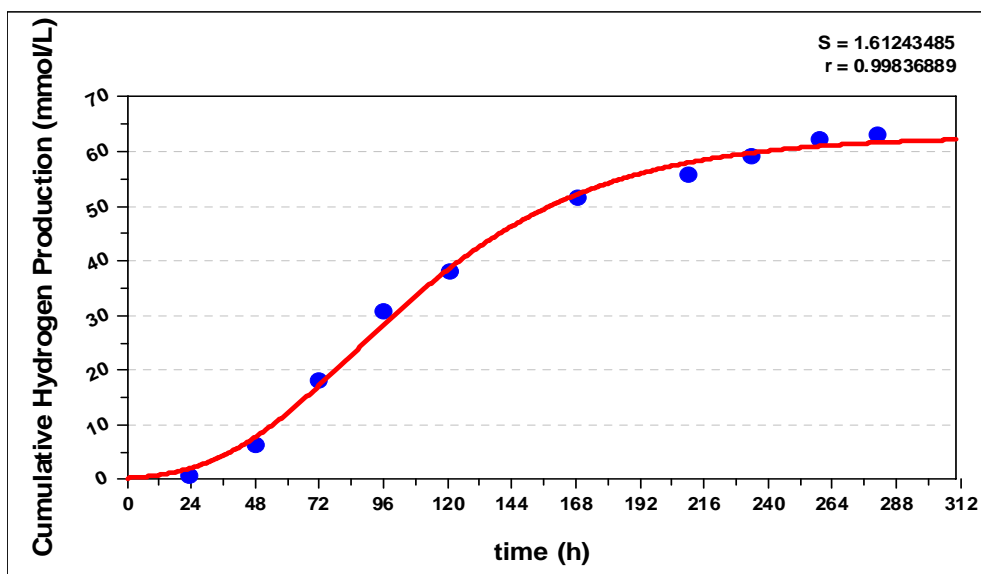


Figure F.9 The Modified Gompertz Model at 30°C and 3000 lux

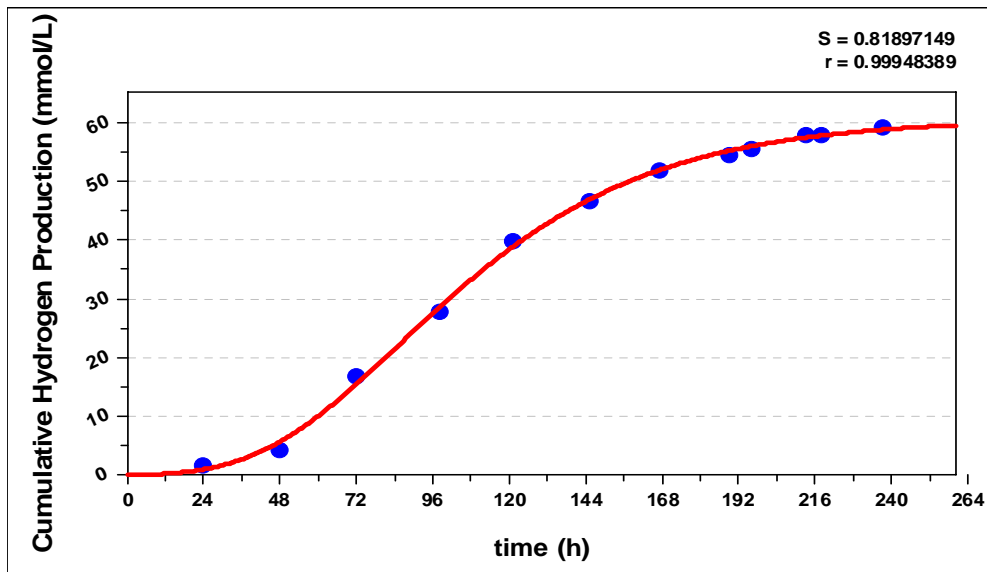


Figure F.10 The Modified Gompertz Model at 30°C and 4000 lux

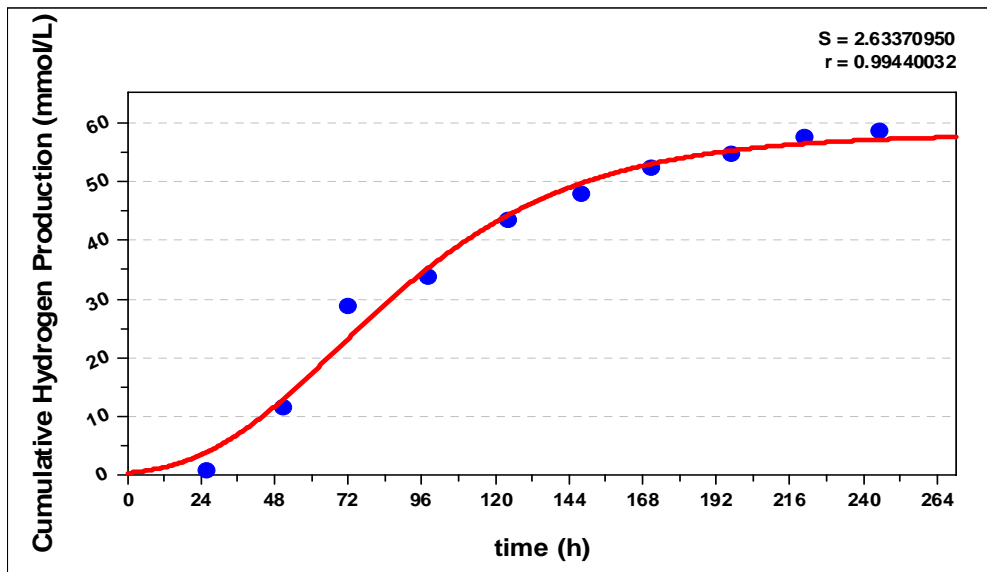


Figure F.11 The Modified Gompertz Model at 30°C and 5000 lux

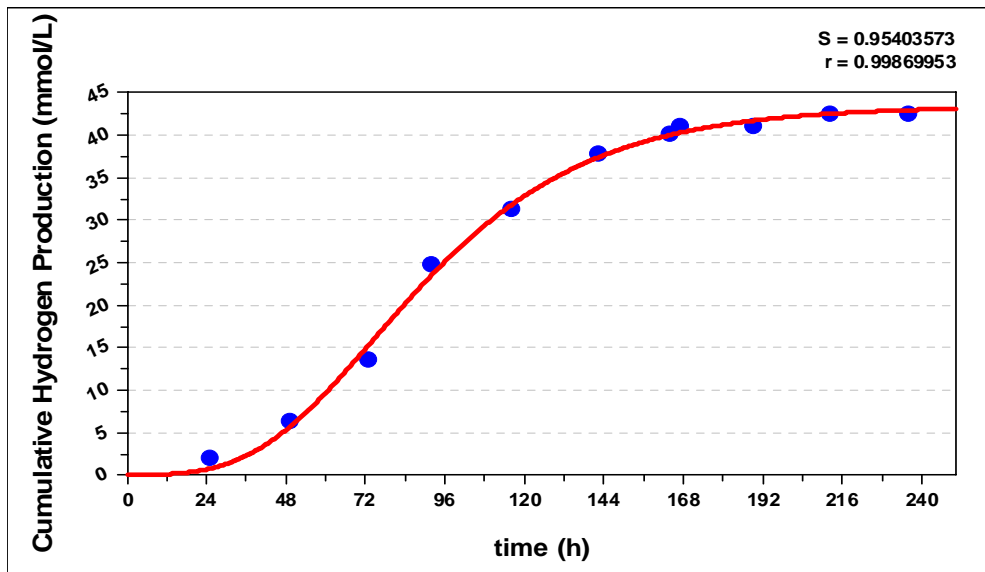


Figure F.12 The Modified Gompertz Model at 30°C and 6000 lux

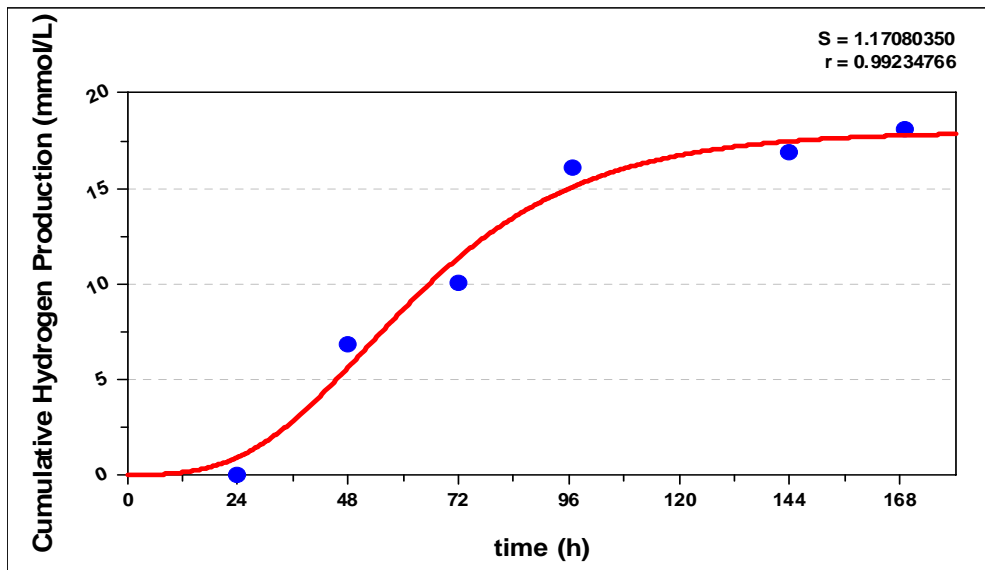


Figure F.13 The Modified Gompertz Model at 30°C and 7000 lux

F14-F18 . Curves fitted to the Modified Gompertz Model together with the experimental data for different light intensities at 38°C

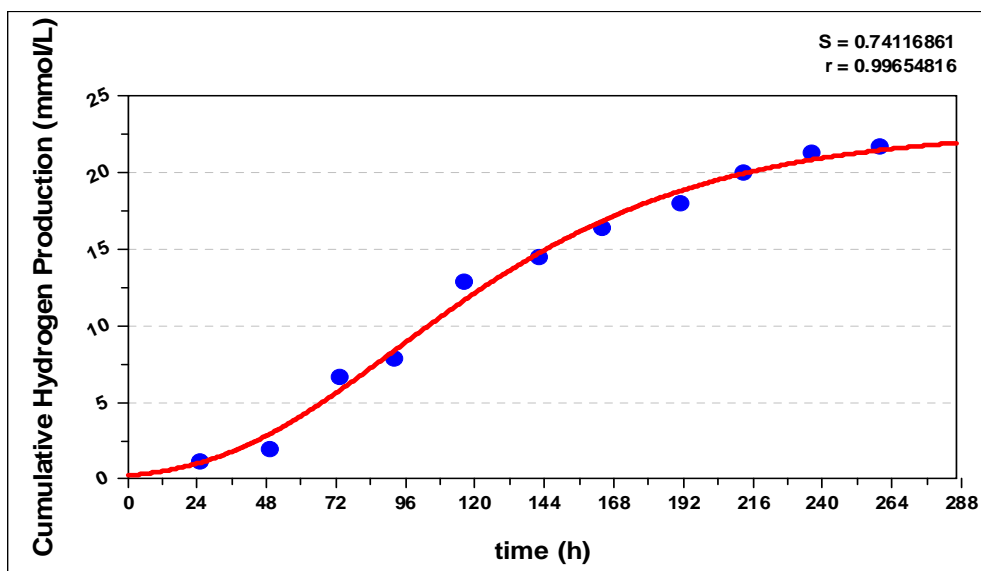


Figure F.14 The Modified Gompertz Model at 38°C and 1500 lux

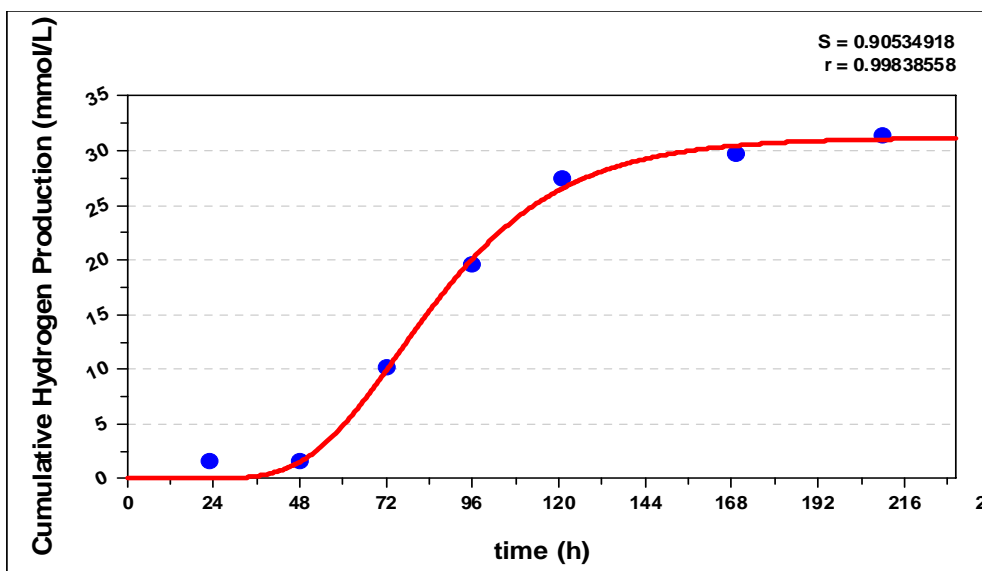


Figure F.15 The Modified Gompertz Model at 38°C and 2000 lux

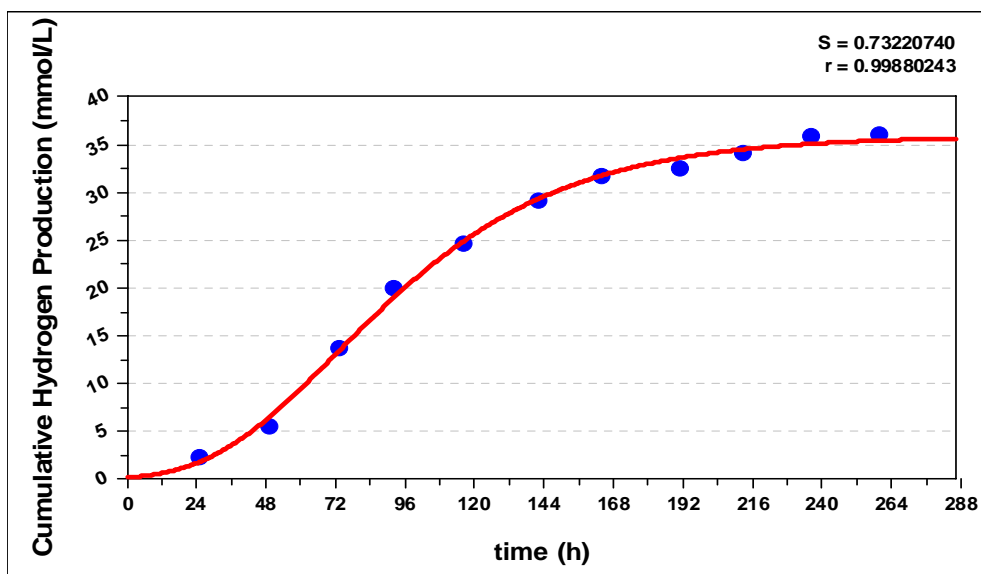


Figure F.16 The Modified Gompertz Model at 38°C and 3000 lux

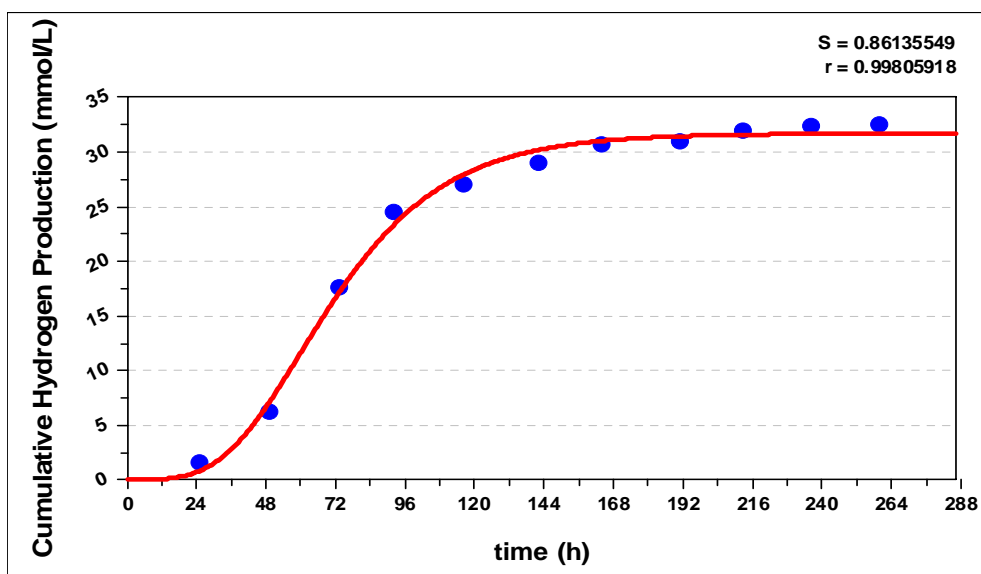


Figure F.17 The Modified Gompertz Model at 38°C and 4000 lux

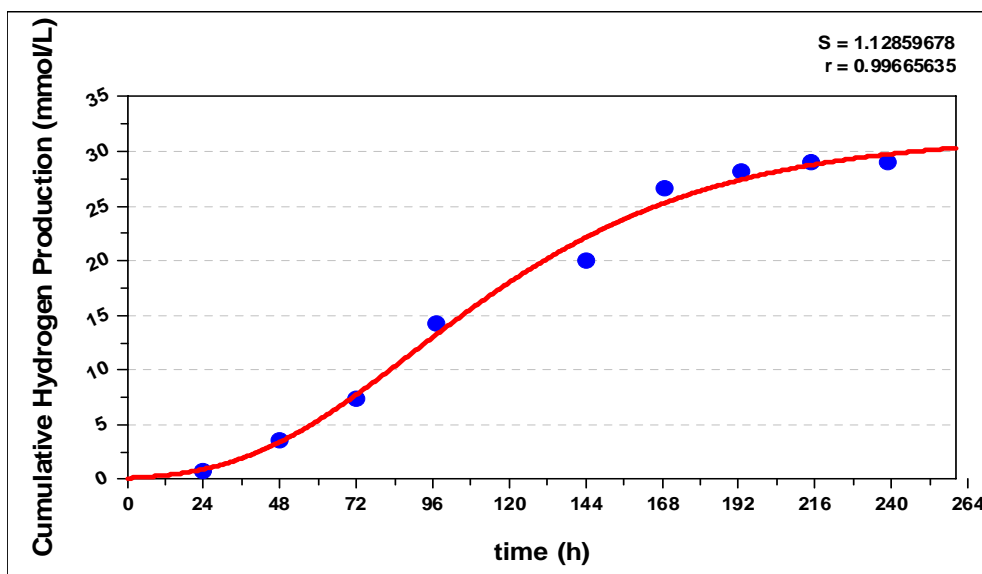


Figure F.18 The Modified Gompertz Model at 38°C and 5000 lux

APPENDIX G

LACTIC ACID CONSUMPTION KINETICS

G1-G7. Lactic Acid Consumption Kinetics together with the experimental data for different light intensities at 20°C

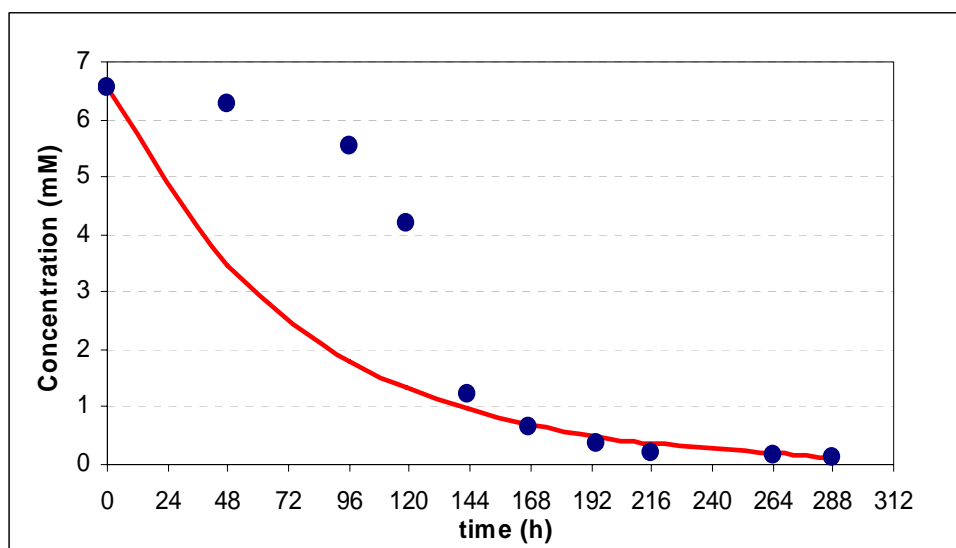


Figure G.1 First Order Kinetics for Lactic acid Consumption at 20°C 1500 lux

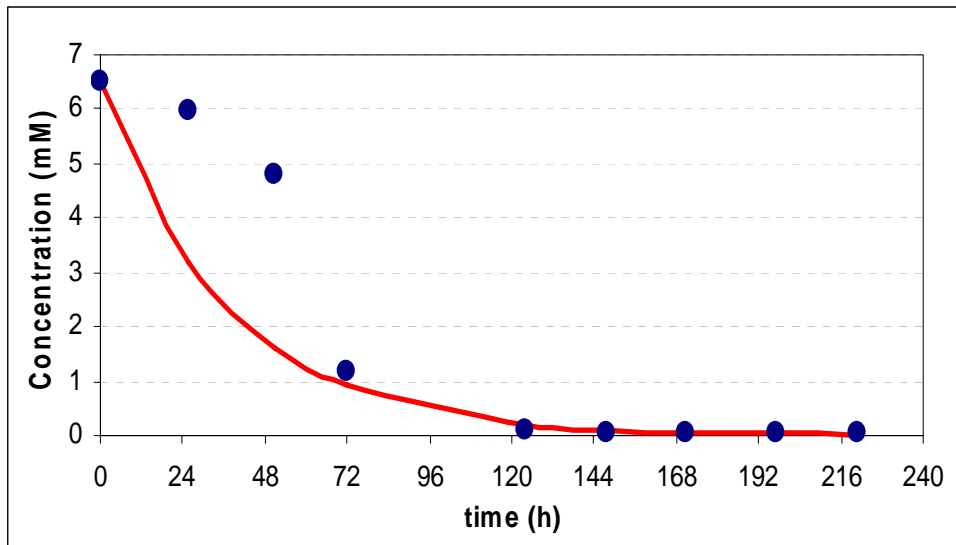


Figure G.2 First Order Kinetics for Lactic acid Consumption at 20°C 2000 lux

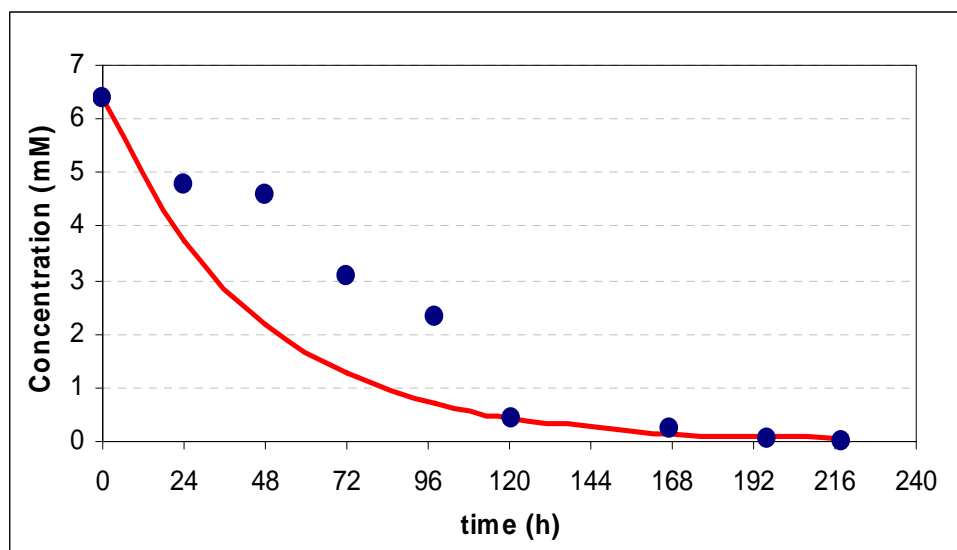


Figure G.3 First Order Kinetics for Lactic acid Consumption at 20°C 3000 lux

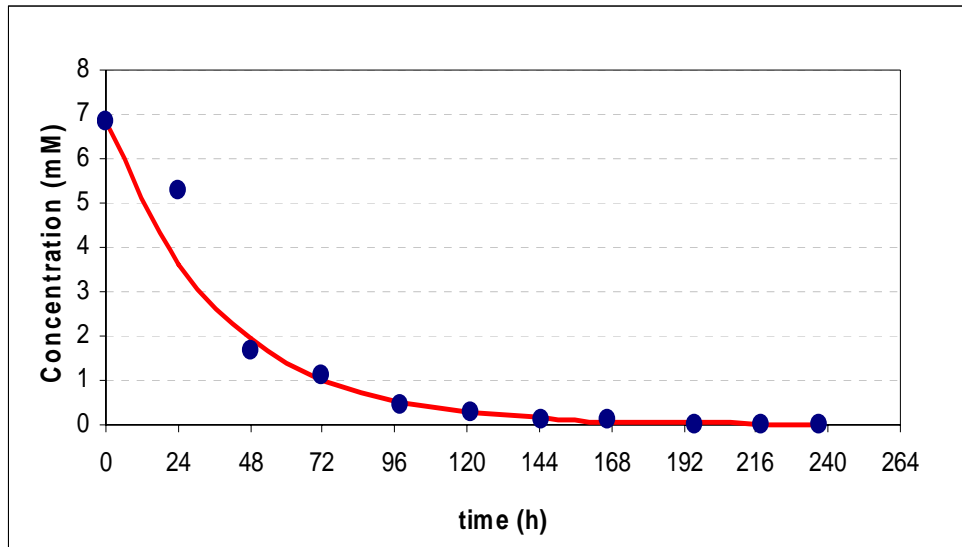


Figure G.4 First Order Kinetics for Lactic acid Consumption at 20°C 4000 lux

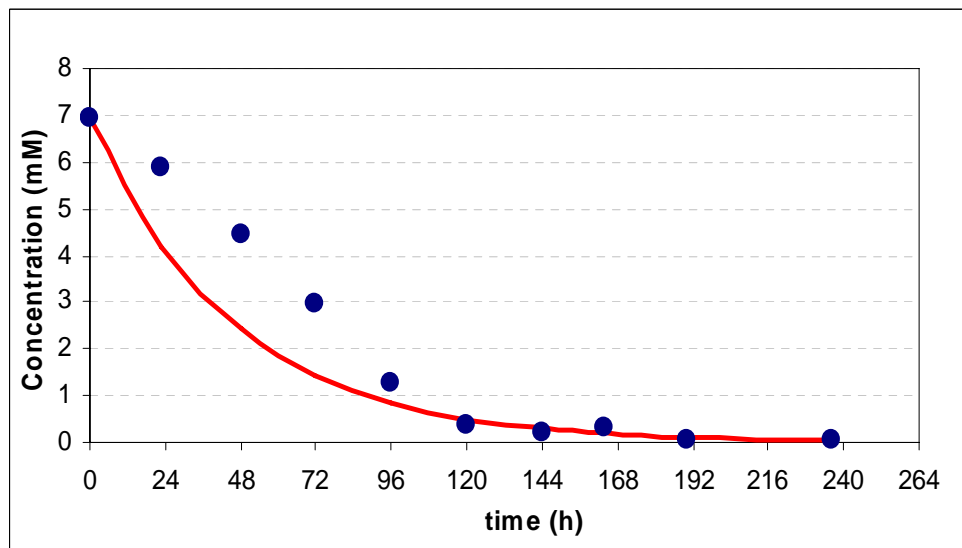


Figure G.5 First Order Kinetics for Lactic acid Consumption at 20°C 5000 lux

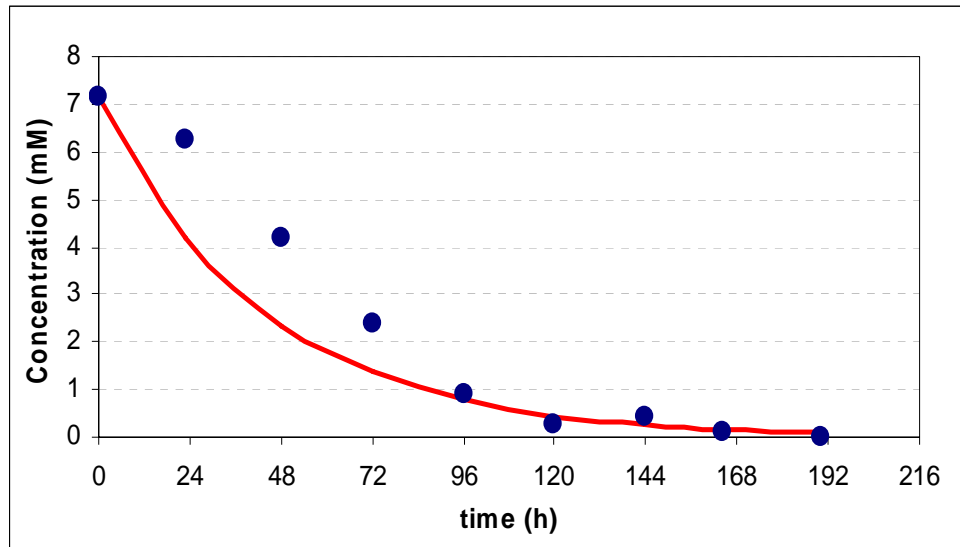


Figure G.6 First Order Kinetics for Lactic acid Consumption at 20°C 6000 lux

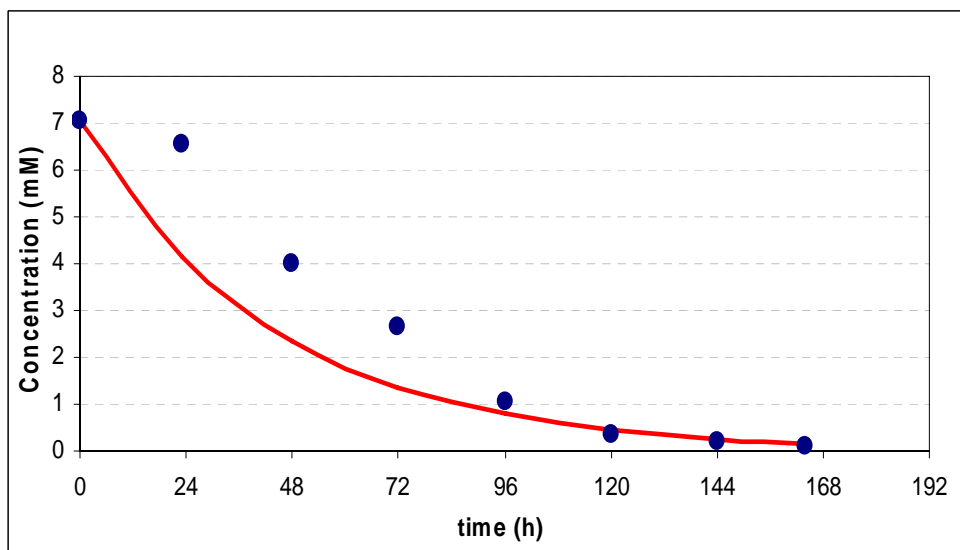


Figure G.7 First Order Kinetics for Lactic acid Consumption at 20°C 7000 lux

G8-G13 . Lactic Acid Consumption Kinetics together with the experimental data for different light intensities at 30°C

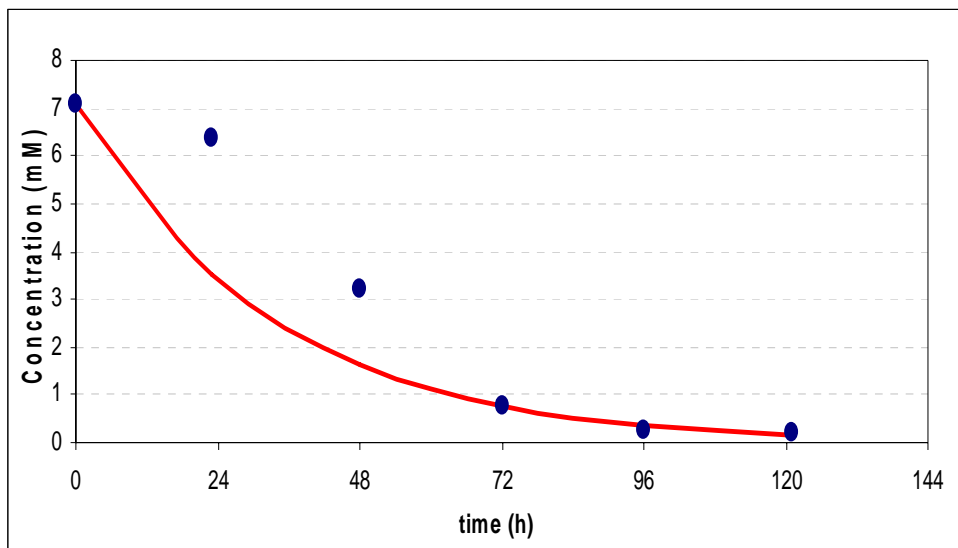


Figure G.8 First Order Kinetics for Lactic acid Consumption at 30°C 1500 lux

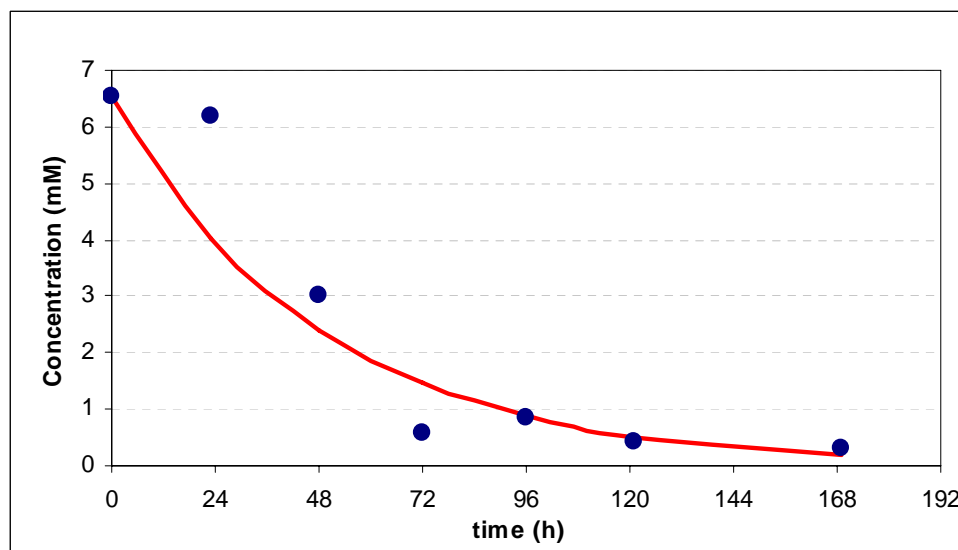


Figure G.9 First Order Kinetics for Lactic acid Consumption at 30°C 2000 lux

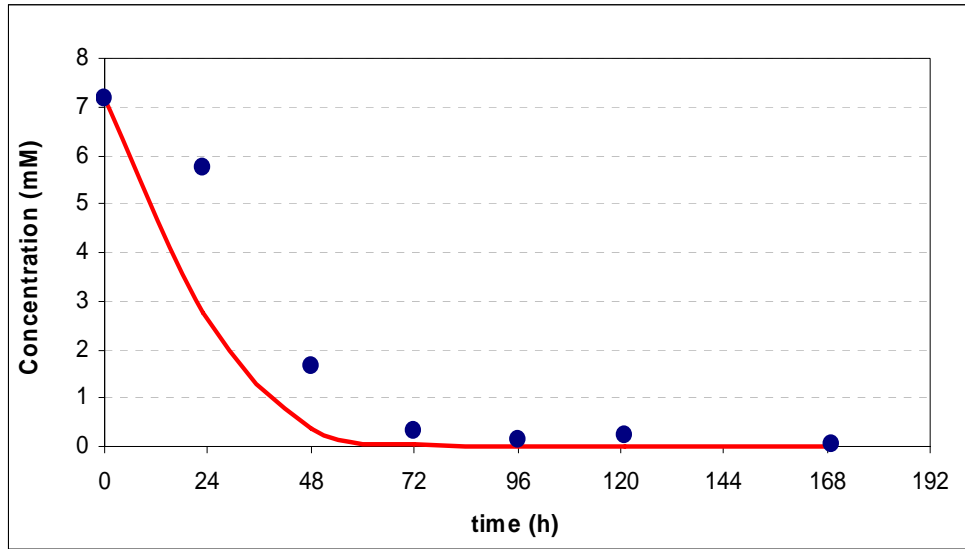


Figure G.10 First Order Kinetics for Lactic acid Consumption at 30°C 3000 lux

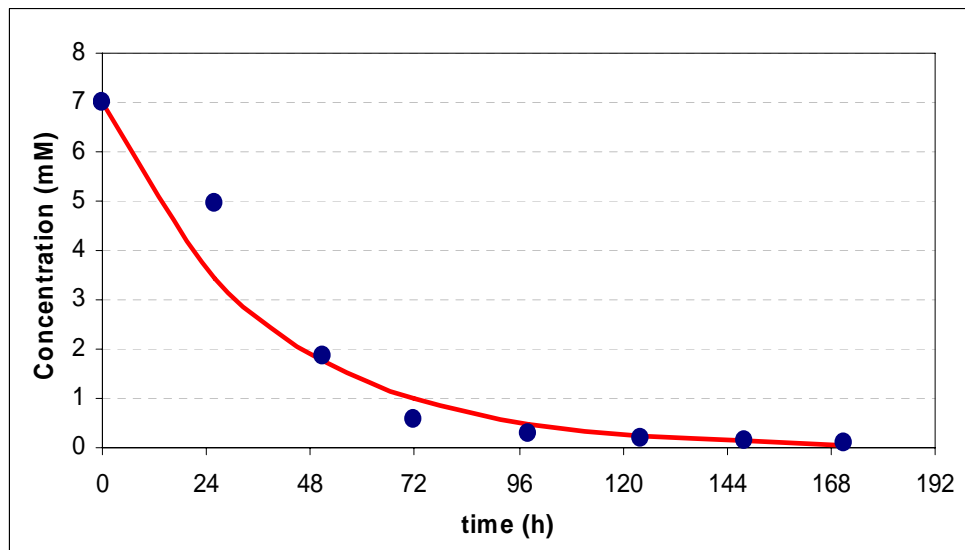


Figure G.11 First Order Kinetics for Lactic acid Consumption at 30°C 5000 lux

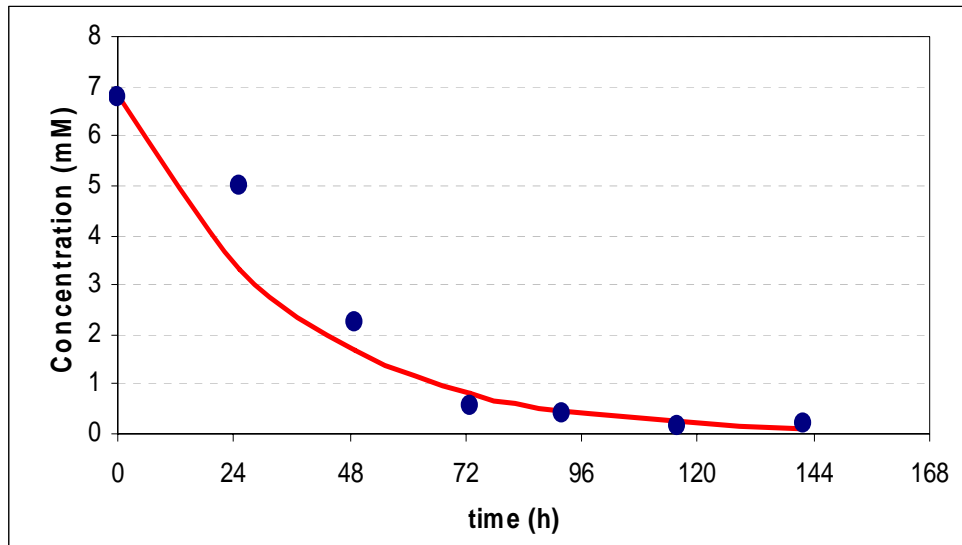


Figure G.12 First Order Kinetics for Lactic acid Consumption at 30°C 6000 lux

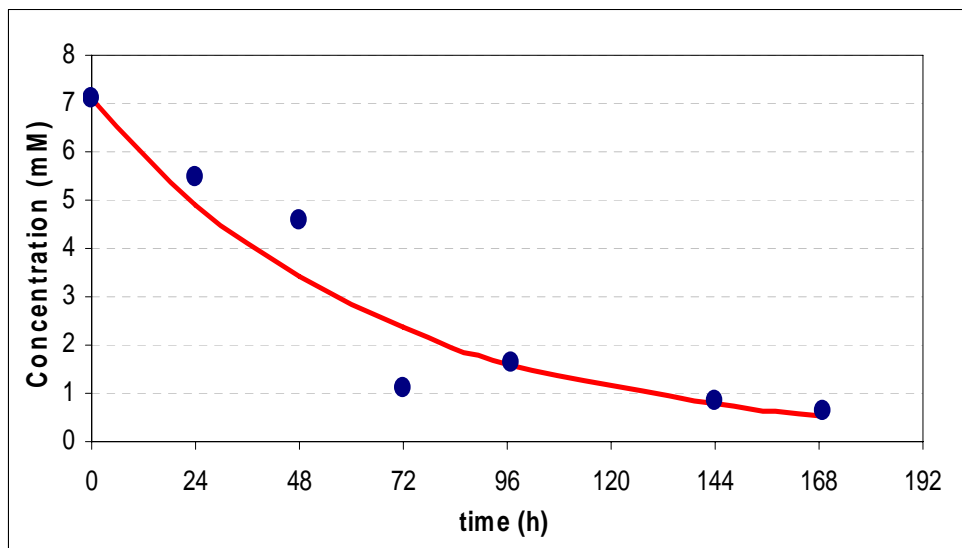


Figure G.13 First Order Kinetics for Lactic acid Consumption at 30°C 7000 lux

G14-G18 . Lactic Acid Consumption Kinetics together with the experimental data for different light intensities at 38°C

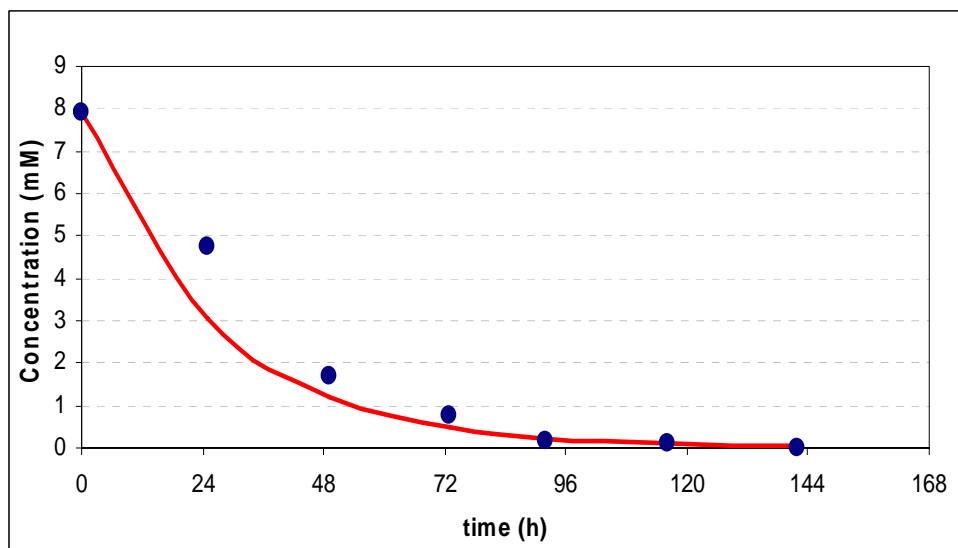


Figure G.14 First Order Kinetics for Lactic acid Consumption at 38°C 1500 lux

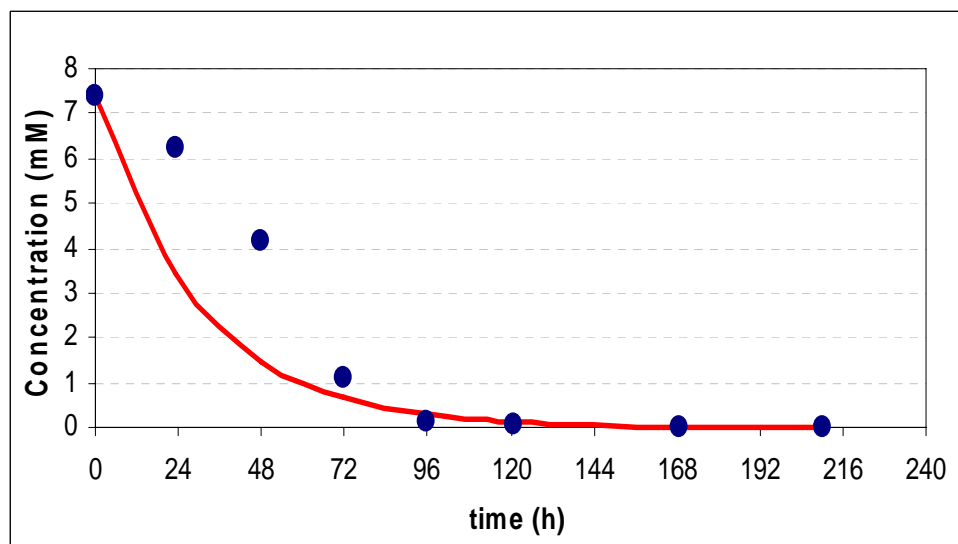


Figure G.15 First Order Kinetics for Lactic acid Consumption at 38°C 2000 lux

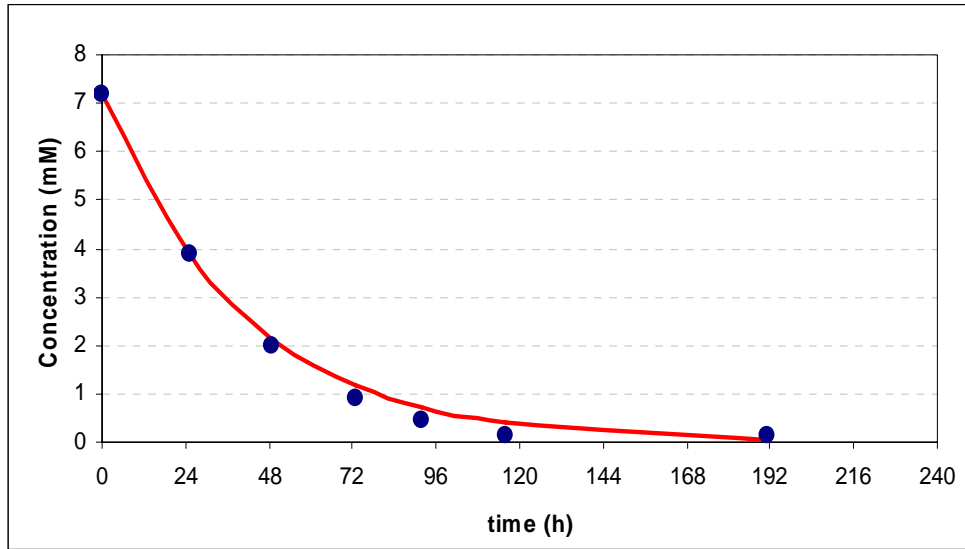


Figure G.16 First Order Kinetics for Lactic acid Consumption at 38°C 3000 lux

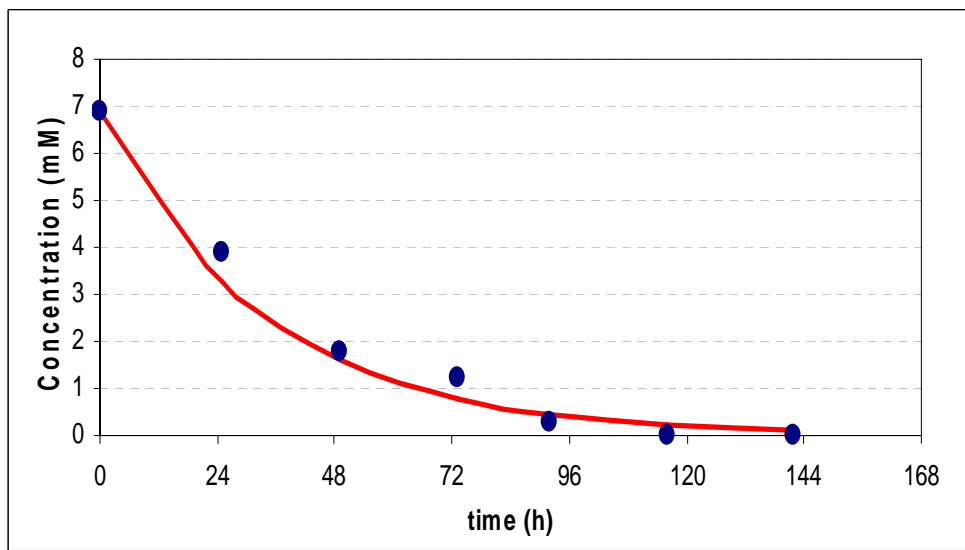


Figure G.17 First Order Kinetics for Lactic acid Consumption at 38°C 4000 lux

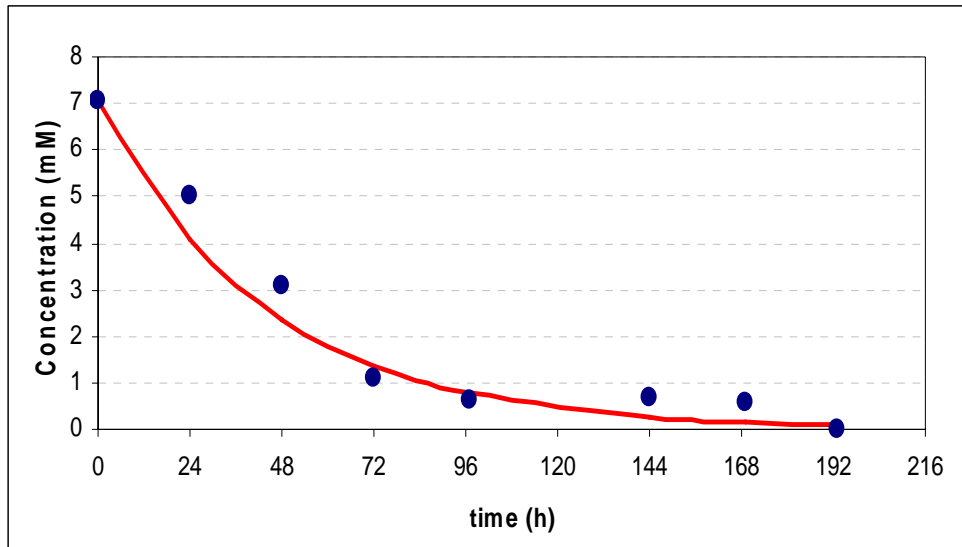


Figure G.18 First Order Kinetics for Lactic acid Consumption at 38°C 5000 lux

APPENDIX H

ACETIC ACID CONSUMPTION KINETICS

H1-H6. Acetic Acid Consumption Kinetics together with the experimental data for different light intensities at 20°C

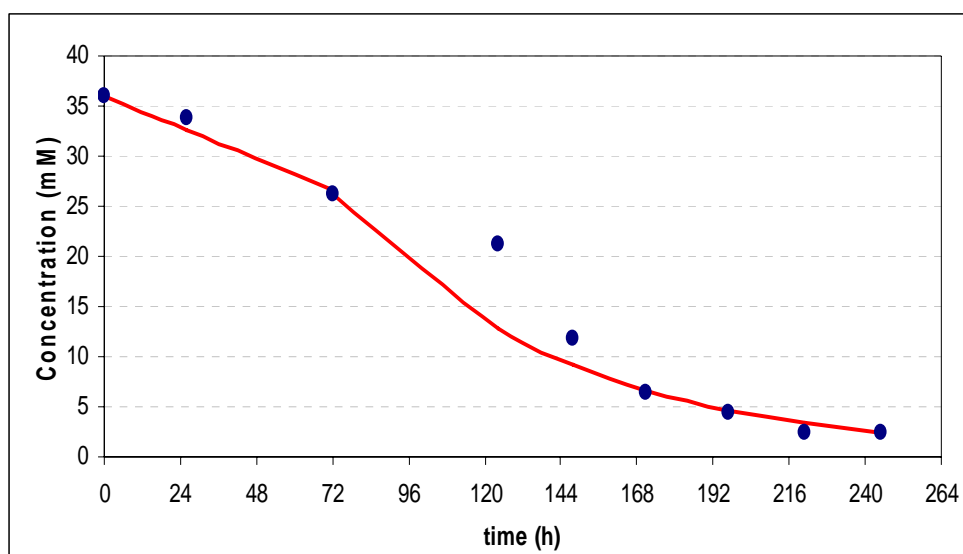


Figure H.1 Kinetic Curves for Acetic Acid Consumption at 20°C 2000 lux

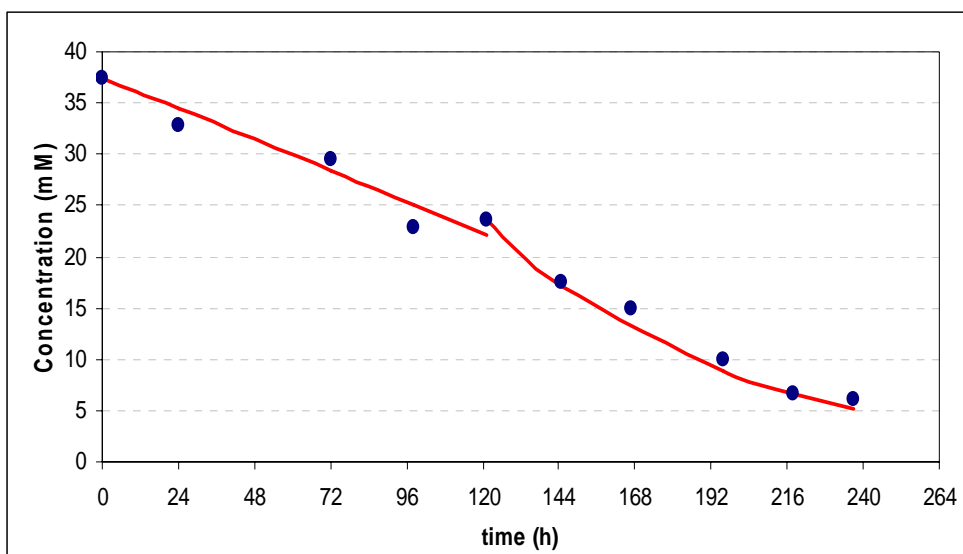


Figure H.2 Kinetic Curves for Acetic Acid Consumption at 20°C 3000 lux

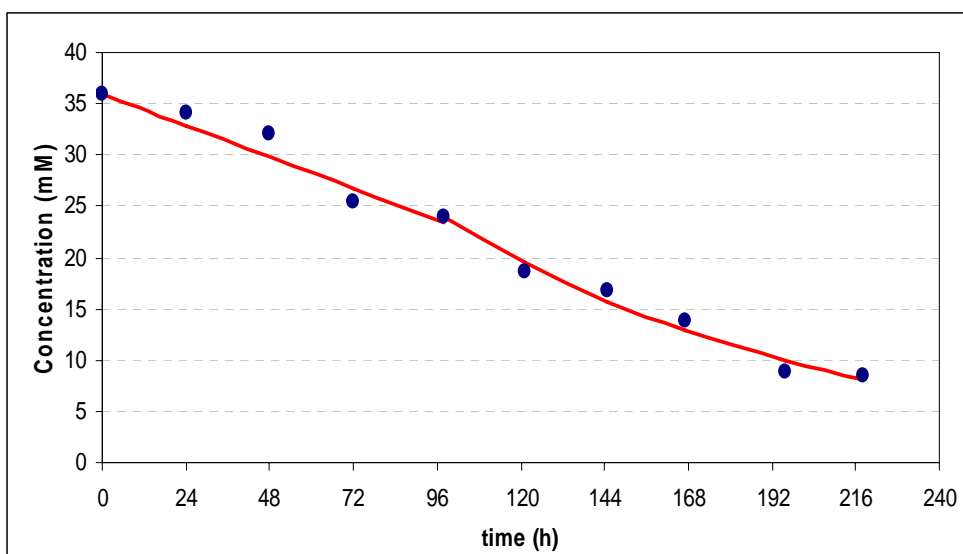


Figure H.3 Kinetic Curves for Acetic Acid Consumption at 20°C 4000 lux

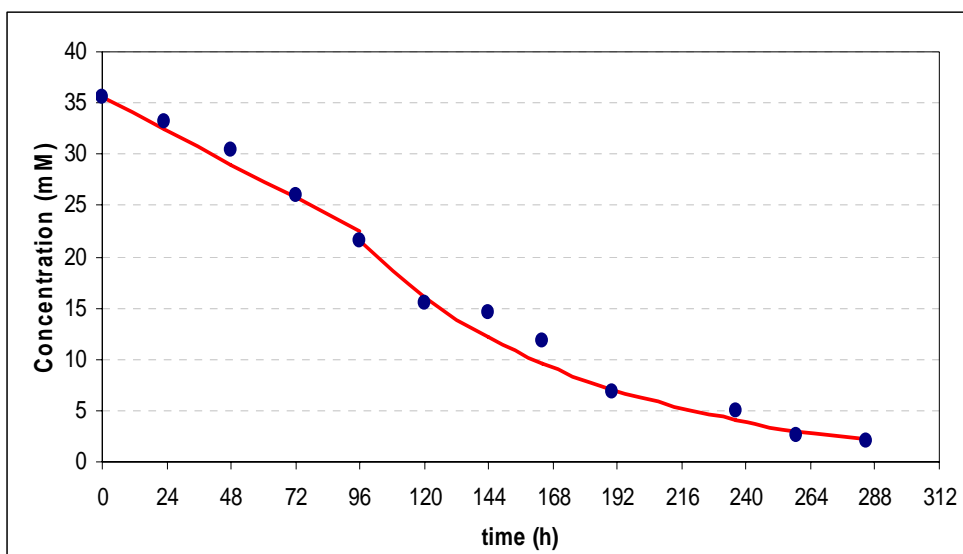


Figure H.4 Kinetic Curves for Acetic Acid Consumption at 20°C 5000 lux

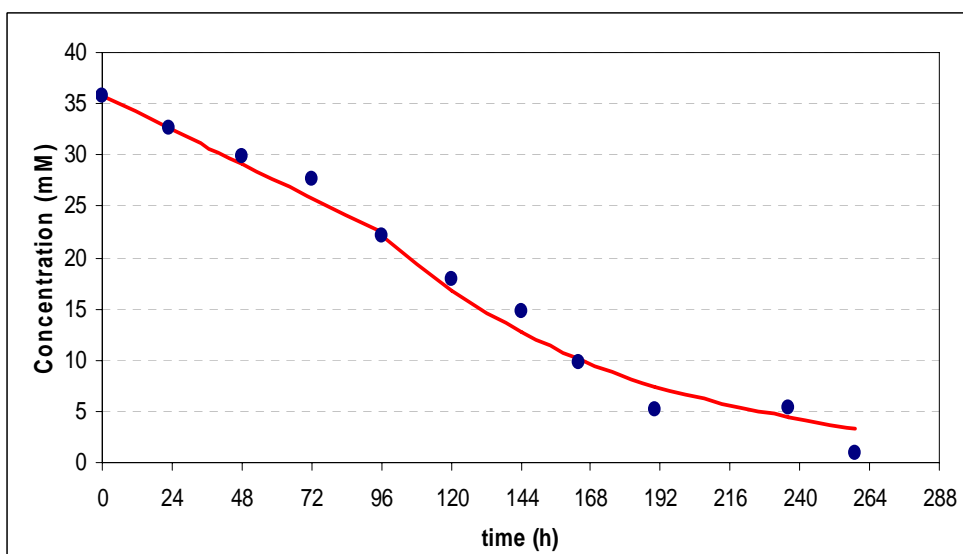


Figure H.5 Kinetic Curves for Acetic Acid Consumption at 20°C 6000 lux

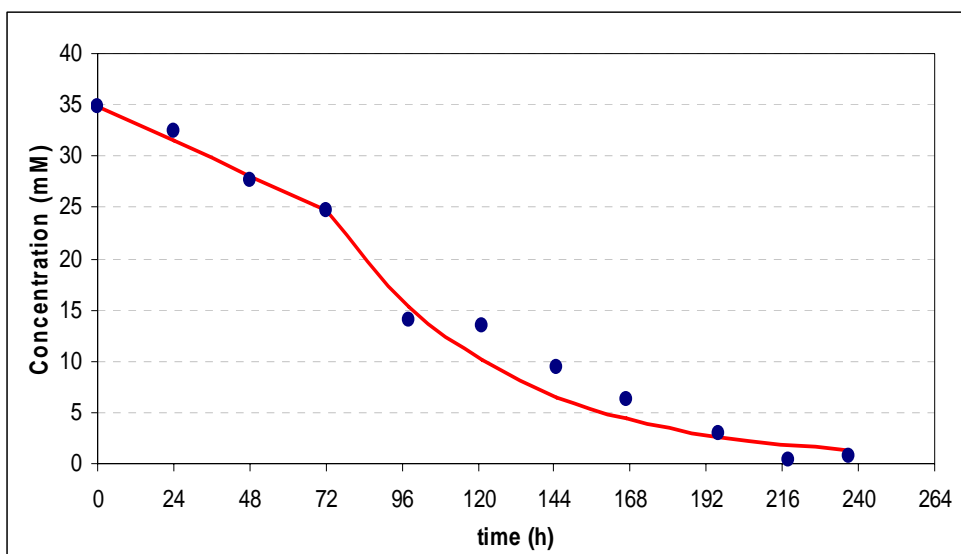


Figure H.6 Kinetic Curves for Acetic Acid Consumption at 20°C 7000 lux

H7-H13. Acetic Acid Consumption Kinetics together with the experimental data for different light intensities at 30°C

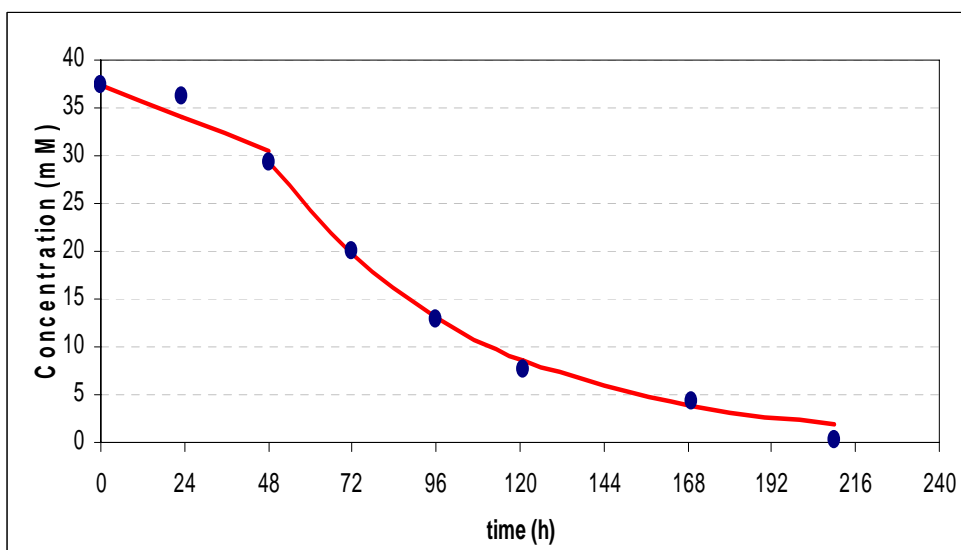


Figure H.7 Kinetic Curves for Acetic Acid Consumption at 30°C 1500 lux

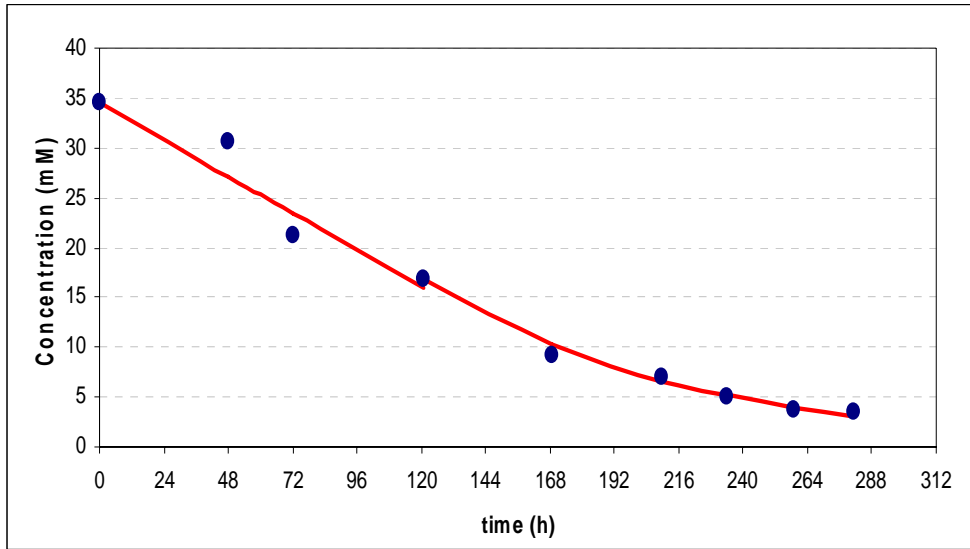


Figure H.8 Kinetic Curves for Acetic Acid Consumption at 30°C 2000 lux

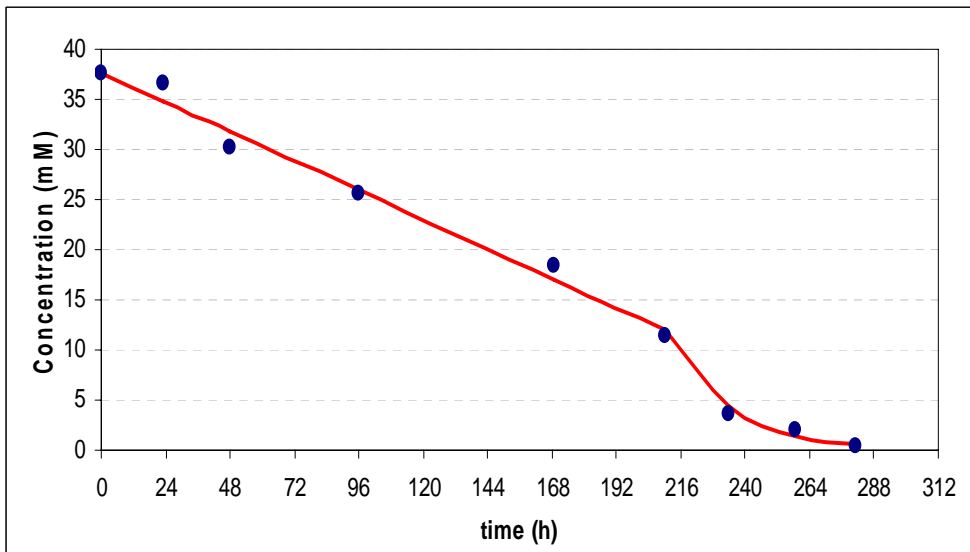


Figure H.9 Kinetic Curves for Acetic Acid Consumption at 30°C 3000 lux

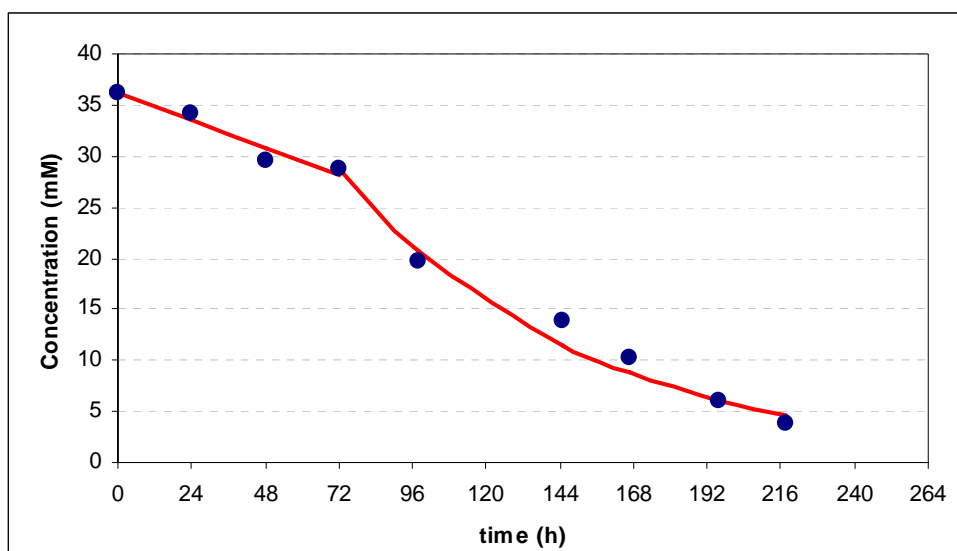


Figure H.10 Kinetic Curves for Acetic Acid Consumption at 30°C 4000 lux

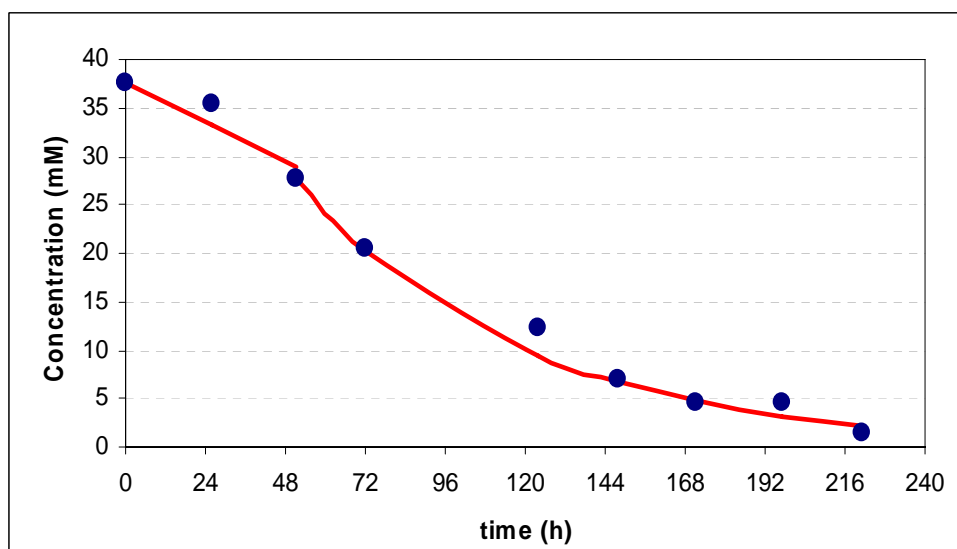


Figure H.11 Kinetic Curves for Acetic Acid Consumption at 30°C 5000 lux

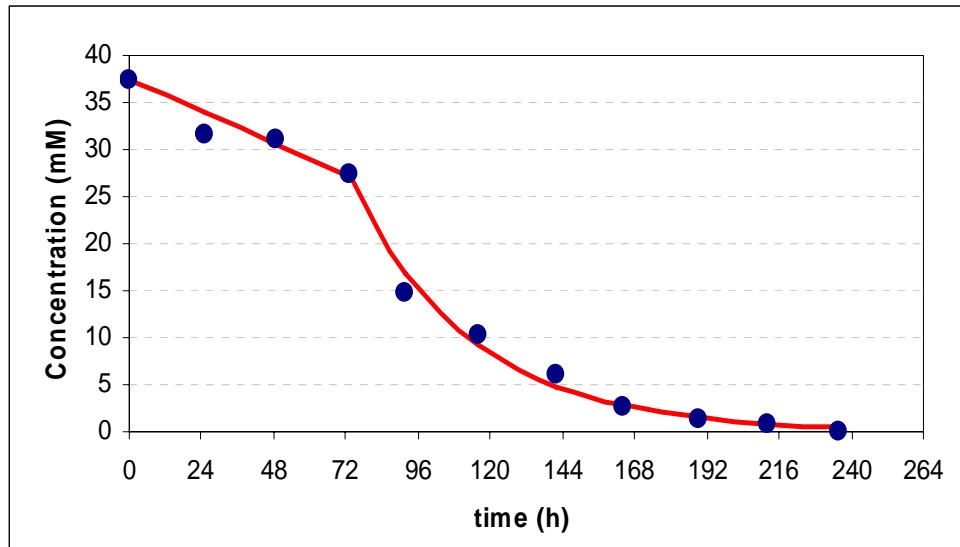


Figure H.12 Kinetic Curves for Acetic Acid Consumption at 30°C 6000 lux

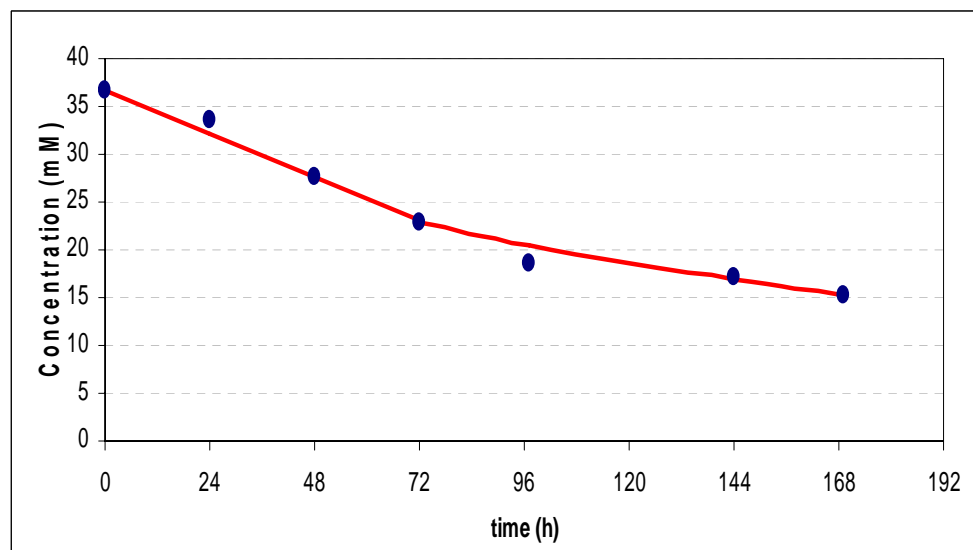


Figure H.13 Kinetic Curves for Acetic Acid Consumption at 30°C 7000 lux

H14-H18. Acetic Acid Consumption Kinetics together with the experimental data for different light intensities at 38°C

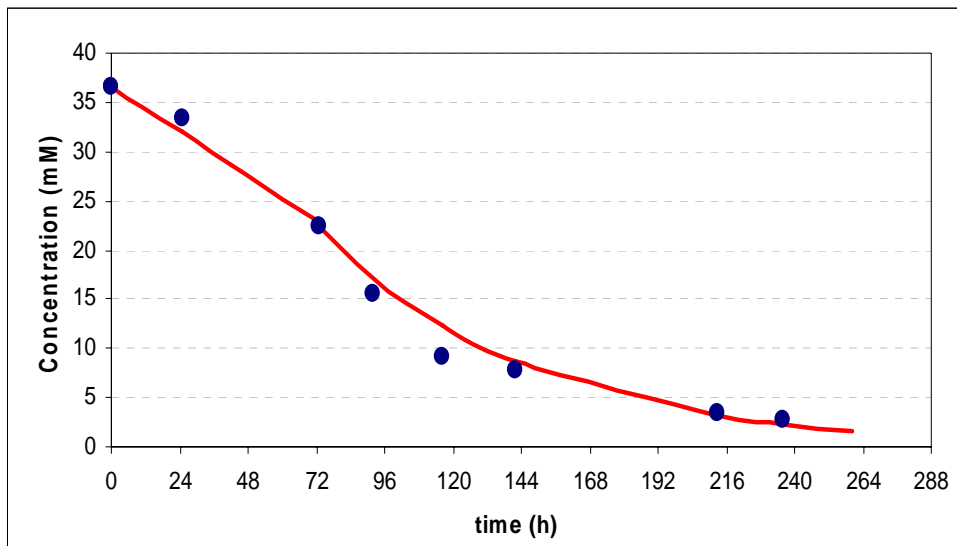


Figure H.14 Kinetic Curves for Acetic Acid Consumption at 38°C 1500 lux

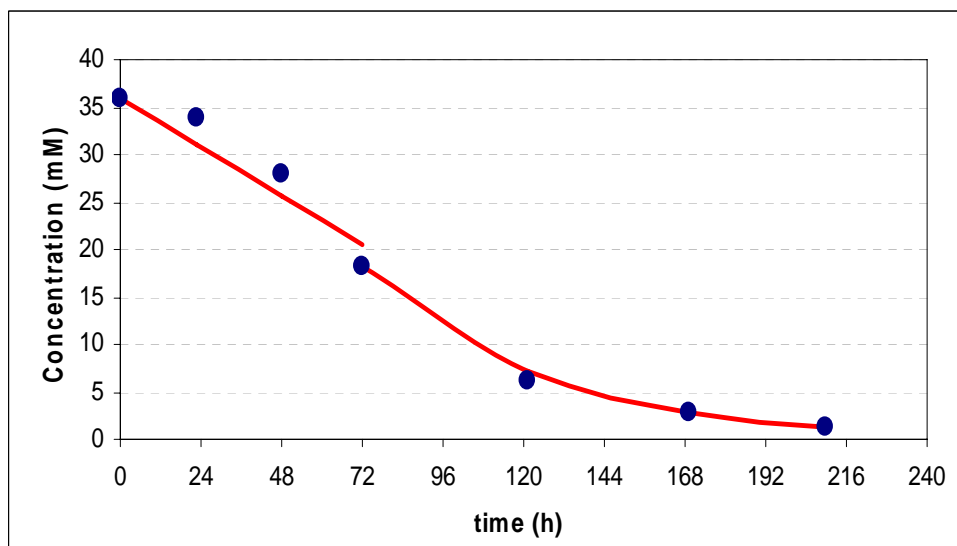


Figure H.15 Kinetic Curves for Acetic Acid Consumption at 38°C 2000 lux

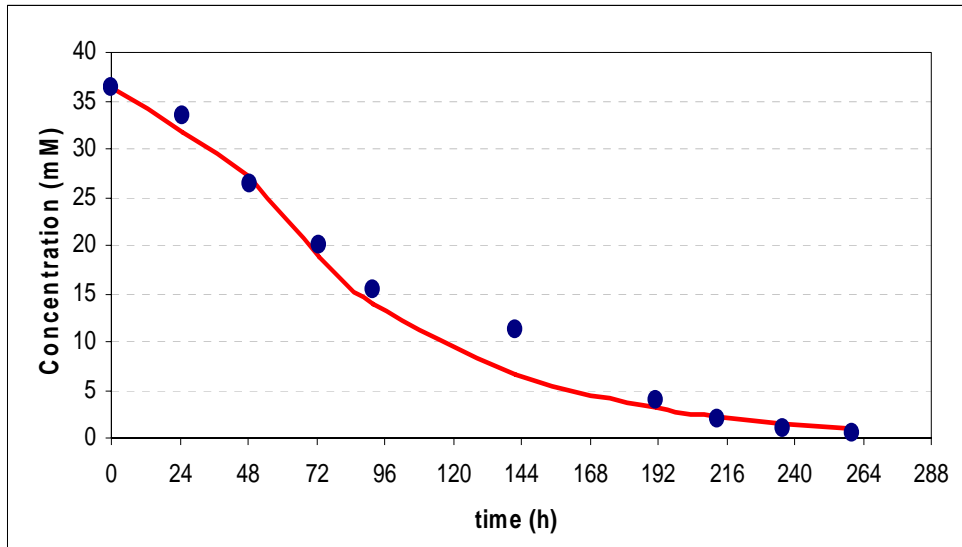


Figure H.16 Kinetic Curves for Acetic Acid Consumption at 38°C 3000 lux

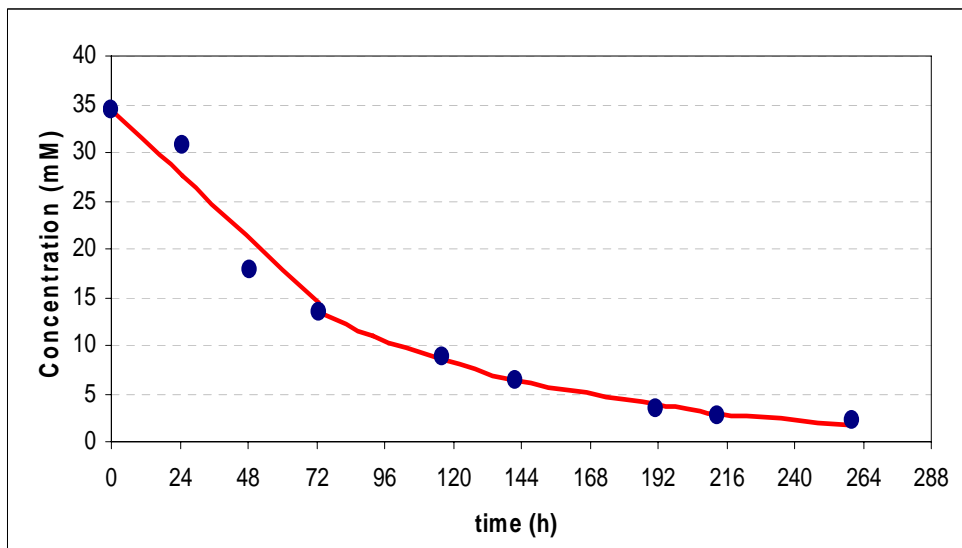


Figure H.17 Kinetic Curves for Acetic Acid Consumption at 38°C 4000 lux

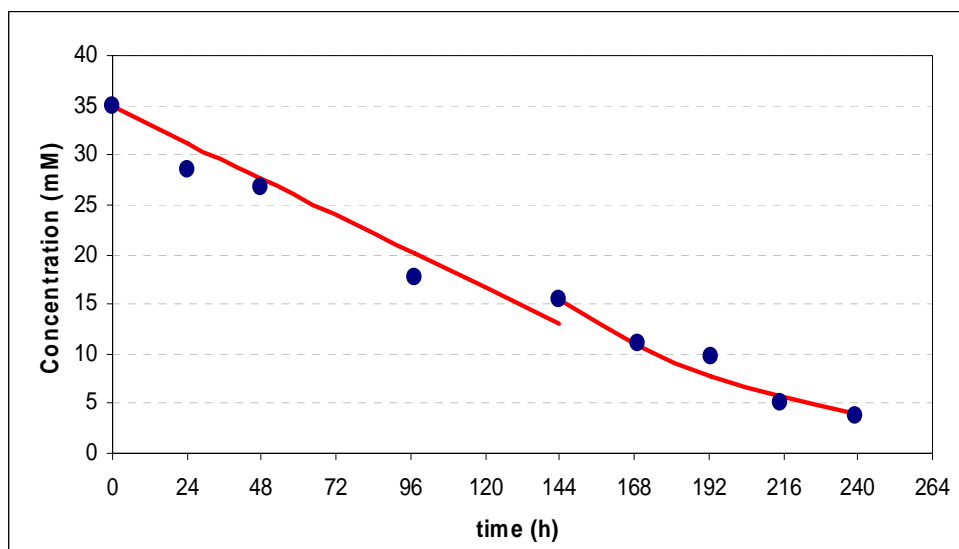


Figure H.18 Kinetic Curves for Acetic Acid Consumption at 38°C 5000 lux

APPENDIX I

EXPERIMENTAL DATA

Table I1- OD, cell dry weight, pH and cumulative hydrogen produced values for 20°C and 1500 lux (Mean of 2 runs)

time	OD	gdw/Lc	pH	Cumulative Hydrogen Produced (ml)	Cumulative Hydrogen Produced (mmol)
0	0.379	0.206	6.53	0	0
48	0.385	0.209	6.49	0.5	0.019
96	0.448	0.243	6.66	0.9	0.038
119	0.770	0.418	6.77	0.9	0.038
143	1.299	0.705	7.05	6.2	0.256
167	1.338	0.726	7.29	12.8	0.532
194	-	-	7.38	21.3	0.884
216	1.583	0.859	7.33	25.8	1.074
239	-	-	-	32.7	1.360
264	1.526	0.828	7.21	36.3	1.510
288	-	-	-	36.3	1.510

Table I2- Organic Acid concentrations for 20°C and 1500 lux (Mean of 2 runs)

time	Acetic Acid (mM)	Lactic Acid (mM)	Formic Acid (mM)	Butyric Acid (mM)	Propionic Acid (mM)
0	35.08	6.55	0	0	0
48	33.80	6.28	2.13	0	0
96	31.81	5.55	4.17	0	0
119	30.91	4.21	7.22	0	0
143	27.69	1.24	12.94	0	0
167	24.83	0.67	11.91	0	0
194	16.02	0.36	12.11	0	0
216	12.61	0.22	8.65	0	0
239	9.21	0.14	7.47	0	0
264	-	-	-	-	-
288	5.07	0.11	6.60	0	0

Table I3- OD, cell dry weight, pH and cumulative hydrogen produced values for 20°C and 2000 lux (Mean of 2 runs)

time	OD	gdw/Lc	pH	Cumulative Hydrogen Produced (ml)	Cumulative Hydrogen Produced (mmol)
0	0.335	0.182	6.46	0	0
26	0.411	0.223	6.525	0	0
51	0.523	0.284	6.635	0	0
72	0.993	0.539	6.85	5.3	0.218
124	1.153	0.626	6.97	33.3	1.383
148	1.259	0.683	7.1235	37.5	1.560
171	1.263	0.685	7.04	41.3	1.716
197	1.330	0.722	7.02	43.8	1.820
221	1.465	0.795	7.12	44.8	1.861
245	1.461	0.793	7.09	44.8	1.861

Table I4- Organic Acid concentrations for 20°C and 2000 lux (Mean of 2 runs)

time	Acetic Acid (mM)	Lactic Acid (mM)	Formic Acid (mM)	Butyric Acid (mM)	Propionic Acid (mM)
0	35.91	6.49	0	0	0
26	33.73	5.98	1.93	0	0
51	34.59	4.80	3.79	0	0
72	26.27	1.19	6.55	0	0
124	21.16	0.12	11.74	0	0
148	11.89	0.05	10.81	0	0
171	6.30	0.04	12.11	0	0
197	4.37	0.03	10.98	0	0
221	2.50	0.04	7.84	0	0
245	2.42	0	5.99	0	0

Table I5- OD, cell dry weight, pH and cumulative hydrogen produced values for 20°C and 3000 lux (Mean of 2 runs)

time	OD	gdw/Lc	pH	Cumulative Hydrogen Produced (ml)	Cumulative Hydrogen Produced (mmol)
0	0.208	0.113	6.42	0	0
24	0.246	0.134	6.50	0	0
48	0.778	0.422	6.72	1.5	0.062
72	0.868	0.471	6.77	6.0	0.250
98	1.078	0.585	6.81	17.5	0.728
121	1.070	0.581	6.84	28.5	1.185
145	-	-	6.90	35.5	1.477
167	0.896	0.486	7.06	38.3	1.591
189	-	-	-	39.5	1.643
196	0.983	0.534	7.19	39.5	1.643
213	-	-	-	43.3	1.799
218	0.967	0.525	7.10	47.3	1.965
237	0.752	0.408	6.81	48.3	2.070

Table I6- Organic Acid concentrations for 20°C and 3000 lux (Mean of 2 runs)

time	Acetic Acid (mM)	Lactic Acid (mM)	Formic Acid (mM)	Butyric Acid (mM)	Propionic Acid (mM)
0	37.45	6.37	0	0	0
24	32.80	4.78	0	0	0
48	27.58	4.58	2.23	0	0
72	29.50	3.06	4.53	0	0
98	22.83	2.30	4.89	0	0
121	23.51	0.41	5.27	0	0
145	17.47	-	-	0	0
167	14.93	0.23	6.76	0	0
189	-	-	-	-	-
196	9.97	0.07	9.06	0	0
213	-	-	-	-	-
218	6.56	0.02	10.78	0	0
237	6.03	0	14.06	0	0

Table I7- OD, cell dry weight, pH and cumulative hydrogen produced values for 20°C and 4000 lux (Mean of 2 runs)

time	OD	gdw/Lc	pH	Cumulative Hydrogen Produced (ml)	Cumulative Hydrogen Produced (mmol)
0	0.208	0.113	6.65	0	0
24	0.517	0.281	6.77	1	0.042
48	0.709	0.385	6.94	2.3	0.094
72	1.022	0.554	7.05	6.0	0.250
98	1.088	0.591	6.83	27.0	1.123
121	0.981	0.532	6.86	27.0	1.123
145	-	-	-	34.0	1.414
167	0.712	0.387	6.83	39.0	1.622
196	0.755	0.410	6.97	47.5	1.976
218	0.718	0.389	6.96	51.5	2.142
237	0.644	0.349	6.81	51.8	2.153

Table I8- Organic Acid concentrations for 20°C and 4000 lux (Mean of 2 runs)

time	Acetic Acid (mM)	Lactic Acid (mM)	Formic Acid (mM)	Butyric Acid (mM)	Propionic Acid (mM)
0	35.93	6.83	0	0	0
24	34.06	5.26	1.49	0	0
48	32.02	1.64	4.14	0	0
72	25.53	1.13	4.52	0	0
98	24.01	0.44	10.31	0	0
121	18.57	0.26	14.17	0	0
145	16.74	0.13	-	0	0
167	13.84	0.10	15.26	0	0
196	8.92	0	14.92	0	0
218	8.52	0	11.58	0	0.009
237	4.36	0	-	0	0

Table I9- OD, cell dry weight, pH and cumulative hydrogen produced values for 20°C and 5000 lux (Mean of 2 runs)

time	OD	gdw/Lc	pH	Cumulative Hydrogen Produced (ml)	Cumulative Hydrogen Produced (mmol)
0	0.286	0.155	6.62	0	0
23	0.608	0.330	6.78	2.5	0.104
48	0.815	0.442	6.83	16.0	0.666
72	0.900	0.488	6.93	29.0	1.206
96	0.936	0.508	6.88	39.8	1.653
120	0.927	0.503	6.79	47.8	1.986
144	0.904	0.491	6.76	52.5	2.184
164	0.811	0.440	7.21	56.8	2.361
190	0.831	0.451	6.79	60.8	2.527
236	0.735	0.399	6.96	67.5	2.808
259	0.711	0.386	-	69.0	2.870
285	0.659	0.358	6.76	69.5	2.891

Table I10- Organic Acid concentrations for 20°C and 5000 lux (Mean of 2 runs)

time	Acetic Acid (mM)	Lactic Acid (mM)	Formic Acid (mM)	Butyric Acid (mM)	Propionic Acid (mM)
0	35.50	6.93	0	0	0
23	33.09	5.87	1.11	0	0
48	30.48	4.46	2.99	0	0
72	25.94	2.94	4.77	0	0.43
96	21.50	1.29	6.88	0	0.62
120	15.50	0.37	9.81	0.13	0.59
144	14.60	0.22	10.13	0.07	0.36
164	11.74	0.30	-	0.09	0.23
190	6.73	0.07	12.51	0.05	0.08
236	4.92	0.03	-	0	0
259	2.85	0	12.47	0	0
285	1.95	0	11.14	0	0

Table II1- OD, cell dry weight, pH and cumulative hydrogen produced values for 20°C and 6000 lux (Mean of 2 runs)

time	OD	gdw/Lc	pH	Cumulative Hydrogen Produced (ml)	Cumulative Hydrogen Produced (mmol)
0	0.291	0.158	6.60	0.0	0
23	0.578	0.314	6.75	1.0	0.560
48	0.888	0.482	6.86	14.0	0.599
72	0.906	0.492	6.90	32.0	1.329
96	0.916	0.497	6.88	42.0	1.741
120	0.887	0.481	6.78	50.0	2.059
144	0.882	0.479	6.74	55.0	2.302
164	0.796	0.432	7.10	61.0	2.518
190	0.816	0.443	6.77	67.0	2.770
214	-	-	-	70.0	2.892
236	0.682	0.370	6.70	71.0	2.957
259	0.593	0.322	-	75.0	3.107
285	0.596	0.324	6.76	75.0	3.107

Table I12- Organic Acid concentrations for 20°C and 6000 lux (Mean of 2 runs)

time	Acetic Acid (mM)	Lactic Acid (mM)	Formic Acid (mM)	Butyric Acid (mM)	Propionic Acid (mM)
0	35.74	7.13	0	0	0
23	32.70	6.24	1.09	0	0
48	29.86	4.17	2.60	0	0
72	27.63	2.37	2.22	0	0.24
96	22.18	0.91	6.92	0.07	0.36
120	17.88	0.25	10.45	0	0.36
144	14.71	0.40	10.63	0	0.14
164	9.78	0.10	-	0	0
190	5.12	0.01	12.82	0	0
214	-	-	-	-	-
236	5.35	0	12.15	0	0
259	0.92	0	13.30	0	0
285	0	0	-	0	0

Table I13- OD, cell dry weight, pH and cumulative hydrogen produced values for 20°C and 7000 lux (Mean of 2 runs)

time	OD	gdw/Lc	pH	Cumulative Hydrogen Produced (ml)	Cumulative Hydrogen Produced (mmol)
0	0.292	0.158	6.61	0	0
23	0.607	0.329	6.72	3.0	0.116
48	0.837	0.454	6.79	14.0	0.576
72	0.876	0.475	6.86	29.0	1.208
96	0.930	0.505	6.83	37.0	1.556
120	0.907	0.492	6.76	44.0	1.814
144	0.905	0.492	6.68	48.0	1.978
164	0.821	0.446	6.99	51.0	2.131
190	0.823	0.447	6.75	53.0	2.217
214	-	-	-	58.0	2.408
236	0.763	0.414	6.79	60.0	2.476
259	0.739	0.401	6.78	62.0	2.572
285	0.709	0.385	6.68	62.0	2.591

Table I14- Organic Acid concentrations for 20°C and 7000 lux (Mean of 2 runs)

time	Acetic Acid (mM)	Lactic Acid (mM)	Formic Acid (mM)	Butyric Acid (mM)	Propionic Acid (mM)
0	34.90	7.06	0	0	0
23	32.47	6.55	0.93	0	0
48	27.65	3.98	2.22	0	0
72	24.66	2.67	3.67	0	0.38
96	13.94	1.03	6.47	0.09	0.63
120	13.50	0.37	8.42	0.12	0.62
144	9.41	0.21	10.31	0.14	0.56
164	6.32	08	10.74	0.12	0.30
190	2.92	08	9.55	0.03	0.06
214	-	-	-	-	-
236	0.41	0.07	11.88	0.06	0
259	0.72	0.01	-	0	0
285	0	0.00	12.54	0	0

Table I15- OD, cell dry weight, pH and cumulative hydrogen produced values for 30°C and 1500 lux (Mean of 2 runs)

time	OD	gdw/Lc	pH	Cumulative Hydrogen Produced (ml)	Cumulative Hydrogen Produced (mmol)
0	0.292	0.158	6.68	0	0
23	0.375	0.204	6.63	0	0
48	0.862	0.468	6.92	3.0	0.121
72	1.492	0.810	7.10	17.5	0.704
96	1.399	0.759	7.15	29.0	1.166
121	1.581	0.858	7.23	34.0	1.368
169	1.374	0.746	7.46	46.0	1.850
210	1.324	0.718	7.30	46.0	1.850

Table I16- Organic Acid concentrations for 30°C and 1500 lux (Mean of 2 runs)

time	Acetic Acid (mM)	Lactic Acid (mM)	Formic Acid (mM)	Butyric Acid (mM)	Propionic Acid (mM)
0	37.35	7.09	0	0	0
23	36.10	6.38	0	0	0.03
48	29.36	3.20	0.21	0	0.01
72	20.30	0.75	0.58	0	0
96	12.96	0.24	1.63	0	0
121	7.63	0.18	1.94	0	0
169	4.24	0.00	2.50	0	0
210	0.19	0.00	2.61	0	0

Table I17- OD, cell dry weight, pH and cumulative hydrogen produced values for 30°C and 2000 lux (Mean of 2 runs)

time	OD	gdw/Lc	pH	Cumulative Hydrogen Produced (ml)	Cumulative Hydrogen Produced (mmol)
0	0.290	0.158	6.68	0	0
23	0.389	0.211	6.65	0	0
48	0.755	0.410	6.84	5.2	0.210
72	1.344	0.729	7.08	22.8	0.915
96	1.330	0.722	7.08	38.5	1.549
121	1.257	0.682	7.14	47.3	1.901
169	1.277	0.693	7.33	70.0	2.816
210	1.236	0.671	7.32	72.0	2.896
234	1.174	0.637	7.22	73.1	2.941
259	0.949	0.515	7.17	75.0	3.017
281	0.961	0.521	7.22	75.8	3.047

Table I18- Organic Acid concentrations for 30°C and 2000 lux (Mean of 2 runs)

time	Acetic Acid (mM)	Lactic Acid (mM)	Formic Acid (mM)	Butyric Acid (mM)	Propionic Acid (mM)
0	34.44	6.53	0	0	0
23	36.19	6.20	0	0	0
48	30.55	3.0	0.07	0	0
72	21.22	0.59	0.54	0	0
96	-	0.85	0.94	0	0
121	16.83	0.42	1.37	0	0.20
169	9.14	0.30	1.85	0.06	0
210	7.06	0	2.55	0.06	0
234	4.96	0	2.73	0.02	0
259	3.61	0	2.58	0.13	0
281	3.39	0	2.80	0.11	0

Table I19- OD, cell dry weight, pH and cumulative hydrogen produced values for 30°C and 3000 lux (Mean of 2 runs)

time	OD	gdw/Lc	pH	Cumulative Hydrogen Produced (ml)	Cumulative Hydrogen Produced (mmol)
0	0.283	0.153	6.67	0	0
23	0.428	0.232	6.67	0.8	0.033
48	0.855	0.464	6.92	7.8	0.312
72	1.328	0.721	7.10	22.5	0.905
96	1.317	0.715	7.11	38.3	1.539
121	1.234	0.670	7.17	47.3	1.901
169	1.182	0.641	7.37	64.0	2.574
210	1.095	0.594	7.32	69.5	2.796
234	1.064	0.578	7.22	73.6	2.961
259	0.656	0.356	7.14	77.5	3.117
281	0.627	0.340	7.17	78.5	3.158

Table I20- Organic Acid concentrations for 30°C and 3000 lux (Mean of 2 runs)

time	Acetic Acid (mM)	Lactic Acid (mM)	Formic Acid (mM)	Butyric Acid (mM)	Propionic Acid (mM)
0	37.67	7.17	0	0	0.05
23	36.56	5.76	0	0	0
48	30.11	1.68	0.17	0	0
72	19.18	0.31	0.69	0	0
96	25.50	0.15	1.44	0	0
121	26.98	0.24	1.64	0	0.33
169	18.41	0.05	2.49	0.01	0.47
210	11.32	0.00	2.58	0.01	0
234	3.52	0.00	2.60	0.02	0.29
259	2.10	0.00	2.85	0.05	0.97
281	0.43	0.00	3.02	0.04	0.60

Table I21- OD, cell dry weight, pH and cumulative hydrogen produced values for 30°C and 4000 lux (Mean of 2 runs)

time	OD	gdw/Lc	pH	Cumulative Hydrogen Produced (ml)	Cumulative Hydrogen Produced (mmol)
0	0.234	0.127	6.77	0	0
24	0.651	0.353	6.90	2.0	0.080
48	1.080	0.586	6.89	5.5	0.221
72	1.206	0.655	6.96	21.0	0.845
98	1.151	0.625	6.98	34.5	1.388
121	1.192	0.647	7.15	49.5	1.991
145	-	-	7.13	58.0	2.333
167	1.186	0.644	7.06	64.3	2.584
196	1.038	0.563	7.24	69.0	2.775
218	0.953	0.517	7.30	72.0	2.896
237	0.911	0.494	7.23	73.5	2.956

Table I22- Organic Acid concentrations for 30°C and 4000 lux (Mean of 2 runs)

time	Acetic Acid (mM)	Lactic Acid (mM)	Formic Acid (mM)	Butyric Acid (mM)	Propionic Acid (mM)
0	36.20	7.18	0	0	0
24	34.27	4.32	0	0	0
48	29.51	1.90	0	0	0
72	28.69	0.74	5.35	0	0
98	19.70	0.22	4.26	0	0
121	19.38	0.18	4.16	0	0
145	13.90	0.21	5.30	0	0
167	10.16	0.13	6.77	0	0
196	6.12	0.00	8.41	0	0.06
218	3.83	0.00	8.87	0	0.22
237	1.72	0.00	10.08	0	0.24

Table I23- OD, cell dry weight, pH and cumulative hydrogen produced values for 30°C and 5000 lux (Mean of 2 runs)

time	OD	gdw/Lc	pH	Cumulative Hydrogen Produced (ml)	Cumulative Hydrogen Produced (mmol)
0	0.355	0.193	6.46	0	0
26	0.667	0.362	6.66	1.0	0.040
51	1.397	0.758	6.96	14.5	0.583
72	1.571	0.853	7.10	36.0	1.448
98	-	-	-	42.0	1.689
124	1.599	0.868	7.26	54.0	2.172
148	1.544	0.838	7.27	59.5	2.393
171	1.532	0.832	7.14	65.0	2.615
197	1.423	0.772	7.18	68.0	2.735
221	1.342	0.728	7.20	71.5	2.876
245	1.192	0.647	7.18	72.8	2.926

Table I24- Organic Acid concentrations for 30°C and 5000 lux (Mean of 2 runs)

time	Acetic Acid (mM)	Lactic Acid (mM)	Formic Acid (mM)	Butyric Acid (mM)	Propionic Acid (mM)
0	37.69	7.00	0	0	0
26	35.38	4.96	9.46	0	0
51	27.72	1.85	20.02	0	0
72	20.36	0.58	15.15	0	0
98	-	0.28	-	-	-
124	12.39	0.18	15.23	0	0
148	6.95	0.14	9.99	0	0
171	4.66	0.12	3.51	0	0
197	4.55	0	-	0	0
221	1.48	0	0	0	0
245	0	0	0	0	0

Table I25- OD, cell dry weight, pH and cumulative hydrogen produced values for 30°C and 6000 lux (Mean of 2 runs)

time	OD	gdw/Lc	pH	Cumulative Hydrogen Produced (ml)	Cumulative Hydrogen Produced (mmol)
0	0.287	0.156	6.66	0	0
25	0.607	0.329	6.425	2.5	0.101
49	1.522	0.826	7.265	8.0	0.322
73	1.474	0.800	7.325	16.5	0.664
92	-	-	-	31.0	1.247
116	1.561	0.847	7.255	39.3	1.579
142	1.457	0.791	7.535	46.5	1.870
164	1.336	0.725	7.72	50.3	2.021
167	-	-	-	50.8	2.041
189	1.135	0.616	7.79	50.8	2.041
212	1.151	0.625	7.83	52.5	2.112
236	0.953	0.517	7.415	52.5	2.112

Table I26- Organic Acid concentrations for 30°C and 6000 lux (Mean of 2 runs)

time	Acetic Acid (mM)	Lactic Acid (mM)	Formic Acid (mM)	Butyric Acid (mM)	Propionic Acid (mM)
0	37.45	6.8	0	0	0
25	31.55	4.97	1.11	0	0
49	31.15	2.24	6.27	0	0
73	27.28	0.54	12.20	0	0.32
92	14.63	0.4	9.50	0.18	0.40
116	10.21	0.17	4.84	0.12	0.06
142	6.08	0.18	5.13	0.20	0.00
164	2.62	0	5.93	0.17	0.17
167	-	-	-	-	-
189	1.37	0	5.96	0	0.11
212	0.82	0	6.38	0	0.11
236	0	0	5.44	0	0.09

Table I27- OD, cell dry weight, pH and cumulative hydrogen produced values for 30°C and 7000 lux (Mean of 2 runs)

time	OD	gdw/Lc	pH	Cumulative Hydrogen Produced (ml)	Cumulative Hydrogen Produced (mmol)
0	0.282	0.153	6.85	0	0
24	0.594	0.322	6.70	0	0
48	1.224	0.664	6.97	8.50	0.342
72	1.249	0.678	6.94	12.50	0.503
97	0.859	0.466	7.02	20.00	0.804
144	0.847	0.460	6.89	21.00	0.845
169	0.803	0.436	6.63	22.50	0.905

Table I28- Organic Acid concentrations for 30°C and 7000 lux (Mean of 2 runs)

time	Acetic Acid (mM)	Lactic Acid (mM)	Formic Acid (mM)	Butyric Acid (mM)	Propionic Acid (mM)
0	36.71	7.08	0	0	0
24	33.59	5.46	2.00	0	0
48	27.57	4.58	5.45	0.05	0.51
72	22.83	1.12	15.60	0	0.67
97	18.48	1.65	25.17	0	0.62
144	17.24	0.83	-	0	0.75
169	15.30	0.63	4.65	0	0.43

Table I29- OD, cell dry weight, pH and cumulative hydrogen produced values for 38°C and 1500 lux (Mean of 2 runs)

time	OD	gdw/Lc	pH	Cumulative Hydrogen Produced (ml)	Cumulative Hydrogen Produced (mmol)
0	0.218	0.118	6.68	0	0
25	0.463	0.251	6.50	1.5	0.059
49	1.050	0.570	6.91	2.5	0.098
73	1.655	0.898	6.79	8.5	0.333
92	1.599	0.868	6.69	9.8	0.382
116	1.716	0.931	6.66	16.5	0.647
142	1.728	0.938	6.86	18.5	0.725
164	-	-	-	21.0	0.823
191	1.558	0.846	7.25	23.0	0.901
213	1.445	0.784	7.88	25.5	0.999
236	1.382	0.750	8.08	27.3	1.068
260	1.184	0.643	7.44	27.8	1.087

Table I30- Organic Acid concentrations for 38°C and 1500 lux (Mean of 2 runs)

time	Acetic Acid (mM)	Lactic Acid (mM)	Formic Acid (mM)	Butyric Acid (mM)	Propionic Acid (mM)
0	36.65	7.90	0	0	0
25	33.35	4.77	1.03	0	0
49	23.25	1.70	-	0	0
73	22.40	0.75	-	0.12	0.12
92	15.50	0.16	3.09	0.64	0.49
116	9.23	0.12	2.50	0.63	0.16
142	7.74	0.02	3.05	0.43	0.00
164	-	-	-	-	-
191	-	-	2.57	0.53	0
213	3.32	0	2.81	0.26	0.08
236	2.68	0	2.96	0.20	0.19
260	2.49	0	1.51	0.12	0.05

Table I31- OD, cell dry weight, pH and cumulative hydrogen produced values for 38°C and 2000 lux (Mean of 2 runs)

time	OD	gdw/Lc	pH	Cumulative Hydrogen Produced (ml)	Cumulative Hydrogen Produced (mmol)
0	0.311	0.169	6.62	0.0	0.00
23	0.578	0.314	6.73	2.0	0.078
48	1.073	0.582	7.08	2.0	0.078
72	1.570	0.852	7.48	13.0	0.509
96	1.765	0.958	7.45	25.0	0.980
121	1.800	0.977	7.53	35.0	1.372
169	1.836	0.997	7.48	38.0	1.489
210	1.924	1.044	7.70	40.0	1.568

Table I32- Organic Acid concentrations for 38°C and 2000 lux (Mean of 2 runs)

time	Acetic Acid (mM)	Lactic Acid (mM)	Formic Acid (mM)	Butyric Acid (mM)	Propionic Acid (mM)
0	35.85	7.37	0	0	0
23	33.75	6.22	0.74	0	0
48	28.02	4.16	1.72	0	0
72	18.22	1.10	2.30	0	0
96	16.40	0.11	-	0	0
121	6.19	0.07	0.06	0	0
169	2.73	0.02	0.09	0	0
210	1.38	0.01	0	0	0

Table I33- OD, cell dry weight, pH and cumulative hydrogen produced values for 38°C and 3000 lux (Mean of 2 runs)

time	OD	gdw/Lc	pH	Cumulative Hydrogen Produced (ml)	Cumulative Hydrogen Produced (mmol)
0	0.306	0.166	6.86	0	0
25	0.613	0.333	6.61	3.0	0.118
49	-	-	-	7.0	0.274
73	1.747	0.948	6.83	17.5	0.686
92	1.641	0.890	6.84	25.5	0.999
116	1.781	0.967	7.00	31.5	1.234
142	1.758	0.954	7.09	37.3	1.460
191	1.974	1.071	7.29	41.5	1.626
213	1.780	0.966	7.89	43.5	1.705
236	1.776	0.964	7.89	45.8	1.793
260	1.569	0.851	7.15	46.0	1.803

Table I34- Organic Acid concentrations for 38°C and 3000 lux (Mean of 2 runs)

time	Acetic Acid (mM)	Lactic Acid (mM)	Formic Acid (mM)	Butyric Acid (mM)	Propionic Acid (mM)
0	36.24	7.21	0.00	0	0
25	33.30	3.88	3.86	0	0
49	26.30	2.00	2.70	0	0
73	20	0.91	1.38	0.14	0.96
92	15.35	0.47	1.19	0.36	1.15
116	11.18	0.16	1.57	0.91	1.56
142	-	-	-	-	-
191	3.86	0.16	2.71	1.23	0.32
213	1.90	0	2.56	1.21	0.12
236	0.94	0	2.32	1.05	0
260	0.59	0	-	0.69	0

Table I35- OD, cell dry weight, pH and cumulative hydrogen produced values for 38°C and 4000 lux (Mean of 2 runs)

time	OD	gdw/Lc	pH	Cumulative Hydrogen Produced (ml)	Cumulative Hydrogen Produced (mmol)
0	0.298	0.162	6.67	0	0
25	0.492	0.267	6.42	2.0	0.078
49	0.872	0.473	7.36	8.0	0.314
73	1.747	0.948	7.22	22.5	0.882
92	-	-	-	31.3	1.225
116	-	-	-	34.5	1.352
142	1.971	1.070	7.10	37.0	1.450
191	1.897	1.030	7.86	39.5	1.548
213	1.953	1.060	8.06	40.8	1.597
236	1.182	0.641	8.05	41.3	1.617
260	1.050	0.570	7.44	41.5	1.626

Table I36- Organic Acid concentrations for 38°C and 4000 lux (Mean of 2 runs)

time	Acetic Acid (mM)	Lactic Acid (mM)	Formic Acid (mM)	Butyric Acid (mM)	Propionic Acid (mM)
0	34.41	6.88	0.26	0	0
25	30.80	3.89	1.76	0	0
49	17.80	1.79	1.44	0	0
73	13.39	1.22	1.91	0	0
92	9.00	0.30	1.60	0.18	0
116		-	-	-	-
142	8.69	0	1.59	0.09	0
191	6.34	0	1.73	0.10	0.26
213	3.35	0	1.53	0.07	0
236	2.61	0	1.54	0.04	0
260	2.19	0	1.34	0.00	0

Table I37- OD, cell dry weight, pH and cumulative hydrogen produced values for 38°C and 5000 lux (Mean of 2 runs)

time	OD	gdw/Lc	pH	Cumulative Hydrogen Produced (ml)	Cumulative Hydrogen Produced (mmol)
0	0.364	0.197	6.67	0	0
24	0.462	0.251	6.40	1.0	0.039
48	0.589	0.320	7.10	4.5	0.176
72	1.041	0.565	6.99	9.5	0.372
97	1.867	1.013	6.90	18.3	0.715
144	-	-	-	25.5	0.999
169	1.974	1.071	7.55	34.0	1.332
193	1.913	1.038	8.11	36.0	1.411
215	1.174	0.637	8.17	37.0	1.450
239	1.070	0.581	7.46	37.0	1.450
260	-	-	-	37.5	1.470

Table I38- Organic Acid concentrations for 38°C and 5000 lux (Mean of 2 runs)

time	Acetic Acid (mM)	Lactic Acid (mM)	Formic Acid (mM)	Butyric Acid (mM)	Propionic Acid (mM)
0	34.88	7.04	0	0	0
25	28.51	5.00	1.09	0	0
49	26.83	3.07	2.41	0	0
73	18.16	1.09	-	0.11	0.11
92	17.72	0.65	2.36	0.41	0.20
116	15.49	0.67	-	0.33	0.08
142	11.13	0.58	2.99	0.40	0.19
191	9.72	0.01	2.13	0.32	0.08
213	5.10	0	0.65	0.17	0.12
236	3.87	0	0.64	0.14	0.27
260	0.74	0	0.70	0.05	0